JAEA-Data/Code
2025-005
DOI:10.11484/jaea-data-code-2025-005

JAEA-Data/Code

Input Data Preparation for PWR Large-Break LOCA Analysis with RELAP5/MOD3.3 Code

Takeshi TAKEDA

Nuclear Safety Research Center
Nuclear Safety and Emergency Preparedness Institute

June 2025

Japan Atomic Energy Agency

日本原子力研究開発機構

国立研究開発法人日本原子力研究開発機構　研究開発推進部　科学技術情報課
〒 319-1112　茨城県那珂郡東海村大字村松 4 番地 49
E-mail: ird-support@jaea.go.jp

JAEA-Data/Code 2025-005

Input Data Preparation for PWR Large-Break LOCA Analysis with RELAP5/MOD3.3 Code

Takeshi TAKEDA

Nuclear Safety Research Center
Nuclear Safety and Emergency Preparedness Institute
Japan Atomic Energy Agency
Tokai-mura, Naka-gun, Ibaraki-ken

(Received March 25, 2025)

JAEA has been creating input data for pressurized water reactor (PWR) analysis with RELAP5/MOD3.3 code, mainly based on design information for the four-loop PWR's Tsuruga Power Station Unit-2 as the reference reactor of the Large Scale Test Facility (LSTF). The cold leg large-break loss-of-coolant accident (LBLOCA) calculation in the flamework of the BEMUSE program is cited as a representative OECD/NEA activity related to the PWR analysis. The new regulatory requirements for PWRs in Japan include the event of loss of recirculation functions from emergency core cooling system (ECCS) in the cold leg LBLOCA. This event should be evaluated the effectiveness of measures against severe core damage.

The input data for this study were made preparations to analyze the PWR LBLOCA, which is one of the design basis accidents that should be postulated in the safety design. This report describes the main features of the input data for the PWR LBLOCA analysis. The PWR model comprised a reactor vessel, pressurizer (PZR), hot legs, steam generators (SGs), SG secondary-side system, crossover legs, cold legs, and ECCS. A four-loop PWR was simulated by two loops in the LBLOCA calculation. Specifically, loop-A attached with the PZR corresponded to three loops, and loop-B mounted with the break was equal to one loop. The nodalization schemes of the PWR components were referred to those of the LSTF components. Moreover, interpretations were added to the main input data for the PWR LBLOCA analysis, and further information such as the basis for determining the input data was provided.

In addition, transient analysis was performed employing the prepared input data for the loss of ECCS recirculation functions event. The present transient analysis was confirmed to be appropriate generally by comparing with the calculation in the previous study using the RELAP5/MOD3.3 code. Furthermore, sensitivity analyses were executed exploiting the RELAP5/MOD3.3 code to clarify the effects of a discharge coefficient through the break and water injection flow rate of the alternative recirculation on the fuel rod cladding surface temperature. This report explains the results of the sensitivity analyses within the defined ranges, which complement some of the content of the previous study's calculation for the loss of ECCS recirculation functions event.

Keywords: PWR, LSTF, Large-Break LOCA, Cold Leg, RELAP5 Code, Input Data, ECCS, New Regulatory Requirements, Design Information, Sensitivity Analysis

JAEA-Data/Code 2025-005

RELAP5/MOD3.3 コードによる PWR 大破断 LOCA 解析のための入力データの整備

日本原子力研究開発機構 原子力安全・防災研究所
安全研究センター

竹田 武司

（2025 年 3 月 25 日受理）

JAEA では、加圧水型軽水炉(PWR)解析のための RELAP5/MOD3.3 コードの入力データを、主に大型非定常実験装置(LSTF)の参照 4 ループ PWR である敦賀発電所 2 号機の設計情報を基に作成してきた。PWR 解析に関する代表的な OECD/NEA の活動として、BEMUSE プログラムの枠組みにおける低温側配管大破断冷却材喪失事故(LBLOCA)の計算が挙げられる。また、わが国の新規制基準に係る PWR の炉心損傷防止対策の有効性評価事象には、低温側配管 LBLOCA 時の非常用炉心冷却系(ECCS)の再循環機能喪失事象が含まれる。

本検討において、PWR の安全設計上想定すべき設計基準事故の一つである LBLOCA を解析するための入力データを整備した。本報告書では、PWR LBLOCA 解析の入力データの主な特徴を示す。PWR の原子炉容器、加圧器(PZR)、高温側配管、蒸気発生器(SG)、SG 二次系、クロスオーバーレグ、低温側配管、ECCS などをモデル化し、参照 4 ループ PWR を 2 ループで模擬した。その際、PZR は 3 ループ分を模擬するループ A に接続し、破断口は 1 ループ分を模擬するループ B に設置した。PWR のコンポーネントのノード分割は、LSTF のコンポーネントのノード分割を参照した。また、PWR LBLOCA 解析の主な入力データに対して、解釈を加えるとともに、設定根拠などの付加情報を提供した。

さらに、整備した入力データを用いて、ECCS 再循環機能喪失事象を対象とした過渡解析を実施した。RELAP5/MOD3.3 コードによる既往研究の計算と比較することにより、過渡解析は概ね妥当であることを確認した。加えて、RELAP5/MOD3.3 コードを用いて感度解析を実施し、破断口の流出係数や代替再循環注水流量が燃料棒被覆管表面温度に及ぼす影響を明らかにした。本報告書では、設定した条件の範囲内での感度解析結果について示し、ECCS 再循環機能喪失事象に対する既往研究の計算内容の一部を補完する。

原子力科学研究所：〒319-1195　茨城県那珂郡東海村大字白方 2-4

Contents

1. Introduction ··· 1
2. PWR LBLOCA Analysis and Steady-State Analysis with RELAP5 Code ··· 3
   2.1 Major Features of Input Data for PWR LBLOCA Analysis ··· 3
   2.2 Overview of Main Input Data Classified into Nine Categories ··· 5
   2.3 Steady-State Analysis ··· 9
3. Loss of ECCS Recirculation Functions Event Analysis with RELAP5 Code ··· 13
   3.1 Outline of Loss of ECCS Recirculation Functions Event ··· 13
   3.2 Transient Analysis for Loss of ECCS Recirculation Functions Event ··· 13
   3.3 Sensitivity Analyses for Loss of ECCS Recirculation Functions Event ··· 15
4. Summary ··· 28

Acknowledgement ··· 29

References ··· 29

Appendix A List of Main Input Data for PWR LBLOCA Analysis ··· 32

目次

1. 緒言 ・・・1
2. RELAP5 コードによる PWR LBLOCA 解析および定常解析 ・・・・・・・・・・・・・・・・・・・・・・・3
2.1 PWR LBLOCA 解析のための入力データの主な特徴・・・・・・・・・・・・・・・・・・・・・・・・・・・3
2.2 9 つのカテゴリーに分類した主な入力データの概要・・・・・・・・・・・・・・・・・・・・・・・・・・5
2.3 定常解析 ・・・9
3. RELAP5 コードによる ECCS 再循環機能喪失事象解析・・・・・・・・・・・・・・・・・・・・・・・・・・・13
3.1 ECCS 再循環機能喪失事象の概要 ・・・・・・・・・・・・・・・・・・・・・・・・・・・・・・・・・・・・13
3.2 ECCS 再循環機能喪失事象の過渡解析 ・・・・・・・・・・・・・・・・・・・・・・・・・・・・・・・・・13
3.3 ECCS 再循環機能喪失事象の感度解析 ・・・・・・・・・・・・・・・・・・・・・・・・・・・・・・・・・15
4. 結言 ・・28
謝辞 ・・29
参考文献 ・・・29
付録 A PWR LBLOCA 解析のための主な入力データリスト ・・・・・・・・・・・・・・・・・・・・・・・・・32

List of Tables

Table 2-1 Comparison of specified value and convergence value for each estimation parameter in steady-state analysis ····· 10
Table 3-1 Variable parameter in RELAP5 code for each estimation parameter in transient analysis ····· 17
Table 3-2 Sensitivity parameters and maximum cladding surface temperatures in sensitivity analyses ····· 18

List of Figures

Fig. 2-1 Noding schematic of overall PWR system ····· 11
Fig. 2-2 Noding schematic of PWR reactor vessel portion ····· 12
Fig. 3-1 PWR coolant distribution in loss of ECCS recirculation functions event ····· 19
Fig. 3-2 Core and vessel downcomer liquid levels (Base Case) ····· 19
Fig. 3-3 Differential pressure between upper plenum and SG portion (Base Case) ····· 20
Fig. 3-4 Fuel rod cladding surface temperatures through Positions 9-5 (Base Case) ··· 20
Fig. 3-5 Fuel rod cladding surface temperatures through Positions 4-1 (Base Case) ··· 21
Fig. 3-6 Reactor thermal power (Base Case) ····· 21
Fig. 3-7 Primary and secondary pressures (Base Case) ····· 22
Fig. 3-8 SG secondary narrow-range liquid levels (Base Case) ····· 22
Fig. 3-9 SG secondary wide-range liquid levels (Base Case) ····· 23
Fig. 3-10 Core and vessel downcomer liquid levels (Cd = 0.6; Case A) ····· 23
Fig. 3-11 Core and vessel downcomer liquid levels (Cd = 0.4; Case B) ····· 24
Fig. 3-12 Fuel rod cladding surface temperatures through Positions 9-5 (Cd = 0.6; Case A) ····· 24
Fig. 3-13 Fuel rod cladding surface temperatures through Positions 9-5 (Cd = 0.4; Case B) ····· 25
Fig. 3-14 Fuel rod cladding surface temperatures through Positions 4-1 (Cd = 0.6; Case A) ····· 25
Fig. 3-15 Fuel rod cladding surface temperatures through Positions 4-1 (Cd = 0.4; Case B) ····· 26
Fig. 3-16 Alternative recirculation water injection flow rate versus maximum cladding surface temperature (Cd = 1.0; Base Case, Cases C and D) ····· 26
Fig. 3-17 Alternative recirculation water injection flow rate versus maximum cladding surface temperature (Cd = 0.6; Cases A, E and F) ····· 27
Fig. 3-18 Alternative recirculation water injection flow rate versus maximum cladding surface temperature (Cd = 0.4; Cases B, G and H) ····· 27

Acronyms and Abbreviations

ACC	Accumulator
AFW	Auxiliary Feedwater
ANS	American Nuclear Society
BEMUSE	Best-Estimate Methods – Uncertainty and Sensitivity Evaluation
Cd	Discharge Coefficient
COL	Crossover Leg
CRGT	Control Rod Guide Tube
CSAU	Code Scaling, Applicability and Uncertainty
DC	Downcomer
ECCS	Emergency Core Cooling System
FSAR	Final Safety Analysis Report
HPI	High Pressure Injection
IET	Integral Effect Test
JAEA	Japan Atomic Energy Agency
LBLOCA	Large-Break Loss-of-Coolant Accident
LOCA	Loss-of-Coolant Accident
LPI	Low Pressure Injection
LSTF	Large Scale Test Facility
MSIV	Main Steam Isolation Valve
NEA	Nuclear Energy Agency
OECD	Organisation for Economic Co-Operation and Development
PORV	Power Operated Relief Valve
PWR	Pressurized Water Reactor
PZR	Pressurizer
RELAP	Reactor Excursion and Leak Analysis Program
ROSA	Rig-of-Safety Assessment
SET	Separate Effect Test
SG	Steam Generator
SI	Safety Injection
USNRC	United States Nuclear Regulatory Commission

1. Introduction

Japan Atomic Energy Agency (JAEA) has been conducting integral effect tests (IETs) and separate effect tests (SETs) for accidents, such as loss-of-coolant accident (LOCA), and transients, such as station blackout, utilizing the Large Scale Test Facility (LSTF) [1] in the Rig-of-Safety Assessment-V (ROSA-V) Program [2]. The LSTF is a full-height and 1/48 volumetrically-scaled simulator with a two-loop system of a Westinghouse-type four-loop 3423 MW (thermal) pressurized water reactor (PWR). The reference PWR of the LSTF is Tsuruga Power Station Unit-2 (Tsuruga Unit-2) of Japan Atomic Power Company. JAEA has also been preparing input data for the PWR analysis with the RELAP5/MOD3.3 code [3], mainly on the basis of design information for Tsuruga Unit-2, for the following reasons. One is to help establish boundary conditions for a variety of the LSTF tests. The other is to look into the impacts of differences in design conditions between the PWR and LSTF on the thermal-hydraulic phenomena and responses during the same accident scenarios.

The LSTF tests under the conditions pre-determined by the PWR calculations involve an IET on loss-of-feedwater transient without scram, with delayed actuation of auxiliary feedwater (AFW) system of steam generator (SG) associated with natural circulation during high core power conditions [4]. The LSTF has provided experimental data including the Mihama Nuclear Power Station Unit-2 SG tube rupture accident simulation for the Nuclear Safety Commission of Japan [5][6]. As a typical OECD/NEA activity concerning PWR calculations, the BEMUSE (Best-Estime Methods – Uncertainty and Sensitivity Evaluation) program has performed uncertainty and sensitivity analysis of a cold leg large-break LOCA (LBLOCA) at the Zion Nuclear Power Plant [7][8]. Regarding other related works, Frepoli has implemented a realistic LBLOCA evaluation model for Westinghouse-type PWR, following the Code Scaling, Applicability and Uncertainty (CSAU) [9]. Kaminski and Diab have developed a machine learning metamodel for the time-series forecasting of a typical PWR undergoing LBLOCA [10].

Preparing input data for this study was done for the analysis of a LBLOCA among the design basis accidents to be taken into account in the PWR safety design [11]. In relation to the LBLOCA, the LSTF tests based on the PWR calculations contain a SET on steam condensation on emergency core cooling system (ECCS) water in cold legs [12]. In the new regulatory requirements for PWRs in Japan, loss of recirculation functions from ECCS in the cold leg LBLOCA was postulated as one of the events, which should be assessed the measures effectiveness against severe core damage [2][13].

The main objective of this study is to prepare the RELAP5/MOD3.3 code input data for PWR LBLOCA analysis based on the available PWR data. A four-loop PWR was simulated using two loops in the LBLOCA calculation. A pressurizer (PZR) was connected to loop-A to simulate three loops, while a break was connected to loop-B to model one loop. Moreover,

interpretations were included in the main input data for the PWR LBLOCA analysis, and additional information (e.g., the ground for setting the input data) was supplied. The main input data were classified into nine categories along with the RELAP5 code user's manual [3]; miscellaneous control cards, time step control cards, trip input data, hydrodynamic components, heat structure input, heat structure thermal property data, general table data, reactor kinetics input, and control system input data.

Code-to-code comparisons in identical scenarios can be used to evaluate the reliability of simulation results when verifications with measured data are limited. In this study, transient analysis was carried out utilizing the prepared input data for the event of loss of ECCS recirculation functions. The validity of the present transient analysis was confirmed by comparing it to the calculation in the previous study taking advantage of the RELAP5/MOD3.3 code [13]. However, it was unclear whether a discharge coefficient (Cd) through the break and water injection flow rate of the alternative recirculation affect the fuel rod cladding surface temperature. Hence, sensitivity analyses were conducted utilizing the RELAP5/MOD3.3 code to elucidate their influences. This report gives the results of the sensitivity analyses under the defined conditions, complementing some of the content of the previous study's calculation for the loss of ECCS recirculation functions event [13].

Chapter 2 of this report presents the major features of the input data, the overview of the main input data for the PWR LBLOCA analysis grouped into the nine categories, and the steady-state analysis. **Chapter 3** of this report explains the outline of the loss of ECCS recirculation functions event, the major conditions and results of the transient and sensitivity analyses for the loss of ECCS recirculation functions event. **Appendix A** of this report summarizes the list of the main input data for the PWR LBLOCA analysis.

2. PWR LBLOCA Analysis and Steady-State Analysis with RELAP5 Code

2.1 Major Features of Input Data for PWR LBLOCA Analysis

The major features of the input data for the PWR LBLOCA analysis are as follows;

1. Design information for four-loop PWR's Tsuruga Unit-2 made of Japan Atomic Power Company [1], which is the LSTF reference reactor, is leveraged as much as possible to create input data for the PWR LBLOCA analysis.
2. The control system input data related to quantities such as PZR heater power and SG secondary narrow-range liquid level are created referring to those for the US Surry Power Plant Units [14]. The reason is that appropriate design information for Tsuruga Unit-2 cannot be acquired.
3. The PWR model includes a reactor vessel, PZR, hot legs, SGs, SG secondary-side system, crossover legs (COLs), cold legs, and ECCS. The COL is a primary piping that connects a reactor coolant pump to the SG.
4. The modeled SG mainly consists of U-tubes, inlet plenum, outlet plenum, downcomer (DC), riser, steam dome, and separator. The U-tubes in each modeled SG are simulated by a single flow channel with ten nodes because the flow among SG U-tubes is expected to be uniform during the PWR LBLOCA.
5. The reactor thermal power is initially fixed to 3423 MW [1][15]. The axial core power profile is a nine-step chopped cosine with a peaking factor of 1.4945. The radial power peaking factors are 1.51, 1.00, and 0.66 for high-power, mean-power, and low-power fuel rods, respectively.
6. The primary pressure, secondary pressure, hot leg fluid temperature, and cold leg fluid temperature are initially set to 15.5 MPa, 6.1 MPa, 598 K, and 562 K, respectively [1][15]. The PZR pressure and SG steam dome pressure represent the primary and secondary pressures, respectively.
7. The initial values of the PZR liquid level and SG secondary narrow-range liquid level are fixed to 58.6% [1] and 44% [4], respectively. The SG secondary narrow-range liquid level is used to monitor the SG secondary liquid level status.
8. The bypass flow between vessel DC and upper head is simulated by providing the proper energy loss coefficient for both forward and reverse flow in the junction between them to better match the specified bypass flow rate [1][15]. The simulation of the bypass flow path between vessel DC and hot legs is done by well modeling the geometry (length, volume, inclination angle, junction area, etc.) to better fit the specified bypass flow rate [1][15].
9. Noding schematics of the overall system and reactor vessel portion of PWR are illustrated in **Figs. 2-1 and 2-2**, respectively. The noding schemes include the connection between

the heat structure and the hydrodynamic component to simulate the heat exchange. A four-loop PWR is modeled by a two-loop noding, except for core bypass region, similar to that for LSTF noding. The volume of the LSTF vessel DC region includes the volume equivalent to the PWR core bypass region. A PZR is connected to loop-A, which corresponds to three loops. A break is installed in loop-B, which is equal to one loop. In relation to the boundary conditions of the heat structure geometry of the PWR components, the environment corresponding to containment is modeled with the single-volume component no. 910, and the connection to the environment (containment) is simulated using the time-dependent volume component no. 900.

10. Following the steady-state analysis, transient analysis begins with a cold leg double-ended guillotine break (200% break) to simulate LBLOCA. As depicted in **Fig. 2-1**, the branch component no. 248 is connected to the pipe component no. 252 through the valve junction component no. 249 for cold leg in loop-B. A break connecting to the branch component no. 248 for cold leg in loop-B is modeled by the valve junction component no. 941. A break connecting to the pipe component no. 252 for cold leg in loop-B is modeled by the valve junction component no. 951. At time zero the two valve junction components no. 941 and 951 are simultaneously open while the valve junction component no. 249 is closed.
11. As drawn in **Fig. 2-2**, the modeled reactor vessel contains upper head, control rod guide tube (CRGT), upper plenum, lower plenum, core, core bypass, and DC. The modeled core with a height of 3.66 m is split into nine equal-height volumes that are stacked perpendicularly, taking account of a nine-step chopped cosine power profile.
12. The nodalization schemes of the PWR components, other than the core bypass region, are similar to those of the LSTF components.
13. In terms of the RELAP5 hydrodynamic component models, quantities such as wall roughness, flow energy loss coefficient, volume and junction control flags for the PWR components are referred to those for the LSTF components.
14. Regarding the PWR reactor coolant pump, the pump characteristic data comprising single-phase homologous curve, two-phase multiplier table, and two-phase difference table for the USNRC's Semiscale test facility built into the RELAP5 code are converted into the input format of the RELAP5 code and applied [3][16].
15. The critical flow model employs the Ransom-Trapp choked-flow model among the built-in models of the RELAP5 code [17].
16. The reflood model integrated into the RELAP5 code is applied to the boundary condition of heat structure geometry of high-power, mean-power, and low-power fuel rods [18].
17. The reactor thermal power is calculated by utilizing the point reactor kinetics model

incorporated into the RELAP5 code. The ANS73 decay heat curve built into the RELAP5 code is employed as the ANS standard data for decay heat data [19]. The Doppler reactivity defined as a function of the temperature is the value evaluated based on the reactivity curve described in the final safety analysis report (FSAR) of the US Surry Power Plant Units [14]. Moreover, the moderator density reactivity defined as a function of the moderator density is the value estimated on the basis of the WCAP-8330 reactivity curve [20]. Additionally, the scram reactivity defined as a function of the time is the value evaluated based on the reactivity curve described in the FSAR of the US Prairie Island Nuclear Generating Plant Units [21].

18. A reactor scram signal is generated when the PZR pressure drops to 12.97 MPa, which causes the termination of SG main feedwater, the closure of SG main steam isolation valves (MSIVs), and the shutdown of PZR heater [15]. In addition, it is assumed that off-site power is lost coincidently with the reactor scram signal, which leads to the coastdown of the reactor coolant pumps [15].
19. The ECCS is simulated such as high pressure injection (HPI) system, accumulator (ACC) system, and low pressure injection (LPI) system. The HPI system is initiated via a safety injection (SI) signal when the PZR pressure drops to 12.27 MPa [15]. The ACC and LPI systems are initiated when the cold leg pressure and lower plenum pressure decline to 4.51 MPa and 1.2 MPa, respectively [15]. The ACC system is terminated when the cold leg pressure drops to 1.7 MPa [22]. The coolant injection temperature is 310 K for the HPI and LPI systems, while it is 320 K for the ACC system, according to the specified value of the LSTF reference reactor [15]. The mass flow rate of coolant from each of the HPI and LPI systems is dependent on the lower plenum pressure.
20. The secondary pressure set points for opening and closure of the SG relief valves are 8.03 MPa and 7.82 MPa respectively, while those of the SG safety valves are 8.68 MPa and 7.69 MPa [15]. The primary pressure set points for opening and closure of the PZR power operated relief valve (PORV) are 16.20 MPa and 16.07 MPa respectively, while those of the PZR safety valve are 17.26 MPa and 17.06 MPa [15].

2.2 Overview of Main Input Data Classified into Nine Categories

Appendix A lists the main input data for the PWR LBLOCA analysis with the RELAP5/MOD3.3 code. The main input data, which are grouped into nine categories along with the RELAP5/MOD3 code manual, are outlined as below.

A. Miscellaneous control cards

Ransom-Trapp choked-flow model is employed, regarding developmental model control. Nitrogen gas is used as non-condensable gas for pressurization of ACC system of ECCS.

B. Time step control cards

The minimum and maximum time steps are chosen 10^{-8} and 0.002, respectively. Quantities edited are plotted every 1 s by multiplying the maximum time step of 0.002 by the minor edit and plot frequency of 500.

C. Trip input data

Cards on trip input data are composed of variable trip cards and logical trip cards. The variable trip cards deal with the following; trip signals for HPI and LPI systems, reactor scram signal, SI signal, break start, on/off signal for SG relief valve, on/off signal for SG safety valve, on/off signal for PZR PORV, on/off signal for PZR safety valve, on/off signal for ACC tank outlet valve, on/off signal for SG AFW system, on/off signal for PZR heater, dummy trip, and reflood model utilization. The logical trip cards treat the following; on/off signal for SG relief valve, on/off signal for SG safety valve, on/off signal for PZR PORV, on/off signal for PZR safety valve, on/off signal for ACC tank outlet valve, on/off signal for SG AFW system, reactor scram signal, trip signal for cold leg in loop-B, and trip signals for HPI and LPI systems.

D. Hydrodynamic components

Hydrodynamic components are made up of a variety of component types. The component types consist of single-volume, time-dependent volume, single-junction, time-dependent junction, pipe, annulus, branch, separator, pump, and ACC. The tag names are SV, TDV, SJ, TDJ, P, AN, B, SP, PMP, and ACC, respectively, as mentioned in the PWR noding schematic in **Figs. 2-1 and 2-2**. With regard to the valve junction components, the tag names for trip valve, motor valve, and servo valve are TRP, MTR, and SRV, respectively.

Junction area, volume flow area, and volume of volume for loop-A are three times as large as those for loop-B. This is because loop-A and loop-B simulate three loops and one loop, respectively.

(1) The single-volume components are applied to the following; vessel DC, lower plenum, upper plenum, upper head, SG inlet, SG outlet, SG steam dome, SG steam line, ACC system, ECCS line, and environment.

(2) The time-dependent volume components are applied to the following; connection to SG steam line, connection to SG AFW line, connection to SG main feedwater line, connection to SG relief valve, connection to SG safety valve, connection to PZR PORV, connection to PZR safety valve, connection to HPI system, connection to LPI system, and connection to environment.

(3) The single-junction components are applied to the following; core inlet to core bypass, core bypass to upper plenum, CRGT to upper plenum, upper head to CRGT, hot leg to

SG inlet, SG inlet to SG inlet plenum, SG inlet plenum to SG U-tube, SG U-tube to SG outlet plenum, SG outlet plenum to SG outlet, SG outlet to COL downflow side, SG DC to SG riser, SG riser to SG steam dome, PZR to its surge line, and environment.

(4) The time-dependent junction components are applied to the SG AFW line, SG main feedwater line, and HPI and LPI systems.

(5) The pipe components are applied to the following; core, core bypass, upper head, CRGT, hot leg, SG inlet plenum, SG U-tube, SG outlet plenum, COL downflow side, COL upflow side, cold leg, SG riser, PZR surge line, PZR, and PZR spray line.

(6) The annulus components are applied to the vessel DC and SG DC.

(7) The branch components are applied to the following; vessel DC, lower plenum, core inlet, core exit, upper plenum, upper head, bypass flow path between vessel DC and hot leg, hot leg, cold leg, SG steam dome, SG steam line, ACC system, and ECCS line.

(8) The separator component is applied to the SG separator.

(9) The pump component is applied to the reactor coolant pump.

(10) The ACC component is applied to the ACC tank.

(11) The valve types in the valve junction components employed comprise trip, motor, and servo. The trip valves are applied to the following; SG relief valve, SG safety valve, PZR spray line valve, PZR PORV, PZR safety valve, ACC tank outlet valve, cold leg in loop-B, and break at cold leg in loop-B. The motor valves are applied to the SG MSIV and SG steam line valve. The servo valve is applied to the PZR spray line valve.

E. Heat structure input

The heat structure geometry types are cylindrical, rectangular, or spherical.

(1) The cylindrical geometry is applied to the following; high-power, mean-power, and low-power fuel rods, vessel DC wall, upper head wall, upper core support plate, core barrel, vessel DC internals, lower plenum support, core exit internals, CRGT, control rod, hot leg, SG tube sheet, SG U-tube, COL, reactor coolant pump, cold leg, SG wall, SG DC shroud, SG riser wall, SG internals, PZR surge line, PZR vessel, and PZR heater.

(2) The rectangular geometry is applied to the upper core support plate, lower core support plate, core baffle plate, SG plate, and SG internals.

(3) The spherical geometry is applied to the lower plenum shell, upper head wall, SG inlet, SG inlet plenum, SG outlet plenum, SG outlet, and PZR shell.

The boundary condition for each heat structure geometry number is chosen length, surface area, or factor. The boundary condition for cylindrical and rectangular geometry is selected either the length or the surface area. On the other hand, the boundary condition for spherical

geometry is chosen the factor, considering the actual geometry of the spherical equipment.

As for the left and right boundary numbers of heat structure geometry number, the length, surface area, and factor for loop-A are three times as large as those for loop-B. The reason is that loop-A and loop-B simulate three loops and one loop, respectively.

F. Heat structure thermal property data

Tables that indicate temperature versus thermal conductivity, and volumetric heat capacity (namely, specific heat times density) are prepared in accordance with the requirements for the heat structure thermal property data for each composition. The tables are prepared for compositions such as magnesium oxide, nichrome, stainless steel, calcium silicate as insulator, helium gas in gap, and Inconel 600. In addition, the thermal data stored in the RELAP5 code program are used for other compositions such as carbon steel, uranium dioxide, and zirconium.

G. General table data

The general table data are as follows. The relationship is provided between the SG secondary narrow-range liquid level and the estimated value. The control value, computed based on the difference between PZR pressure and PZR reference pressure (15.5 MPa as the PZR initial pressure), versus PZR proportional heater power is depicted. The heat transfer coefficient of environment (containment) is kept constant at 5 $W/m^2 \cdot K$ as a general heat transfer coefficient for natural convection [23][24]. The scram reactivity is defined as a function of the time following the reactor scram, which is evaluated based on the reactivity curve described in the FSAR of the US Prairie Island Nuclear Generating Plant Units [21].

H. Reactor kinetics input

The reactor thermal power is calculated by utilizing the point reactor kinetics model with the ANS73 decay heat curve. The Doppler reactivity is evaluated based on the reactivity curve described in the FSAR of the US Surry Power Plant Units [19]. The moderator density reactivity is estimated on the basis of the WCAP-8330 reactivity curve [20]. The heat structure weighting factor for the Doppler feedback is given, which refers to the number of heater rods, the radial and axial power peaking factors in the LSTF. The volume weighting factor for density feedback for each of nine vertically divided volumes of the core is adjusted to 0.11111.

I. Control system input data

The control components employed with the self-initialization option are composed of various types; sum, integrating, unit trip, multiplier, lag, and functional. Operations including addition, integration, and multiplication of variables are conducted in the sum component, integrating

component, and multiplier component, respectively. Trip number, lag time, and general table number are used in the unit trip component, lag component, and functional component, respectively. The control system input data related to the PZR heater include the control components on the PZR liquid volume, difference between PZR pressure and PZR reference pressure, PZR heater power, on/off signal for PZR heater, and reactor scram signal. The control system input data comprise the control components on the SG secondary narrow-range liquid level and the opening degree of the SG main feedwater valve, and the liquid levels of the core, vessel DC, and SG secondary wide-range.

2.3 Steady-State Analysis

Steady-state analysis was implemented making use of the RELAP5/MOD3.3 code to verify that the calculated values meet the specified values of the typical PWR primary and secondary system parameters prior to the LBLOCA onset, taking advantage of the prepared input data. **Table 2-1** compares the specified value and convergence value for each estimation parameter in the steady-state analysis. The convergence value was defined to be a null transient value, which represents the calculation result after 100 s, to correctly judge the steady-state. Except for the early stage of the null transient, each estimation parameter exhibited a nearly constant value. The estimation parameters were broadly divided into the primary system parameter and the secondary system parameter. The primary system parameters included the reactor thermal power, primary loop flow rate, primary pressure, PZR liquid level, hot leg fluid temperature, cold leg fluid temperature, core flow rate, core bypass flow rate, bypass flow rate between vessel DC and hot leg, and bypass flow rate between vessel DC and upper head. The secondary system parameters contained the secondary pressure, SG secondary-side narrow-range liquid level, and SG main feedwater flow rate. The PZR pressure and SG steam dome pressure are employed to represent the primary and secondary pressures, respectively. Individual estimation parameters in the RELAP5 code are specified by variable parameters in **Table 2-1**. The variable codes of ‘rktpow’, ‘mflowj’, ‘p’, and ‘tempf’ are utilized to indicate the total reactor power, junction combined liquid and vapor flow rate, volume pressure, and volume liquid temperature, respectively. The variable ‘cntrlvar’ signifies the command for the control variable.

As presented in **Table 2-1**, the convergence values in the steady-state analysis generally matched the specified values for individual estimation parameters. Consequently, the steady-state calculation with the RELAP5/MOD3.3 code was confirmed to be valid.

Table 2-1 Comparison of specified value and convergence value for each estimation parameter in steady-state analysis

Estimation parameter	Specified value	Convergence value*	Variable parameter in RELAP5 code
Reactor thermal power (MW)	3423	3423.0	rktpow 0 / 10^6
Primary loop flow rate			
Loop-A / 3 (kg/s)	4157	4156.7	mflowj 104040000 / 3
Loop-B (kg/s)	4157	4156.7	mflowj 104030000
Primary pressure (MPa)	15.5	15.48	p 610010000 / 10^6
PZR liquid level (%)	58.6	58.55	cntrlvar 612**
Hot leg fluid temperature			
Loop-A (K)	598	598.1	tempf 406010000
Loop-B (K)	598	598.1	tempf 206010000
Cold leg fluid temperature			
Loop-A (K)	562	562.0	tempf 448010000
Loop-B (K)	562	562.0	tempf 248010000
Core flow rate (kg/s)	15873	15846.1	mflowj 132010000
Core bypass flow rate (kg/s)	700.7	699.82	mflowj 123000000
Bypass flow rate between vessel DC and hot leg			
Loop-A / 3 (kg/s)	13.5	13.49	mflowj 402010000 / 3
Loop-B (kg/s)	13.5	13.48	mflowj 202010000
Bypass flow rate between vessel DC and upper head (kg/s)	27	27.0	mflowj 104010000
Secondary pressure			
Loop-A (MPa)	6.1	6.10	p 516010000 / 10^6
Loop-B (MPa)	6.1	6.10	p 316010000 / 10^6
SG secondary narrow-range liquid level			
Loop-A (%)	44	44.1	cntrlvar 508**
Loop-B (%)	44	44.1	cntrlvar 308**
SG main feedwater flow rate			
Loop-A / 3 (kg/s)	466.6	466.14	mflowj 561000000 / 3
Loop-B (kg/s)	466.6	466.10	mflowj 361000000

* Null transient value which represents calculation result after 100 s

** See **Appendix A** for control system input data

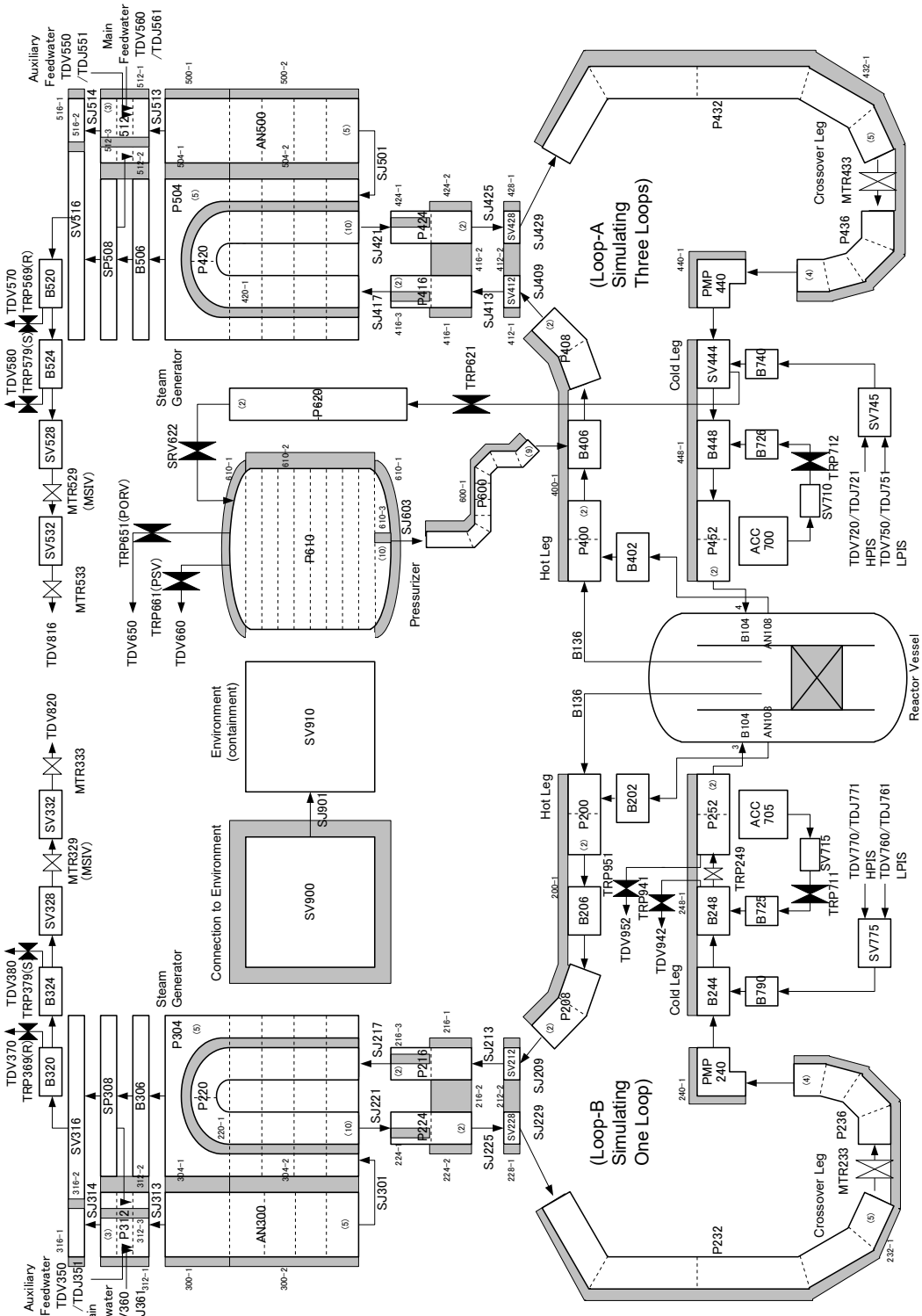

Fig. 2-1 Noding schematic of overall PWR system

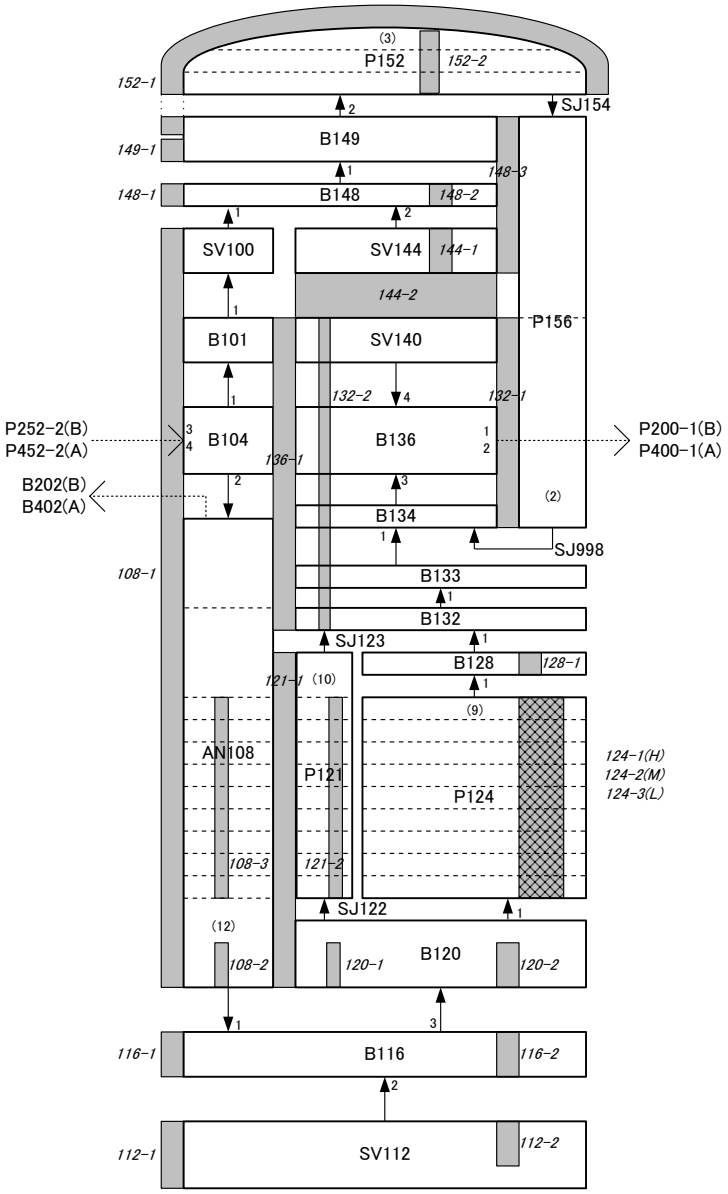

Fig. 2-2 Noding schematic of PWR reactor vessel portion

3. Loss of ECCS Recirculation Functions Event Analysis with RELAP5 Code

3.1 Outline of Loss of ECCS Recirculation Functions Event

Loss of ECCS recirculation functions event in the cold leg LBLOCA is one of events that should be assessed the measures effectiveness against severe core damage. Loss of ECCS recirculation functions is represented by loss of both high-pressure and low-pressure recirculation features in the cold leg LBLOCA where operators have less grace time to provide alternative recirculation water injection compared to smaller break LOCAs. The primary pressure rapidly lowers to near-atmospheric pressure after the break, while the SG secondary-side liquid level remains at a certain high liquid level. Cold water is injected from ECCS into both cold legs shortly after the break. Liquid droplets evaporate in the SG U-tubes on account of heating from the SG secondary-side. The pressure drop increase in the SG U-tubes is ascribed to the steam production, which may bring about a decrease in the core liquid level and a rise in the fuel rod cladding surface temperature. The steam binding phenomenon induced the core liquid level to depress several meters below the vessel DC liquid level in the previous study's calculation for the loss of ECCS recirculation functions event utilizing the RELAP5/MOD3.3 code [13]. By contrast, the electric power company's analysis with the MAAP code overestimated the core liquid level on account of no consideration of the pressure drop in the SG U-tubes, producing that the core uncovery was delayed compared to the previous study's calculation [25]. After the ECCS water sources deplete, failure to switch to alternative recirculation water injection causes to cease the water injection into the core. As an alternative method to the ECCS recirculation features, water is fed into the cold leg via the containment recirculation sump by operating the spray pump for the containment (as illustrated in **Fig. 3-1**). The ECCS recirculation functions can be maintained by exploiting the containment spray pump.

3.2 Transient Analysis for Loss of ECCS Recirculation Functions Event

The validity of the present transient analysis is confirmed by comparison with the previous study's calculation for the loss of ECCS recirculation functions event making use of the RELAP5/MOD3.3 code [13]. The previous study's calculation used standard data that have been developed for Japan's three-loop PWR plant with a reactor thermal power of 2652 MW. The standard data were based on the application for permission to make changes to the nuclear reactor installation. The characteristics of the major parameters involved in the loss of ECCS recirculation functions event gained from the previous study's calculation are comparable to those provided by the nuclear operator's calculation. The present transient analysis assumed that the ECCS water injection stops 1140 s after the break, in accordance with the previous study's calculation. The alternative recirculation water injection was assumed to initiate when the fuel rod cladding surface temperature rose to above 800 K due to the ECCS water injection stop, with reference to the previous study's calculation. Based on this

assumption, the alternative recirculation water injection was begun 440 s after stopping the ECCS water injection. The alternative recirculation water injection flow rate was set to the total flow rate of the HPI and LPI systems owing to the lack of its public information. **Table 3-1** depicts the variable parameter in the RELAP5 code for each estimation parameter in the transient analysis. With regard to the fuel rod cladding surface temperature, the variable parameter is the heat structure geometry number, which is followed by a two-digit mesh point number to indicate the variable code of 'httemp' is the mesh point temperature.

The results of the major parameters were compared between the present transient analysis and the previous study's calculation until the initiation of core uncovery caused by the ECCS water injection stop from the start of the break. The major parameters included the core and vessel DC liquid levels on the basis of the reactor vessel bottom, as well as the fuel rod cladding surface temperatures. In both analyses, the liquid level in the core became lower than that in the vessel DC due to the steam binding until the ECCS water injection stop after the core reflooding onset (**Fig. 3-2**). The core and vessel DC liquid levels gradually declined after the ECCS water injection stop. The liquid level difference reached zero by the time the core was uncovered. The liquid level difference between the core and vessel DC was somewhat higher in the present transient analysis than in the previous study's calculation. In both analyses, the differential pressure between the upper plenum and SG outlet plenum was slightly higher than that between the upper plenum and SG inlet plenum because the SG inlet pressure was a little bit higher than the SG outlet pressure (**Fig. 3-3**). Both analyses revealed that the maximum cladding surface temperature during the reflood phase was higher than that during the blowdown phase (**Figs. 3-4 and 3-5**) because the core liquid level recovered more slowly. The cladding surface temperature tendencies are similar to the conclusions obtained from the OECD/NEA BEMUSE program [7][8]. The maximum cladding surface temperatures during the reflood phase and blowdown phase were 1274 K and 1127 K, respectively, in the present transient analysis. On the other hand, they were about 1190 K and 1100 K, respectively, in the previous study's calculation. The reason was that the ECCS flow rate was lower in the present transient analysis than in the previous study's calculation, which produced a lower liquid level in the core. The maximum cladding surface temperatures during the reflood phase and blowdown phase were well below the allowable limit of 1473 K. This implies that the ECCS water injection should be effective in cooling the core. The whole core was quenched by means of the ECCS water injection during the reflood phase. Although the major parameters had some discrepancies between the present transient analysis and the previous study's calculation, the overall trends were consistent qualitatively. Thus, the present transient analysis was confirmed to be proper generally.

In the present transient analysis, the reactor thermal power drastically dropped following a reactor scram signal (**Fig. 3-6**). The reactor scram signal and SI signal were generated at 4 s

and 5 s, respectively, because of a sudden decrease in the primary pressure (**Fig. 3-7**). The ACC system was activated for a duration of 4 to 21 s. The HPI and LPI systems were actuated at 5 s and 24 s, respectively. The primary pressure fell to near-atmospheric pressure, while a gradual reduction appeared in the secondary pressure. The secondary pressure was lower in loop-B than in loop-A according to the pressures of the primary loops. As plotted in **Fig. 3-8**, the SG secondary narrow-range liquid level degraded on account of the termination of SG main feedwater following the reactor scram signal, and gradually restored because of the AFW injection into the SG secondary-side. At around 300-450 s, a temporary drop appeared in the SG secondary narrow-range liquid level in loop-B, even though the AFW flow rate was kept constant. The reason was that a decrease in the SG secondary fluid temperature was greater in loop-B than in loop-A, relying on the SG primary fluid temperature. The SG secondary narrow-range liquid level was finally held at about 42-44 %. During that period, the SG secondary wide-range liquid level was maintained at about 12.7 m, which was above the SG U-tube height (**Fig. 3-9**).

3.3 Sensitivity Analyses for Loss of ECCS Recirculation Functions Event

Sensitivity analyses were performed to investigate the impacts of Cd through the break and the alternative recirculation water injection flow rate on the fuel rod cladding surface temperature, focusing on the cold leg LBLOCA. The transient analysis conditions denoted in **Section 3.2** were defined as the conditions of the base case employed for the sensitivity analyses. In the base case, specifically, the Cd through the break was 1.0 and the alternative recirculation water injection flow rate was the total flow rate of the HPI and LPI systems. The maximum cladding surface temperature during the alternative recirculation water injection was 942 K in the base case, which resulted in higher than the previous study's calculation of about 880 K [13] due to lower flow rate of the alternative recirculation water injection. **Table 3-2** lists the conditions of the sensitivity analyses. The Cd through the break was adjusted to 1.0, 0.6, or 0.4, with reference to the past studies on spectrum analysis of the cold leg LBLOCA which examined the effects on the fuel rod cladding surface temperature [26][27]. The smaller Cd through the break is, the smaller the break flow rate is. The alternative recirculation water injection flow rate was assumed to be equivalent to the total flow rate, 1/2 of the total flow rate, or 1/3 of the total flow rate of the HPI and LPI systems. This may cover the flow rate ranges of the alternative recirculation water injection as widely as possible, while keeping no excessive rise in the fuel rod cladding surface temperature.

Under the alternative recirculation water injection flow rate equivalent to the total flow rate of the HPI and LPI systems, the core and vessel DC liquid levels on the basis of the reactor vessel bottom when the Cd through the break is 1.0, 0.6, and 0.4, respectively, are indicated in **Figs. 3-2, 3-10, and 3-11**. In the Cd of 0.4 especially, the core and vessel DC liquid levels

oscillated until the ECCS water injection stopped. This gave rise to several relatively large drops in the core liquid level, which led to an increase in the fuel rod cladding surface temperature. The core and vessel DC liquid levels recovered rapidly after the alternative recirculation water injection onset, which produced the entire core being quenched.

Under the alternative recirculation water injection flow rate equivalent to the total flow rate of the HPI and LPI systems, the fuel rod cladding surface temperatures at Positions 9-5 when the Cd through the break is 1.0, 0.6, and 0.4, respectively, are shown in **Figs. 3-4, 3-12, and 3-13**. The fuel rod cladding surface temperatures at Positions 4-1 when the Cd through the break is 1.0, 0.6, and 0.4, respectively, are given in **Figs. 3-5, 3-14, and 3-15**. Positions 9, 5, and 1 correspond to the top, center, and bottom of the core, respectively. The maximum cladding surface temperature appeared at Positions 5 or 6, which was 1.6-2.0 m or 2.0-2.4 m above the core bottom. This was attributed to the axial core power profile (i.e., the 9-step chopped cosine) and the behavior of the core liquid level. Other cladding surface temperatures from the top to the center of the core were higher in the order of Position 7, 8, and 9. The cladding surface temperatures from the center to the bottom of the core were higher in the order of Positions 4, 3, 2, and 1. As set out in **Table 3-2**, the maximum cladding surface temperatures until the stop of the ECCS water injection were 1274 K, 1153 K, and 904 K when the Cd through the break was 1.0, 0.6, and 0.4, respectively. The smaller Cd through the break was, the lower the maximum cladding surface temperatures were, due to the smaller break flow rate. On the other hand, the maximum cladding surface temperatures during the alternative recirculation water injection were 942 K, 1010 K, and 661 K when the Cd through the break was 1.0, 0.6, and 0.4, respectively. The maximum cladding surface temperature in the Cd of 0.6 was higher than that in the Cd of 1.0. The reason was that the core became completely empty of liquid with the primary pressure decrease following the ECCS water injection stop in the Cd of 0.6, resulting in a slower recovery speed of the core liquid level after the alternative recirculation water injection onset. The maximum cladding surface temperature was the lowest in the Cd of 0.4. The reason was that the time until the alternative recirculation water injection initiation after the core uncovery onset was shorter because the core uncovery was slightly delayed owing to the smaller break flow rate in the Cd of 0.4.

Additionally, the relationship between the alternative recirculation water injection flow rate and the fuel rod cladding surface temperature during the alternative recirculation water injection was surveyed, as stated in **Table 3-2**. The maximum cladding surface temperatures during the alternative recirculation water injection in terms of the alternative recirculation water injection flow rates when the Cd through the break is 1.0, 0.6, and 0.4, respectively, are presented in **Figs. 3-16, 3-17, and 3-18**. The maximum cladding surface temperatures during the alternative recirculation water injection were 1040 K, 1066 K, and 780 K when the Cd through the break was 1.0, 0.6, and 0.4, respectively, under the alternative recirculation water

injection flow rate equivalent to 1/2 of the total flow rate of the HPI and LPI systems. On the other hand, they were 1082 K, 1142 K, and 923 K when the Cd through the break was 1.0, 0.6, and 0.4, respectively, under the alternative recirculation water injection flow rate equivalent to 1/3 of the total flow rate of the HPI and LPI systems. The maximum cladding surface temperature during the alternative recirculation water injection was the highest in the Cd of 0.6. The lower the alternative recirculation water injection flow rate, the higher the maximum cladding surface temperature during the alternative recirculation water injection.

Table 3-1 Variable parameter in RELAP5 code for each estimation parameter in transient analysis

Estimation parameter	Variable parameter in RELAP5 code	Estimation parameter	Variable parameter in RELAP5 code
Core liquid level (m)	cntrlvar 125*	SG wide-range liquid level (loop-A) (m)	cntrlvar 512*
Vessel DC liquid level (m)	cntrlvar 109*	SG wide-range liquid level (loop-B) (m)	cntrlvar 312*
Upper plenum pressure (MPa)	p 132010000 / 10^6	Cladding surface temp. (Position 9) (K)	httemp 124100908
SG outlet pressure (loop-A) (MPa)	p 420100000 / 10^6	Cladding surface temp. (Position 8) (K)	httemp 124100808
SG inlet pressure (loop-A) (MPa)	p 420010000 / 10^6	Cladding surface temp. (Position 7) (K)	httemp 124100708
Reactor thermal power (MW)	rktpow 0 / 10^6	Cladding surface temp. (Position 6) (K)	httemp 124100608
Primary pressure (MPa)	p 610010000 / 10^6	Cladding surface temp. (Position 5) (K)	httemp 124100508
Secondary pressure (loop-A) (MPa)	p 516010000 / 10^6	Cladding surface temp. (Position 4) (K)	httemp 124100408
Secondary pressure (loop-B) (MPa)	p 316010000 / 10^6	Cladding surface temp. (Position 3) (K)	httemp 124100308
SG narrow-range liquid level (loop-A) (%)	cntrlvar 508*	Cladding surface temp. (Position 2) (K)	httemp 124100208
SG narrow-range liquid level (loop-B) (%)	cntrlvar 308*	Cladding surface temp. (Position 1) (K)	httemp 124100108

* See **Appendix A** for control system input data

Table 3-2 Sensitivity parameters and maximum cladding surface temperatures in sensitivity analyses

Case	Parameter		Maximum cladding surface temperature	
	Cd through break	Water injection flow rate of alternative recirculation	Until stop of ECCS water injection	During alternative recirculation water injection
Base Case	1.0	Total flow rate*	1274 K	942 K
Case A	0.6	Total flow rate	1153 K	1010 K
Case B	0.4	Total flow rate	904 K	661 K
Case C	1.0	1/2 of total flow rate	1274 K	1040 K
Case D	1.0	1/3 of total flow rate	1274 K	1082 K
Case E	0.6	1/2 of total flow rate	1153 K	1066 K
Case F	0.6	1/3 of total flow rate	1153 K	1142 K
Case G	0.4	1/2 of total flow rate	904 K	780 K
Case H	0.4	1/3 of total flow rate	904 K	923 K

* Total flow rate of HPI and LPI systems

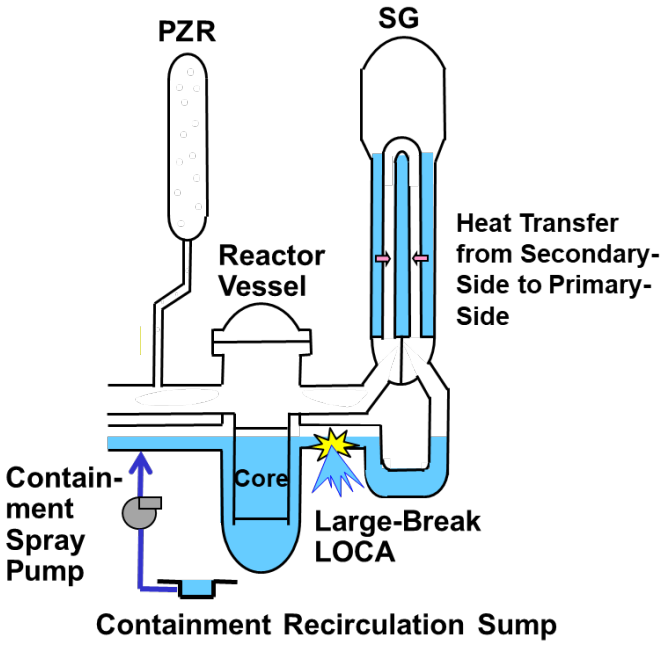

Fig. 3-1 PWR coolant distribution in loss of ECCS recirculation functions event

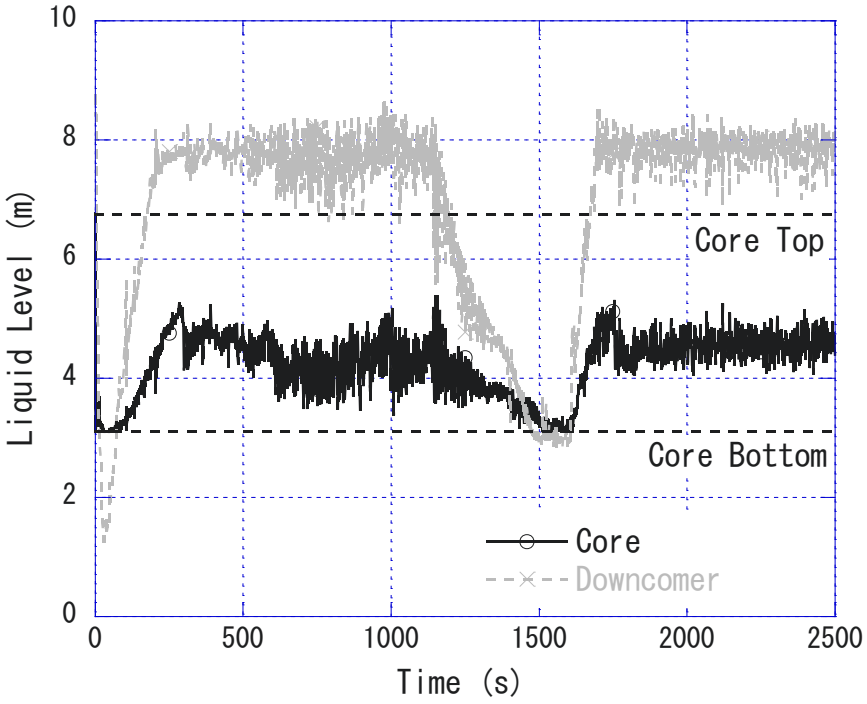

Fig. 3-2 Core and vessel downcomer liquid levels (Base Case)

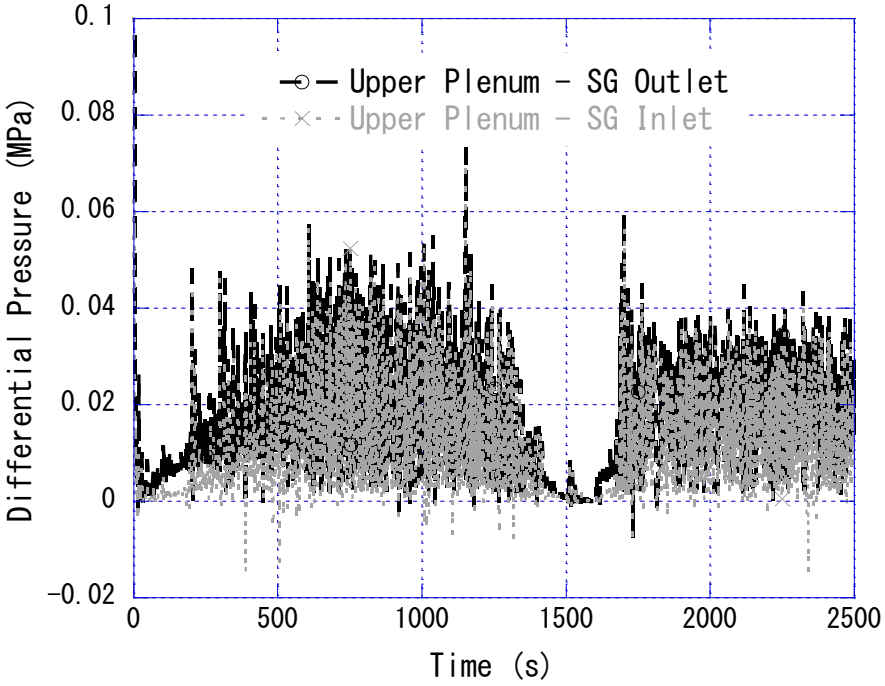

Fig. 3-3 Differential pressure between upper plenum and SG portion (Base Case)

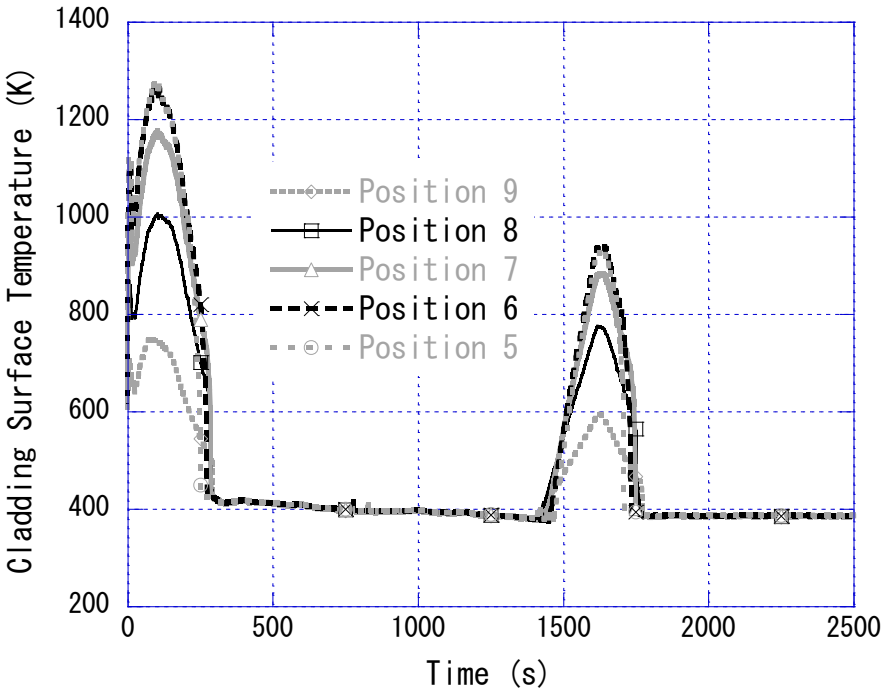

Fig. 3-4 Fuel rod cladding surface temperatures through Positions 9-5 (Base Case)

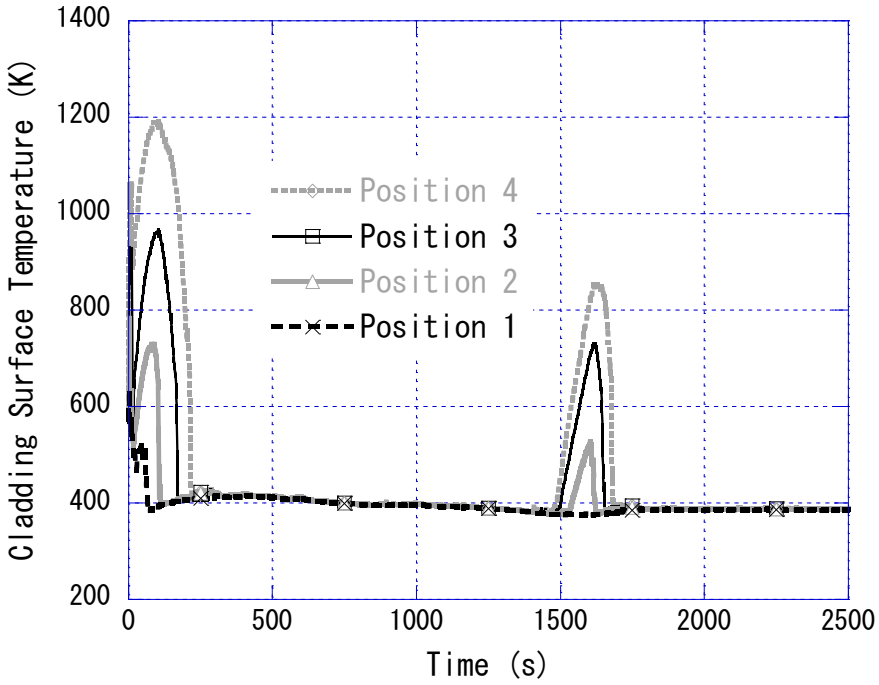

Fig. 3-5 Fuel rod cladding surface temperatures through Positions 4-1 (Base Case)

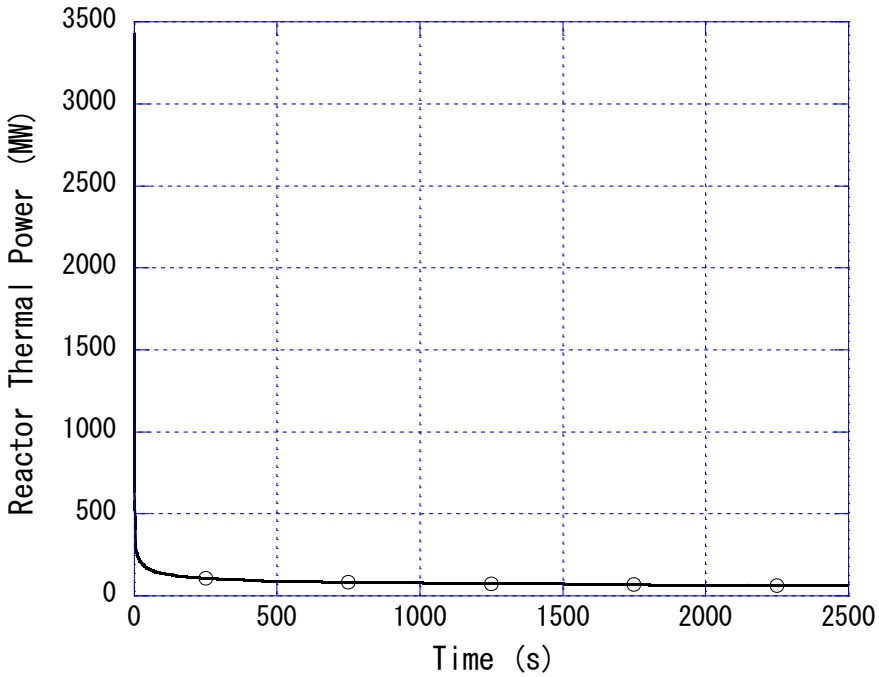

Fig. 3-6 Reactor thermal power (Base Case)

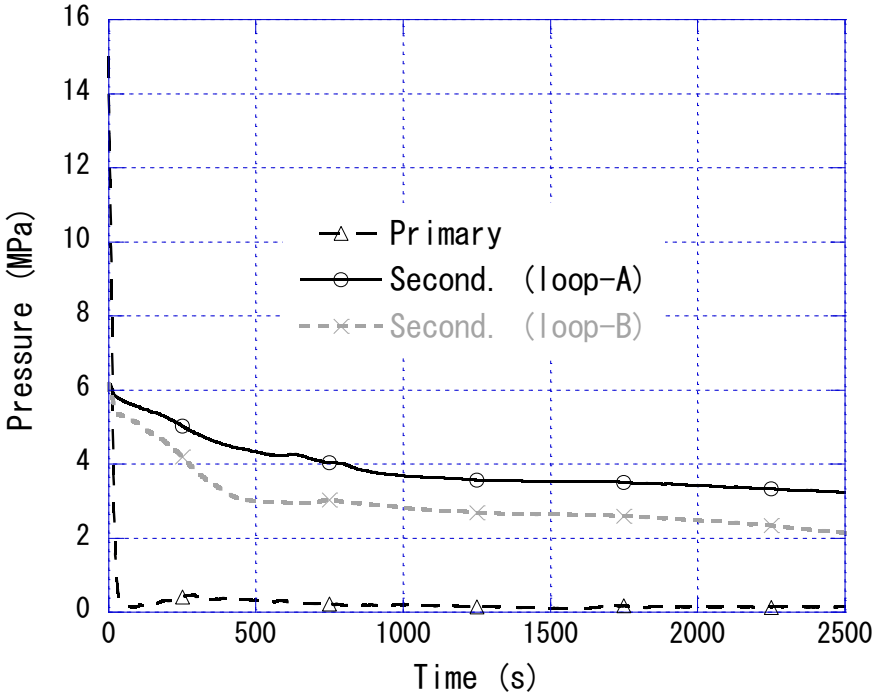

Fig. 3-7 Primary and secondary pressures (Base Case)

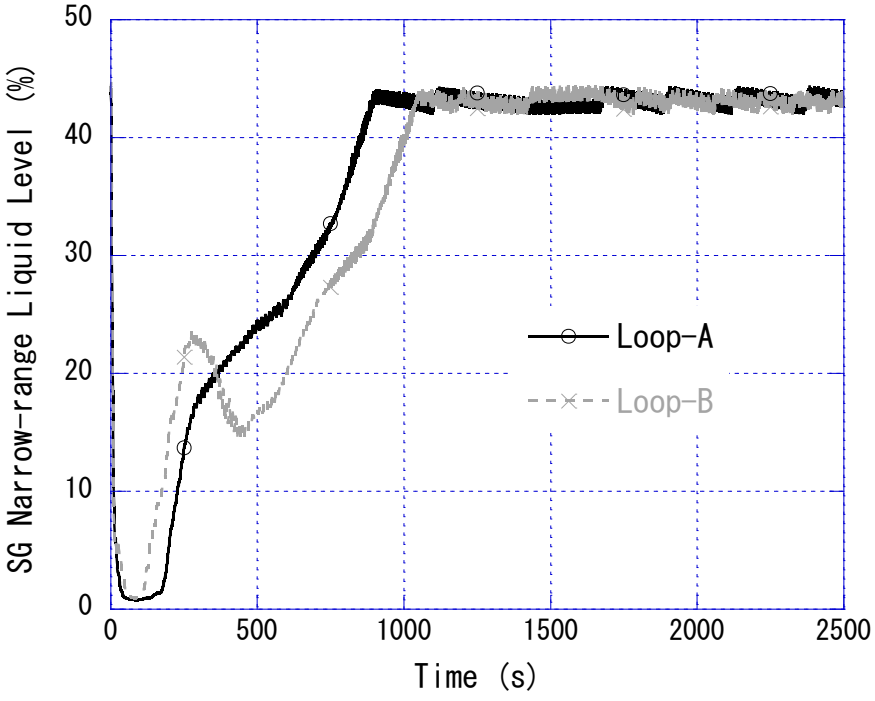

Fig. 3-8 SG secondary narrow-range liquid levels (Base Case)

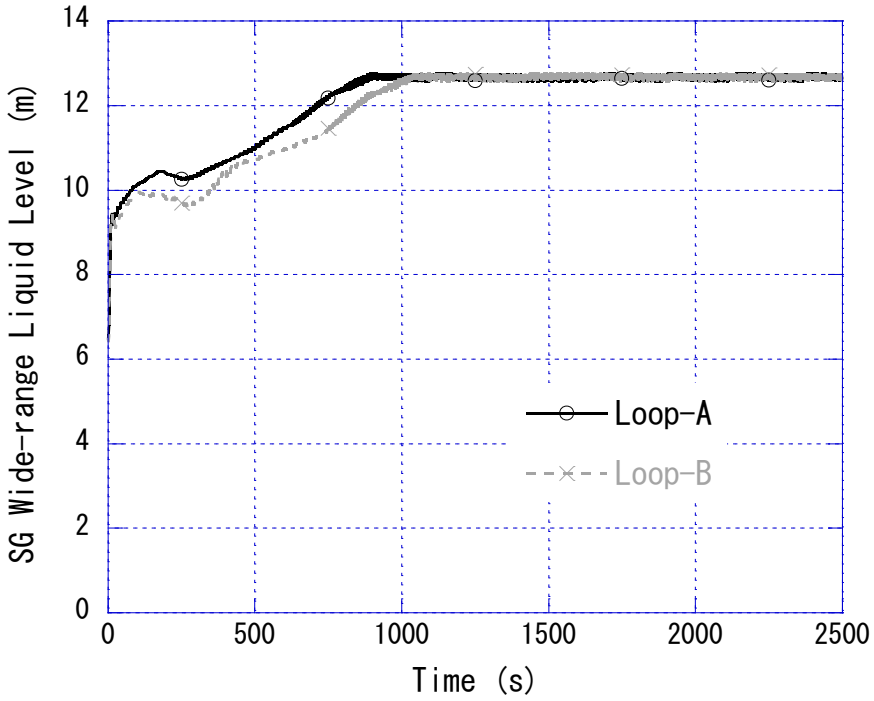

Fig. 3-9 SG secondary wide-range liquid levels (Base Case)

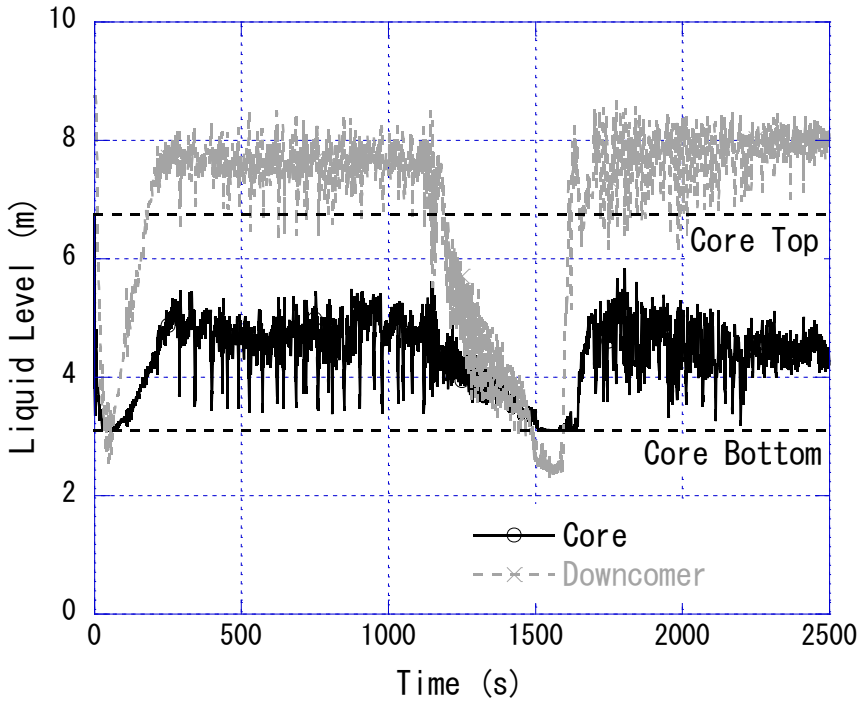

Fig. 3-10 Core and vessel downcomer liquid levels (Cd = 0.6; Case A)

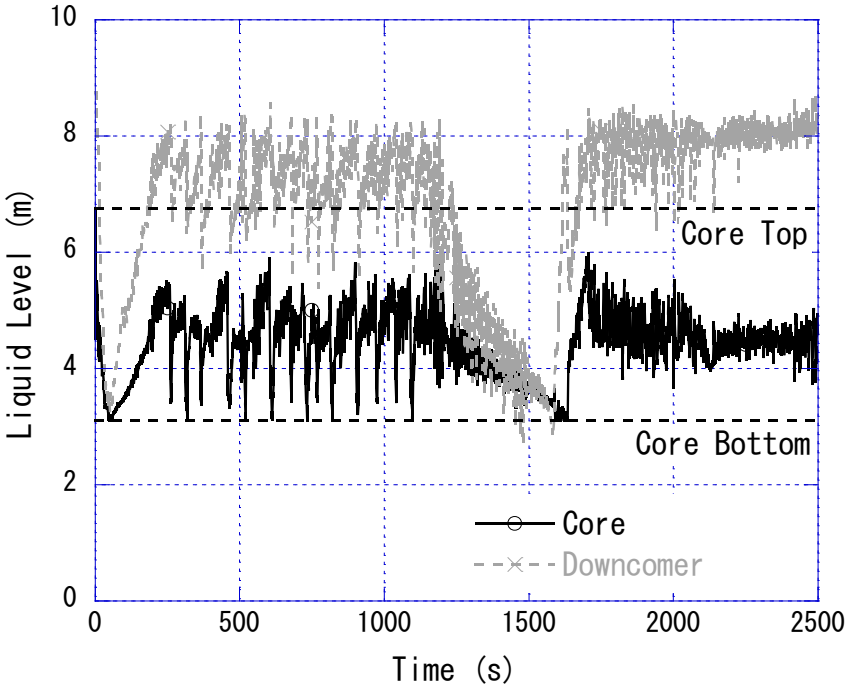

Fig. 3-11 Core and vessel downcomer liquid levels (Cd = 0.4; Case B)

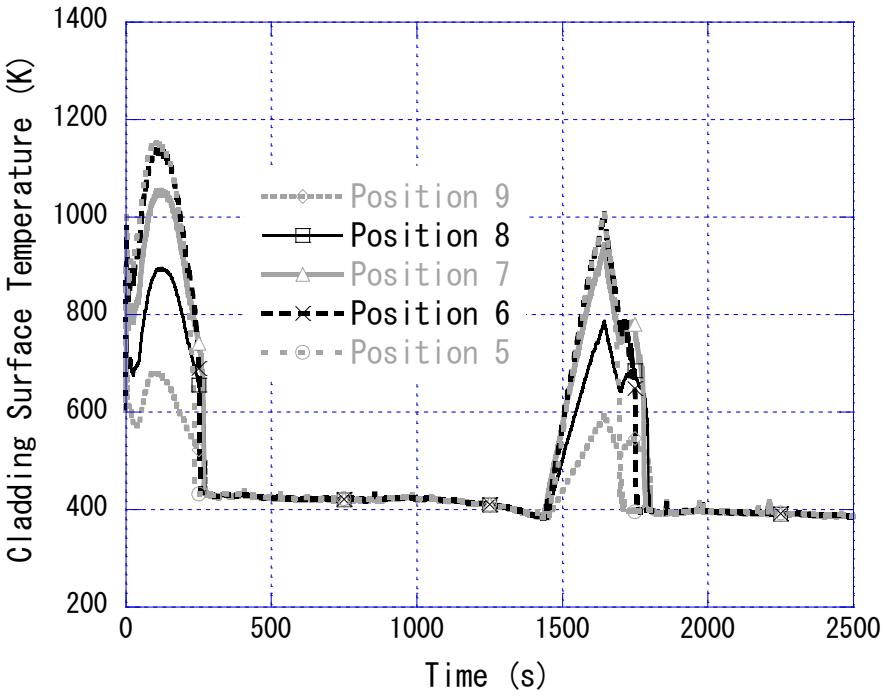

Fig. 3-12 Fuel rod cladding surface temperatures through Positions 9-5 (Cd = 0.6; Case A)

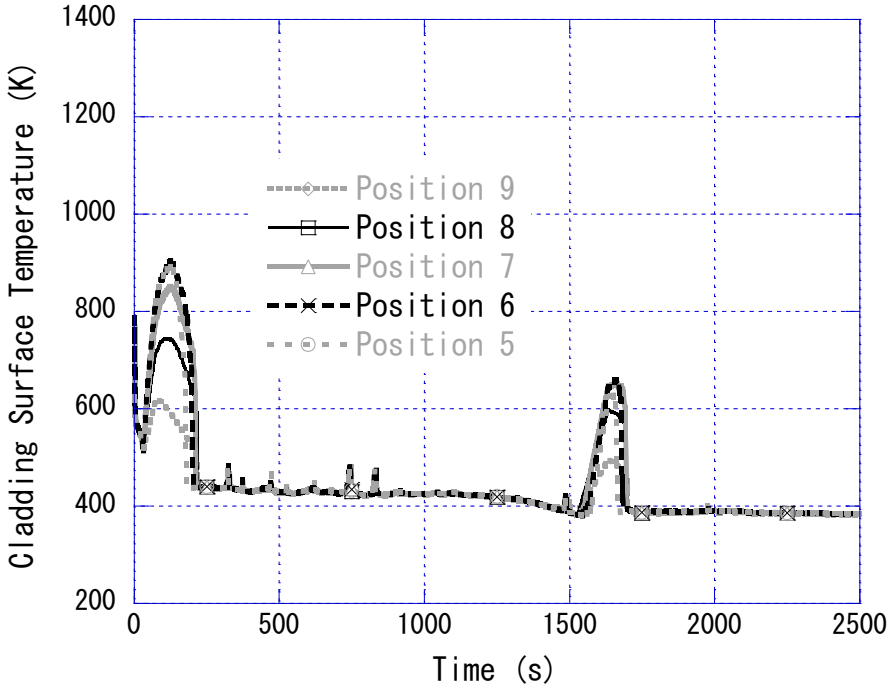

Fig. 3-13 Fuel rod cladding surface temperatures through Positions 9-5 (Cd = 0.4; Case B)

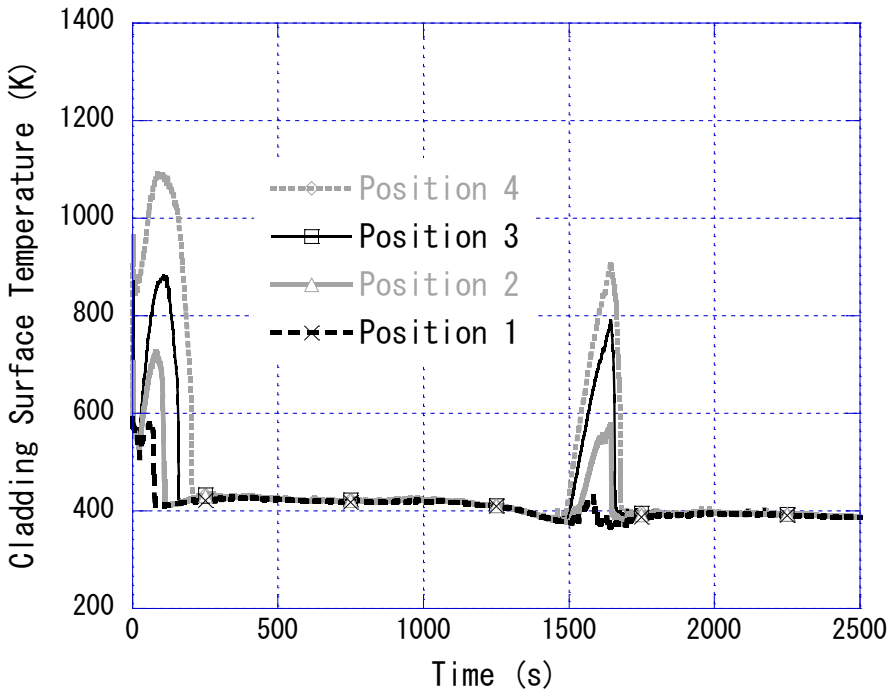

Fig. 3-14 Fuel rod cladding surface temperatures through Positions 4-1 (Cd = 0.6; Case A)

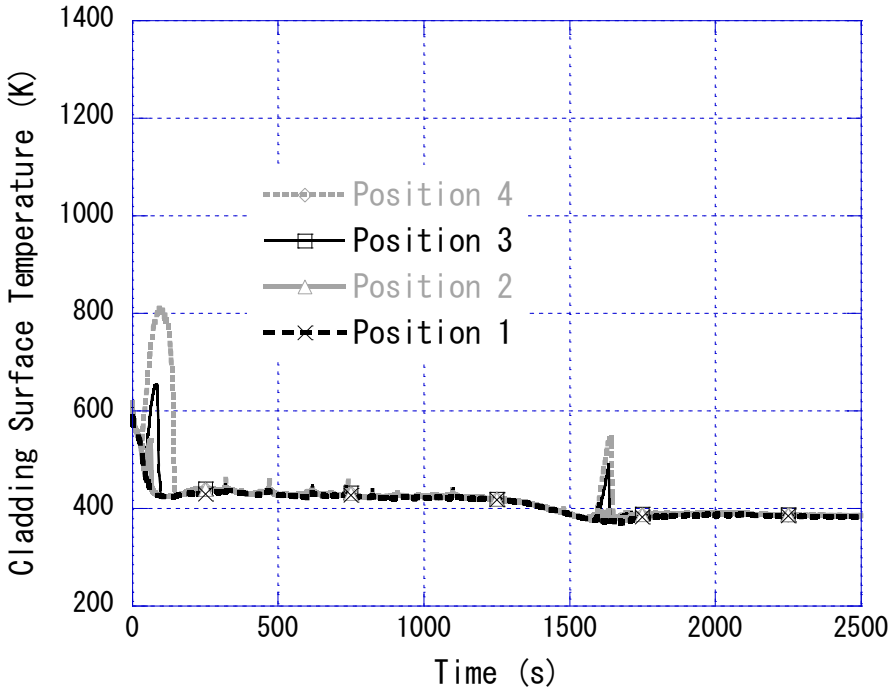

Fig. 3-15 Fuel rod cladding surface temperatures through Positions 4-1 (Cd = 0.4; Case B)

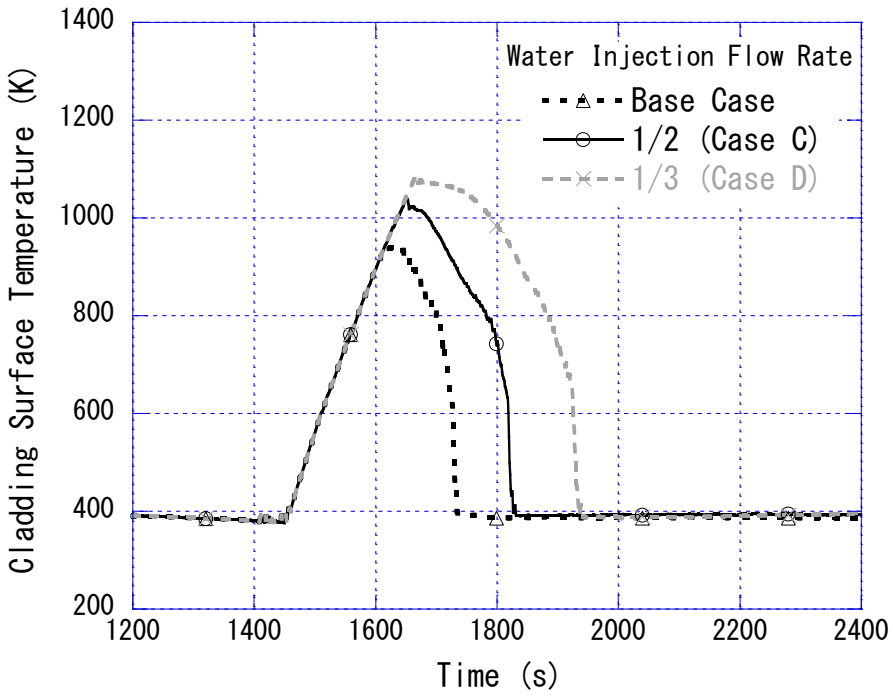

Fig. 3-16 Alternative recirculation water injection flow rate versus maximum cladding surface temperature (Cd = 1.0; Base Case, Cases C and D)

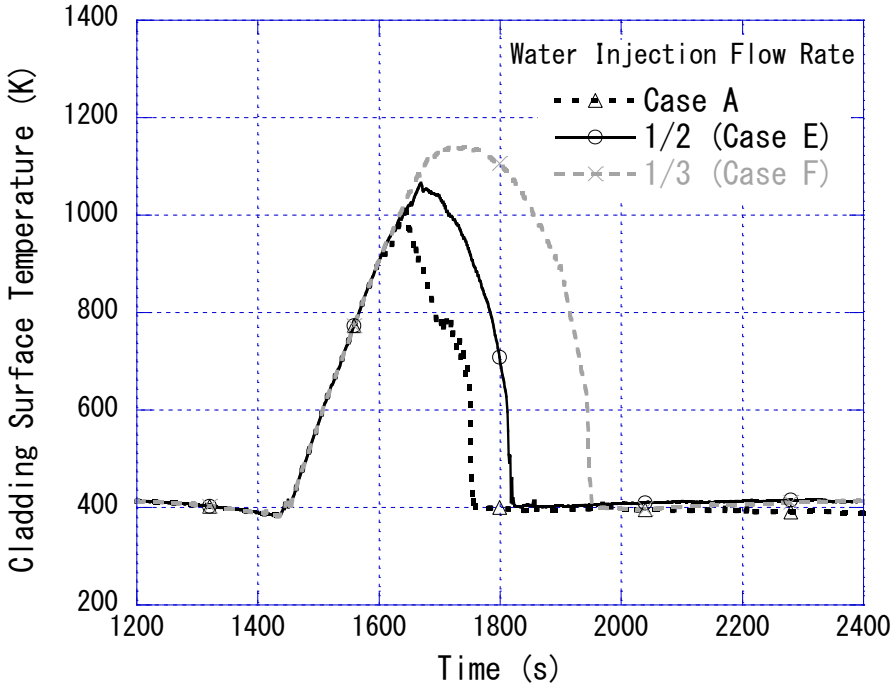

Fig. 3-17 Alternative recirculation water injection flow rate versus maximum cladding surface temperature (Cd = 0.6; Cases A, E and F)

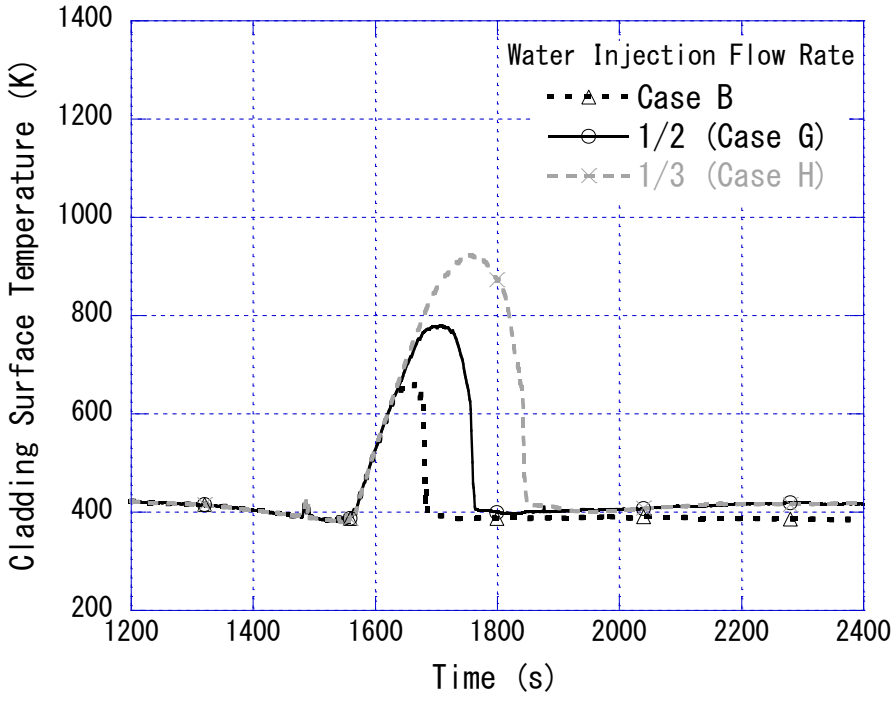

Fig. 3-18 Alternative recirculation water injection flow rate versus maximum cladding surface temperature (Cd = 0.4; Cases B, G and H)

4. Summary

JAEA has been creating input data for the PWR LBLOCA analysis using the RELAP5/MOD3.3 code, mostly on the basis of design information for Tsuruga Unit-2, which is the reference four-loop PWR of the LSTF. The PWR model involved a reactor vessel, PZR, hot legs, SGs, SG secondary-side system, crossover legs, cold legs, and ECCS. The PWR was modeled with two loops in the LBLOCA calculation. The PZR was connected to loop-A, simulating three loops. The break was installed in loop-B, modeling one loop. The node divisions of the PWR components, other than the core bypass region, were analogous to those of the LSTF components.

Steady-state analysis was practiced to ensure that the calculated values satisfy the specified values of the representative parameters of the PWR primary and secondary systems before starting the LBLOCA, leveraging the input data that were developed. The steady-state calculation was valid because the convergence values in the steady-state analysis were generally in line with the specified values.

Transient analysis was executed for the loss of ECCS recirculation functions event in the cold leg LBLOCA. The present transient analysis was compared with the calculation in the previous study exploiting the RELAP5/MOD3.3 code until the initiation of core uncovery induced by the ECCS water injection stop from the break start. Both analyses showed that the liquid level in the core became lower than that in the vessel DC because of the steam binding until the ECCS water injection termination after the core reflooding initiation. In both analyses, the maximum cladding surface temperature was higher during the reflood phase than during the blowdown phase. In addition, the ECCS water injection brought about the entire core being quenched during the reflood phase. The results of the major parameters were somewhat different between the present transient analysis and the previous study’s calculation, but the overall tendencies were reproducible qualitatively. Therefore, the present transient analysis was confirmed to be suitable in general.

Moreover, sensitivity analyses were carried out for the loss of ECCS recirculation functions event to identify how the Cd through the break and the alternative recirculation water injection flow rate affect the fuel rod cladding surface temperature. The Cd through the break was fixed to 1.0, 0.6, or 0.4. The alternative recirculation water injection flow rate was settled to be equivalent to the total flow rate, 1/2 of the total flow rate, or 1/3 of the total flow rate of the HPI and LPI systems. The maximum cladding surface temperature until the ECCS water injection stop reduced as the Cd through the break decreased. The maximum cladding surface temperatures during the alternative recirculation water injection were higher in the order of the Cd of 0.6, 1.0, and 0.4. When the alternative recirculation water injection flow rate was lower, the maximum cladding surface temperature during the alternative recirculation water injection

was higher.

The consequences acquired from the transient and sensitivity analyses were the information that served as the basis for deciding the boundary conditions for the LSTF SET concerning the loss of ECCS recirculation functions event.

The content of this report will be helpful in making input data for similar PWR accident analysis scenarios using other computer codes or by coupling them with other computer codes.

Acknowledgement

This study was conducted under the auspices of Nuclear Regulation Authority, Japan (NRA). The author would like to thank the relevant members of CSA of Japan Co., Ltd. for their assistance in creating input data for the PWR LBLOCA analysis with the RELAP5/MOD3.3 code, Dr. M. Sekine of NRA for his useful advice on the code's calculation for the loss of ECCS recirculation functions event, and Drs. Y. Udagawa, J. Katsuyama, and Y. Sibamoto of JAEA for their in-depth discussion about the PWR LBLOCA analysis.

References

[1] The ROSA-V Group, ROSA-V Large Scale Test Facility (LSTF) System Description for the Third and Fourth Simulated Fuel Assemblies, JAERI-Tech 2003-037, 2003, 479p.

[2] Takeda, T., Wada, Y., Sibamoto, Y., Major outcomes through recent ROSA/LSTF experiments and future plans, World Journal of Nuclear Science and Technology, 11, 2021, pp. 17-42.

[3] USNRC, RELAP5/MOD3 Code Manual – User's Guide and Input Requirements, NUREG/CR-5535, INEL-95/0174, Vol. 2, 1995, 344p.

[4] Takeda, T., Asaka, H., Nakamura, H., RELAP5 Analysis of OECD/NEA ROSA Project Experiment Simulating a PWR Loss-of-Feedwater Transient with High-Power Natural Circulation, Science and Technology of Nuclear Installations, 2012, Article ID 957285, 2012, 15p.

[5] Watanabe, T., Kukita, Y., Effects of ECCS and Pressurizer Auxiliary Spray on the Experiment Simulating Mihama Unit-2 Steam Generator U-tube Rupture Incident, Proceedings of the 5th International Topical Meeting on Nuclear Reactor Thermal-Hydraulics, Salt Lake, USA, 1992.

[6] Anoda, Y., Nakamura, H., Watanabe, T., Hirano, M., Kukita, Y., Experimental and Analytical Simulations of the Mihama Unit-2 Steam Generator Tube Rupture Incident, Proceedings of the 1993 Simulation Multiconference (Session on Simulation Approaches to Safety Assessment and Diagnostics), Washington, D.C., USA, 1993, pp. 242-247.

[7] NEA, BEMUSE Phase V Report: Uncertainty and Sensitivity Analysis of a LB-LOCA in ZION Nuclear Power Plant, NEA/CSNI/R(2009)13, 2009, 94p.

[8] Perez, M., Reventos, F., Batet, L., et al., Uncertainty and sensitivity analysis of a LBLOCA in a PWR Nuclear Power Plant: Results of the Phase V of the BEMUSE programme, Nuclear Engineering and Design, 241, 2011, pp. 4206-4222.

[9] Frepoli, C., An Overview of Westinghouse Realistic Large Break LOCA Evaluation Model, Science and Technology of Nuclear Installations, 2008, Article ID 498737, 2008, 15p.

[10] Kaminski, M., Diab, A., Time-Series Forecasting of a Typical PWR Undergoing Large Break LOCA, Science and Technology of Nuclear Installations, 2024, Article ID 6162232, 2024, 16p.

[11] Tregoning, R., Abramson, L., Scott, P., Csontos, A, Estimating Loss-of-Coolant Accident (LOCA) Frequencies Through the Elicitation Process, USNRC Report, NUREG-1829, 2008.

[12] Takeda, T., Ohtsu, I., Nakamura, H., OECD/NEA ROSA Project Experiment on Steam Condensation in PWR Horizontal Legs during Large-Break LOCA, Journal of Energy and Power Engineering, 7, 2013, pp. 1009-1022.

[13] NRA, Analyses of Events for the Evaluation of the Effectiveness of Measures against Severe Core Damage (PWR), NRA Technical Report Series, NTEC-2014-1001, 2014, (in Japanese).

[14] USNRC, Surry Power Plant Units Final Safety Analysis Report 1 and 2, DOCKET 50-280, Part B, Vol.1, 1970.

[15] Kumamaru, H., Hirata, K., Nakamura, H., et al., ROSA-IV/LSTF 5% Cold Leg Break LOCA Experiment Run SB-CL-18 Data Report, JAERI-M 89-027, 1989, 105p.

[16] Veloso, M. A., de Mattos, J. R. L., Polar representation of centrifugal pump homologous curves, Proceedings of the 12th Brazilian Congress of Thermal Engineering and Sciences, Belo Horizonte, MG, Brazil, 2008.

[17] Ransom, V. H., Trapp, J. A., The RELAP5 chocked flow model and application to a large scale flow test, Proceedings of the ANS/ASME/NRC International Topical Meeting on Nuclear Reactor Thermal-Hydraulics, Saratoga Springs, New York, USA, 1980.

[18] Li, D., Liu, X., Yang, Y., Improvement of reflood model in RELAP5 code based on sensitivity analysis, Nuclear Engineering and Design, 303, 2016, pp. 163-172.

[19] ANS, Decay Energy Release Rates Following Shutdown of Uranium Fueled Thermal Reactors, Draft ANS-5.1/N18.6, 1973.

[20] Salvatori, R., Westinghouse anticipated transients without trip analysis, Technical Report WCAP-8330, Westinghouse Electric Corp., 1974.

[21] USNRC, Prairie Island Nuclear Generating Plant Units Final Safety Analysis Report, DOCKET 50-282, 1973.

[22] Yoshihara, K., Current situation of safety assurance measures in the light of Fukushima Daiichi accident taken by Kansai Electric Power Co., Inc., Journal of the Atomic Energy Society of Japan, 54 (7), 2012, pp. 441-446, (in Japanese).

[23] Khalifa, A. J. N., Natural convective heat transfer coefficient – a review: I. Isolated vertical and horizontal surfaces, Energy Conversion and Management, 42 (4), pp. 491-504, 2001.

[24] Khalifa, A. J. N., Natural convective heat transfer coefficient – a review: II. Surfaces in two- and three-dimensional enclosure, Energy Conversion and Management, 42 (4), pp. 505-517, 2001.

[25] Hokkaido Electric Power Company, Severe accident analysis code for evaluating effectiveness of measures against major accidents (Part 3 MAAP), Nuclear Regulatory Authority 58th judging meeting material, 2013 (in Japanese), Available from https://www.hepco.co.jp/energy/atomic/safety_improve/info/pdf/examination_meeting_58_5.pdf (accessed on 2025-1-22).

[26] MAPI, Mitsubishi PWR emergency core cooling system performance evaluation break spectrum analysis, MAPI 1069 MOD1, 1990, 919p., (in Japanese).

[27] Hokkaido Electric Power Company, Responses to issues at Tomari Power Station Unit 3 judging meeting [Confirmation of feasibility: Evaluation of effectiveness of measures against major accidents], Nuclear Regulatory Authority 70th judging meeting material, 2014 (in Japanese), Available from https://www.hepco.co.jp/energy/atomic/safety_improve/info/pdf/examination_meeting_70_2.pdf (accessed on 2025-1-22).

Appendix A List of Main Input Data for PWR LBLOCA Analysis

An attempt is made to overview a list of the main input data, along with the explanations for individual data, for the PWR LBLOCA analysis with the RELAP5/MOD3.3 code. The list of the main input data is divided into the following nine categories;

A. Miscellaneous control cards
B. Time step control cards
C. Trip input data
D. Hydrodynamic components
E. Heat structure input
F. Heat structure thermal property data
G. General table data
H. Reactor kinetics input
I. Control system input data

The RELAP5/MOD3 code manual involving the user's guide and input requirements [A-1] is useful in interpreting the list of the main input data.

Reference

[A-1] USNRC, RELAP5/MOD3 Code Manual – User's Guide and Input Requirements, NUREG/CR-5535, INEL-95/0174, Vol. 2, 1995, 344p.

A. Miscellaneous control cards (cards 1 through 110)

<developmental model control>
option: 50 (Namely, Ransom-Trapp chocked-flow model is employed.)

<problem type and option>
problem type: new (i.e., new simulation problem)
problem option: transnt (i.e., transient simulation)

<input check or run option>
option: run (Namely, problem is executed if no input errors are detected.)

<units selection>
input units: si (i.e., SI units)

<noncondensable gas species>
noncondensable gas type: nitrogen (Namely, nitrogen gas is used as non-condensable gas for pressurization of ACC system of ECCS.)

B. Time step control cards (cards 200 through 299)

time end: 2500.0 s minimum time step: 1.0d-8 maximum time step: 0.002
control option: 3 (i.e., semi-implicit scheme) minor edit and plot frequency: 500

***Note*:** The time end of transient simulation is 2500 s. The quantities edited are plotted every 1 s by multiplying the maximum time step of 0.002 by the minor edit and plot frequency of 500.

C. Trip input data (cards 400 through 799)

C.1 Variable trip card

relationship: ge (greater than/equal to), gt (greater than), le (less than/equal to), or lt (less than)
variable code: null (Namely, specifies null field. Allowed only on trip cards. Parameter is zero.) or timeof (i.e., time of trip occurring. Parameter is trip number. This is allowed only on trip cards.)
latch indicator: l (Namely, trip once set true remains true, even if condition later is not met.) or
n (Namely, trip is tested each time advancement.)

Variable ‘cntrlvar’ corresponds to control variable command used in the RELAP5 code.

trip signals for HPI and LPI systems

card no.	variable	parameter	relationship	variable	parameter	additive constant	latch
401	time	0	ge	null	0	1140.0 s	l
402	time	0	ge	timeof	401	440.0 s	l

***Note*:** Two trip cards no. 401 and 402 mean the following. HPI and LPI systems in both loops are stopped 1140 s after break. Next, the HPI and LPI systems in both loops are restarted 440 s after stopping, for the alternative recirculation water injection.

reactor scram signal and SI signal

card no.	variable	parameter	relationship	variable	parameter	additive constant	latch
501	p	610010000	lt	null	0	1.297d+7 Pa	l
502	time	0	ge	timeof	501	0.0 s	l

***Note*:** Two trip cards no. 501 and 502 mean that a reactor scram signal is generated when pressure of the pipe component no. 610 for PZR drops to 12.97 MPa.

card no.	variable	parameter	relationship	variable	parameter	additive constant	latch
505	p	610010000	lt	null	0	1.227d+7 Pa	l

***Note*:** A trip card no. 505 means that a SI signal is obtained when pressure of the pipe component no. 610 for PZR drops to 12.27 MPa.

card no.	variable	parameter	relationship	variable	parameter	additive constant	latch
511	cntrlvar	521	lt	null	0	10.0 %	l
512	time	0	ge	timeof	511	0.0 s	l

***Note*:** Two trip cards no. 511 and 512 mean that a reactor scram signal is generated when SG secondary narrow-range liquid level in loop-A computed in the 'cntrlvar 521' drops to 10%.

card no.	variable	parameter	relationship	variable	parameter	additive constant	latch
513	cntrlvar	321	lt	null	0	10.0 %	l
514	time	0	ge	timeof	513	0.0 s	l

***Note*:** Two trip cards no. 513 and 514 mean that a reactor scram signal is generated when SG secondary narrow-range liquid level in loop-B computed in the 'cntrlvar 321' drops to 10%.

break start

card no.	variable	parameter	relationship	variable	parameter	additive constant	latch
530	time	0	ge	null	0	0.0 s	l

***Note*:** A trip card no. 530 means that break at cold leg in loop-B starts at time zero.

signal for COL valve

card no.	variable	parameter	relationship	variable	parameter	additive constant	latch
536	time	0	ge	null	0	1.0d+8 s	l
537	time	0	ge	null	0	1.0d+8 s	l
538	time	0	lt	null	0	0.0 s	l
539	time	0	lt	null	0	0.0 s	l

***Note*:** Four trip cards no. 536, 537, 538, and 539 mean that the two valve junction components no. 433 and 233 for COL valves in loop-A and loop-B respectively are always controlled to be open. The COL valves are virtually modeled due to their equipping for the experiment on the LSTF, which is employed as a reference for noding.

on/off signal for SG relief valve

card no.	variable	parameter	relationship	variable	parameter	additive constant	latch
570	p	516010000	gt	null	0	7.82d+6 Pa	n
571	p	516010000	gt	null	0	8.03d+6 Pa	n
572	time	0	gt	null	0	1.0d+8 s	n

***Note*:** Two trip cards no. 570 and 571 mean the following. In loop-A, the valve junction component no. 569 for SG relief valve is closed when pressure of the single-volume component no. 516 for SG steam dome drops to 7.82 MPa. In loop-A, the valve junction component no. 569 is open when the single-volume component no. 516 pressure rises to 8.03 MPa. A trip card no. 572 indicates this operation is invalid because the time is set to a large value of 10^8 s.

card no.	variable	parameter	relationship	variable	parameter	additive constant	latch
560	p	316010000	gt	null	0	7.82d+6 Pa	n
561	p	316010000	gt	null	0	8.03d+6 Pa	n
562	time	0	gt	null	0	1.0d+8 s	n

***Note*:** Two trip cards no. 560 and 561 mean the following. In loop-B, the valve junction component no. 369 for SG relief valve is closed when pressure of the single-volume component no. 316 for SG steam dome drops to 7.82 MPa. In loop-B, the valve junction component no. 369 is open when the single-volume component no. 316 pressure rises to 8.03 MPa. A trip card no. 562 indicates this operation is invalid because the time is set to a large value of 10^8 s.

on/off signal for SG safety valve

card no.	variable	parameter	relationship	variable	parameter	additive constant	latch
540	p	516010000	gt	null	0	7.69d+6 Pa	n
541	p	516010000	gt	null	0	8.68d+6 Pa	n

***Note*:** Two trip cards no. 540 and 541 mean the following. In loop-A, the valve junction component no. 579 for SG safety valve is closed when pressure of the single-volume component no. 516 for SG steam dome drops to 7.69 MPa. In loop-A, the valve junction component no. 579 is open when the single-volume component no. 516 pressure rises to 8.68 MPa.

card no.	variable	parameter	relationship	variable	parameter	additive constant	latch
542	p	316010000	gt	null	0	7.69d+6 Pa	n
543	p	316010000	gt	null	0	8.68d+6 Pa	n

***Note*:** Two trip cards no. 542 and 543 mean the following. In loop-B, the valve junction component no. 379 for SG safety valve is closed when pressure of the single-volume component no. 316 for SG steam dome drops to 7.69 MPa. In loop-B, the valve junction component no. 379 is open when the single-volume component no. 316 pressure rises to 8.68 MPa.

on/off signal for PZR PORV

card no.	variable	parameter	relationship	variable	parameter	additive constant	latch
531	p	610010000	gt	null	0	16.07d+6 Pa	n
532	p	610010000	gt	null	0	16.20d+6 Pa	n
520	time	0	gt	null	0	1.0d+8 s	n

***Note*:** Two trip cards no. 531 and 532 mean the following. The valve junction component no. 651 for PZR PORV is closed when pressure of the pipe component no. 610 for PZR drops to 16.07 MPa. The valve junction component no. 651 is open when the pipe component no. 610 pressure rises to 16.20 MPa. A trip card no. 520 indicates this operation is invalid because the time is set to a large value of 10^8 s.

on/off signal for PZR safety valve

card no.	variable	parameter	relationship	variable	parameter	additive constant	latch
521	p	610010000	gt	null	0	17.06d+6 Pa	n
522	p	610010000	gt	null	0	17.26d+6 Pa	n

***Note*:** Two trip cards no. 521 and 522 mean the following. The valve junction component no. 661 for PZR safety valve is closed when pressure of the pipe component no. 610 for PZR drops to 17.06 MPa. The valve junction component no. 661 is open when the pipe component no. 610 pressure rises to 17.26 MPa.

on/off signal for ACC tank outlet valve

card no.	variable	parameter	relationship	variable	parameter	additive constant	latch
523	p	448010000	gt	null	0	1.70d+6 Pa	n
524	p	448010000	lt	null	0	4.51d+6 Pa	n

***Note*:** Two trip cards no. 523 and 524 mean the following. In loop-A, the valve junction component no. 712 for ACC tank outlet valve is closed when pressure of the branch component no. 448 for cold leg drops to 1.7 MPa. In loop-A, the valve junction component no. 712 is open when the branch component no. 448 pressure declines to 4.51 MPa.

card no.	variable	parameter	relationship	variable	parameter	additive constant	latch
544	p	248010000	gt	null	0	1.70d+6 Pa	n
545	p	248010000	lt	null	0	4.51d+6 Pa	n

***Note*:** Two trip cards no. 544 and 545 mean the following. In loop-B, the valve junction component no. 711 for ACC tank outlet valve is closed when pressure of the branch component no. 248 for cold leg drops to 1.7 MPa. In loop-B, the valve junction component no. 711 is open when the branch component no. 248 pressure declines to 4.51 MPa.

on/off signal for SG AFW system

card no.	variable	parameter	relationship	variable	parameter	additive constant	latch
551	cntrlvar	508	lt	null	0	42.0 %	n
552	cntrlvar	508	lt	null	0	44.0 %	n

***Note*:** Two trip cards no. 551 and 552 mean the following. In loop-A, SG secondary narrow-range liquid level is initially fixed to 44%. In loop-A, SG AFW system is initiated when SG

secondary narrow-range liquid level computed in the ‘cntrlvar 508’ drops to 42%. In loop-A, SG AFW system is terminated when SG secondary narrow-range liquid level rises to 44%.

card no.	variable	parameter	relationship	variable	parameter	additive constant	latch
553	cntrlvar	308	lt	null	0	42.0 %	n
554	cntrlvar	308	lt	null	0	44.0 %	n

***Note*:** Two trip cards no. 553 and 554 mean the following. In loop-B, SG secondary narrow-range liquid level is initially fixed to 44%. In loop-B, SG AFW system is initiated when SG secondary narrow-range liquid level computed in the ‘cntrlvar 308’ drops to 42%. In loop-B, SG AFW system is terminated when SG secondary narrow-range liquid level rises to 44%.

on/off signal for PZR heater

card no.	variable	parameter	relationship	variable	parameter	additive constant	latch
581	cntrlvar	612	le	null	0	5.8 %	n
582	cntrlvar	660	le	null	0	0.0 %	n

Note: As a trip card no. 581 is ‘on’ when PZR liquid volume computed in the ‘cntrlvar 612’ is less than 5.8%, PZR proportional and backup heaters are ‘off’. Namely, PZR proportional and backup heaters remain ‘on’ when PZR liquid volume exceeds 5.8%. The ‘cntrlvar 651’ involved in the ‘cntrlvar 660’ indicates the difference between PZR pressure and PZR reference pressure (15.5 MPa as PZR initial pressure). The PZR liquid volume is less than zero when PZR pressure is below PZR reference pressure. Thus, a trip card no. 582 is ‘on’ when the PZR liquid level computed in the ‘cntrlvar 660’ is less than zero, causing that PZR backup heater is ‘on’. Accordingly, a trip card no. 582 is always ‘on’ because PZR pressure is below 15.5 MPa.

dummy trip

card no.	variable	parameter	relationship	variable	parameter	additive constant	latch
597	time	0	ge	null	0	1.0d+8 s	l

***Note*:** A trip card no. 597 is used to open and close the two valve junction components no. 529 and 533 for SG MSIV and SG steam line valve respectively in loop-A while the two valve junction components no. 329 and 333 for SG MSIV and SG steam line valve respectively in loop-B. A trip card no. 597 is employed as a trip signal to open the four valve junction components no. 529, 533, 329, and 333, while a trip card no. 501 is used to close the four valve junction components. Thus, the four valve junction components are controlled not to reopen after being closed following a reactor scram signal because the time is set to a large value of 10^8 s.

card no.	variable	parameter	relationship	variable	parameter	additive constant	latch
598	time	0	ge	null	0	1.0d+8 s	l

***Note*:** A trip card no. 598 means that the valve junction component no. 621 for PZR spray line valve is always controlled to be closed because the time is set to a large value of 10^8 s.

reflood model utilization

card no.	variable	parameter	relationship	variable	parameter	additive constant	latch
599	time	0	ge	null	0	0.0 s	l

***Note*:** A trip card no. 599 means that reflood model built into the RELAP5 code is employed because the time is set to zero. Specifically, the reflood model is applied to the boundary condition of heat structure geometry of high-power, mean-power, and low-power fuel rods.

C.2 Logical trip card

on/off signal for SG relief valve

card no.	trip card no.	operator	trip card no.	latch
601	-603	and	571	n
602	603	and	570	n
603	601	or	602	n
633	603	or	572	n

***Note*:** A trip card no. 633 means the following. In loop-A, the valve junction component no. 569 for SG relief valve is closed when pressure of the single-volume component no. 516 for SG steam dome drops to 7.82 MPa. In loop-A, the valve junction component no. 569 is open when the single-volume component no. 516 pressure rises to 8.03 MPa.

card no.	trip card no.	operator	trip card no.	latch
607	-609	and	561	n
608	609	and	560	n
609	607	or	608	n
639	609	or	562	n

***Note*:** A trip card no. 639 means the following. In loop-B, the valve junction component no. 369 for SG relief valve is closed when pressure of the single-volume component no. 316 for SG steam dome drops to 7.82 MPa. In loop-B, the valve junction component no. 369 is open when the single-volume component no. 316 pressure rises to 8.03 MPa.

on/off signal for SG safety valve

card no.	trip card no.	operator	trip card no.	latch
651	-653	and	541	n
652	653	and	540	n
653	651	or	652	n

***Note*:** A trip card no. 653 means the following. In loop-A, the valve junction component no. 579 for SG safety valve is closed when pressure of the single-volume component no. 516 for SG steam dome drops to 7.69 MPa. In loop-A, the valve junction component no. 579 is open when the single-volume component no. 516 pressure rises to 8.68 MPa.

card no.	trip card no.	operator	trip card no.	latch
657	-659	and	543	n
658	659	and	542	n
659	657	or	658	n

***Note*:** A trip card no. 659 means the following. In loop-B, the valve junction component no. 379 for SG safety valve is closed when pressure of the single-volume component no. 316 for SG steam dome drops to 7.69 MPa. In loop-B, the valve junction component no. 379 is open when the single-volume component no. 316 pressure rises to 8.68 MPa.

on/off signal for PZR PORV

card no.	trip card no.	operator	trip card no.	latch
623	-625	and	532	n
624	625	and	531	n
625	623	or	624	n
626	625	or	520	n

***Note*:** A trip card no. 626 means the following. The valve junction component no. 651 for PZR PORV is closed when pressure of the pipe component no. 610 for PZR drops to 16.07 MPa. The valve junction component no. 651 is open when the pipe component no. 610 pressure rises to 16.20 MPa.

on/off signal for PZR safety valve

card no.	trip card no.	operator	trip card no.	latch
613	-615	and	522	n
614	615	and	521	n
615	613	or	614	n

***Note*:** A trip card no. 615 means the following. The valve junction component no. 661 for PZR safety valve is closed when pressure of the pipe component no. 610 for PZR drops to 17.06 MPa. The valve junction component no. 661 is open when the pipe component no. 610 pressure rises to 17.26 MPa.

on/off signal for ACC tank outlet valve

card no.	trip card no.	operator	trip card no.	latch
618	523	and	524	n

***Note*:** A trip card no. 618 means the following. In loop-A, the valve junction component no. 712 for ACC tank outlet valve is closed when pressure of the branch component no. 448 for cold leg drops to 1.7 MPa. In loop-A, the valve junction component no. 712 is open when the branch component no. 448 pressure declines to 4.51 MPa.

card no.	trip card no.	operator	trip card no.	latch
619	544	and	545	n

***Note*:** A trip card no. 619 means the following. In loop-B, the valve junction component no. 711 for ACC tank outlet valve is closed when pressure of the branch component no. 248 for cold leg drops to 1.7 MPa. In loop-B, the valve junction component no. 711 is open when the branch component no. 248 pressure declines to 4.51 MPa.

on/off signal for SG AFW system

card no.	trip card no.	operator	trip card no.	latch
641	-643	and	551	n
642	643	and	552	n
643	641	or	642	n
644	643	and	505	n

***Note*:** A trip card no. 644 means the following. A SI signal is obtained when pressure of the pipe component no. 610 for PZR drops to 12.27 MPa. In loop-A, SG AFW system is initiated when SG secondary narrow-range liquid level computed in the ‘cntrlvar 508’ drops to 42%. In loop-A, SG AFW system is terminated when SG secondary narrow-range liquid level rises to 44%.

card no.	trip card no.	operator	trip card no.	latch
645	-647	and	553	n
646	647	and	554	n
647	645	or	646	n
648	647	and	505	n

***Note*:** A trip card no. 648 means the following. A SI signal is obtained when pressure of the pipe component no. 610 for PZR drops to 12.27 MPa. In loop-B, SG AFW system is initiated when SG secondary narrow-range liquid level computed in the ‘cntrlvar 308’ drops to 42%. In loop-B, SG AFW system is terminated when SG secondary narrow-range liquid level rises to 44%.

reactor scram signal

card no.	trip card no.	operator	trip card no.	latch
671	502	or	502	l
672	671	or	512	l
673	671	or	514	l

***Note*:** A trip card no. 673 means the following. A reactor scram signal is generated when pressure of the pipe component no. 610 for PZR drops to 12.97 MPa or when SG secondary narrow-range liquid levels in loop-A and loop-B computed in the ‘cntrlvar 521’ and ‘cntrlvar 321’ respectively drop to 10%, whichever occurs first.

trip signal for cold leg in loop-B

card no.	trip card no.	operator	trip card no.	latch
630	-530	or	-530	n

***Note*:** A trip card no. 630 means the following. Regarding cold leg in loop-B, the branch component no. 248 is connected to the pipe component no. 252 through the valve junction component no. 249. To simulate LBLOCA, the valve junction component no. 941 for break connecting to the branch component no. 248 and the valve junction component no. 951 for break connecting to the pipe component no. 252 are simultaneously open at time zero. By contrast, the valve junction component no. 249 is closed at time zero.

trip signals for HPI and LPI systems

card no.	trip card no.	operator	trip card no.	latch
681	505	and	-401	n
682	505	and	-401	n

***Note*:** Two trip cards no. 681 and 682 mean the following. A SI signal is obtained when pressure of the pipe component no. 610 for PZR drops to 12.27 MPa. HPI and LPI systems in both loops are stopped 1140 s after break.

card no.	trip card no.	operator	trip card no.	latch
683	681	or	402	n
684	682	or	402	n

***Note*:** Two trip cards no. 683 and 684 mean the following. A SI signal is obtained when pressure of the pipe component no. 610 for PZR drops to 12.27 MPa. HPI and LPI systems in both loops are stopped 1140 s after break. Next, the HPI and LPI systems in both loops are restarted 440 s after stopping, for the alternative recirculation water injection.

D. Hydrodynamic components (cards cccxxnn)

The hydrodynamic card numbers are divided into fields, where ccc is the component number, xx is the card type, and nn is the card number within card type. Here, the connection code is represented by 'ccc-vv', where ccc is the component number and vv is the volume number.

Hydrodynamic components are made up of a variety of component types. The component types of single-volume, time-dependent volume, single-junction, time-dependent junction, pipe, annulus, branch, separator, pump, and ACC correspond to the tag names of SV, TDV, SJ, TDJ, P, AN, B, SP, PMP, and ACC, respectively, as mentioned in the PWR noding schematic in **Figs. 2-1 and 2-2**. With regard to the valve junction components, the tag names for trip valve, motor valve, and servo valve are TRP, MTR, and SRV, respectively. The tag name is enclosed in brackets for the component type specified below.

Boundary condition for each hydrodynamic component is chosen either volume flow area or volume of volume. Junction area, volume flow area, and volume of volume for loop-A are three times as large as those for loop-B. This is because loop-A and loop-B simulate three loops and one loop, respectively.

Setting the inclination angle to zero means being horizontal. The positive and negative angles have upward and downward inclination, respectively. The positive and negative values of elevation change increase and decrease, respectively, in elevation.

Quantities such as wall roughness, flow energy loss coefficient, volume and junction control flags for the PWR components are referred to those for the LSTF components. It is noted that the description of volume and junction control flags with packed format concerning various model options is left out in this report. The reason is that the majority of the volume and junction control flags are set to zero.

Volume of volume is equal to volume flow area times length of volume. The hydraulic diameter is computed from 2*(volume flow area/π)**0.5 when it is set to zero. Setting the junction area to zero means the minimum volume area of the adjoining volume.

location: vessel DC

component no. (ccc): 100 component type: snglvol (i.e., single-volume [SV])

length	volume	inclination	elevation chg.	wall roughness	hydraulic dia.
0.89695 m	1.4494 m^3	-90.0 deg	-0.89695 m	3.33d-5	0.2488 m

***Note*:** The single-volume component no. 100 is part of modeled vessel DC.

location: vessel DC

component no. (ccc): 101 component type: branch (i.e., branch [B]) number of junct.: 1

length	volume	inclination	elevation chg.	wall roughness	hydraulic dia.
0.8248 m	2.7851 m^3	-90.0 deg	-0.8248 m	3.33d-5	0.52 m

from ccc-vv	to ccc-vv	junct. area	forward flow coeff.	reverse flow coeff.	junct. hydraulic dia.
101-01	100-01	0.0 m^2	0.0	0.0	0.2488 m

***Note*:** The branch component no. 101 for vessel DC is conjunctive with the single-volume component no. 100 for vessel DC.

location: vessel DC

component no. (ccc): 104 component type: branch (i.e., branch [B]) number of junct.: 4

length	volume	inclination	elevation chg.	wall roughness	hydraulic dia.
0.8245 m	2.7841 m^3	-90.0 deg	-0.8245 m	3.33d-5	0.52 m

from ccc-vv	to ccc-vv	junct. area	forward flow coeff.	reverse flow coeff.	junct. hydraulic dia.
104-01	101-01	0.0 m^2	0.0	0.0	0.52 m
104-01	108-01	0.0 m^2	0.0	0.0	0.52 m
252-02	104-01	0.0 m^2	0.0	0.0	0.6985 m
452-02	104-01	0.0 m^2	0.0	0.0	0.6985 m

***Note*:** The branch component no. 104 for vessel DC is conjunctive with the branch component no. 101 for vessel DC, the annulus component no. 108 for vessel DC, and the two pipe components no. 252 and 452 for cold legs in both loops.

location: vessel DC

component no. (ccc): 108 component type: annulus (i.e., annulus [AN]) number of vol.: 12

ccc-vv	length	volume	inclination	elevation chg.	wall roughness	hydraulic dia.
108-01	0.51075 m	1.6177 m^3	-90.0 deg	-0.51075 m	4.57d-5	0.52 m
108-02	0.655 m	2.1729 m^3	-90.0 deg	-0.655 m	4.57d-5	0.52 m
108-03	0.406666 m	1.2137 m^3	-90.0 deg	-0.406666 m	4.57d-5	0.4451 m
108-04	0.406666 m	1.2137 m^3	-90.0 deg	-0.406666 m	4.57d-5	0.4451 m
108-05	0.406666 m	1.2137 m^3	-90.0 deg	-0.406666 m	4.57d-5	0.4451 m
108-06	0.406666 m	1.2137 m^3	-90.0 deg	-0.406666 m	4.57d-5	0.4451 m
108-07	0.406666 m	1.2137 m^3	-90.0 deg	-0.406666 m	4.57d-5	0.4451 m
108-08	0.406666 m	1.2137 m^3	-90.0 deg	-0.406666 m	4.57d-5	0.4451 m
108-09	0.406666 m	1.2137 m^3	-90.0 deg	-0.406666 m	4.57d-5	0.4451 m
108-10	0.406666 m	1.2137 m^3	-90.0 deg	-0.406666 m	4.57d-5	0.4451 m
108-11	0.406666 m	1.2137 m^3	-90.0 deg	-0.406666 m	4.57d-5	0.4451 m
108-12	1.2588 m	4.2506 m^3	-90.0 deg	-1.2588 m	4.57d-5	0.52 m

forward flow coeff.	reverse flow coeff.	junction hydraulic dia.	junction no.
0.0	0.0	0.52 m	01
0.0	0.0	0.4451 m	02-11

***Note*:** The annulus component no. 108 for vessel DC consists of twelve vertically divided volumes with different lengths.

location: lower plenum

component no. (ccc): 112 component type: snglvol (i.e., single-volume [SV])

length	volume	inclination	elevation chg.	wall roughness	hydraulic dia.
0.64 m	2.3764 m^3	90.0 deg	0.64 m	3.33d-5	1.107 m

***Note*:** The single-volume component no. 112 is part of modeled lower plenum.

location: lower plenum

component no. (ccc): 116 component type: branch (i.e., branch [B]) number of junct.: 3

length	volume	inclination	elevation chg.	wall roughness	hydraulic dia.
1.2 m	13.8843 m^3	90.0 deg	1.2 m	3.33d-5	2.062 m

from ccc-vv	to ccc-vv	junct. area	forward flow coeff.	reverse flow coeff.	junct. hydraulic dia.
108-12	116-01	3.039 m^2	1.0	1.0	0.52 m
112-01	116-01	0.0 m^2	0.0	0.0	1.107 m

116-01	120-01	6.1038 m^2	1.0	1.0	0.362 m

***Note*:** The branch component no. 116 for lower plenum is conjunctive with the annulus component no. 108 for vessel DC, the single-volume component no. 112 for lower plenum, and the branch component no. 120 for core inlet.

location: core inlet

component no. (ccc): 120 component type: branch (i.e., branch [B]) number of junct.: 1

length	volume	inclination	elevation chg.	wall roughness	hydraulic dia.
1.2588 m	11.0162 m^3	90.0 deg	1.2588 m	3.33d-5	0.362 m

from ccc-vv	to ccc-vv	junct. area	forward flow coeff.	reverse flow coeff.	junct. hydraulic dia.
120-01	124-01	2.951 m^2	3.7	3.7	0.01131 m

***Note*:** The branch component no. 120 for core inlet is conjunctive with the pipe component no. 124 for core.

location: core

component no. (ccc): 124 component type: pipe (i.e., pipe [P]) number of volumes: 9

ccc-vv	length	volume	inclination	elevation chg.	wall roughness	hydraulic dia.
124-01	0.406666 m	1.891 m^3	90.0 deg	0.406666 m	3.33d-5	0.01131 m
124-02	0.406666 m	1.891 m^3	90.0 deg	0.406666 m	3.33d-5	0.01131 m
124-03	0.406666 m	1.891 m^3	90.0 deg	0.406666 m	3.33d-5	0.01131 m
124-04	0.406666 m	1.891 m^3	90.0 deg	0.406666 m	3.33d-5	0.01131 m
124-05	0.406666 m	1.891 m^3	90.0 deg	0.406666 m	3.33d-5	0.01131 m
124-06	0.406666 m	1.891 m^3	90.0 deg	0.406666 m	3.33d-5	0.01131 m
124-07	0.406666 m	1.891 m^3	90.0 deg	0.406666 m	3.33d-5	0.01131 m
124-08	0.406666 m	1.891 m^3	90.0 deg	0.406666 m	3.33d-5	0.01131 m
124-09	0.406666 m	1.891 m^3	90.0 deg	0.406666 m	3.33d-5	0.01131 m

forward flow coeff.	reverse flow coeff.	junction hydraulic dia.	junction no.
0.236	0.236	0.01131 m	01-08

***Note*:** The pipe component no. 124 for core with a height of 3.66 m consists of nine vertically divided volumes with identical length (i.e., 0.406666 m each).

location: core bypass

component no. (ccc): 121 component type: pipe (i.e., pipe [P]) number of volumes: 10

ccc-vv	length	volume	inclination	elevation chg.	wall roughness	hydraulic dia.
121-01	0.406666 m	0.70237 m^3	90.0 deg	0.406666 m	3.33d-5	0.0696 m
121-02	0.406666 m	0.70237 m^3	90.0 deg	0.406666 m	3.33d-5	0.0696 m
121-03	0.406666 m	0.70237 m^3	90.0 deg	0.406666 m	3.33d-5	0.0696 m
121-04	0.406666 m	0.70237 m^3	90.0 deg	0.406666 m	3.33d-5	0.0696 m
121-05	0.406666 m	0.70237 m^3	90.0 deg	0.406666 m	3.33d-5	0.0696 m
121-06	0.406666 m	0.70237 m^3	90.0 deg	0.406666 m	3.33d-5	0.0696 m
121-07	0.406666 m	0.70237 m^3	90.0 deg	0.406666 m	3.33d-5	0.0696 m
121-08	0.406666 m	0.70237 m^3	90.0 deg	0.406666 m	3.33d-5	0.0696 m
121-09	0.406666 m	0.70237 m^3	90.0 deg	0.406666 m	3.33d-5	0.0696 m
121-10	0.385 m	0.6649 m^3	90.0 deg	0.385 m	3.33d-5	0.0696 m

forward flow coeff.	reverse flow coeff.	junction hydraulic dia.	junction no.
0.0	0.0	0.0696 m	01-09

***Note*:** The pipe component no. 121 for core bypass consists of ten vertically divided volumes with different lengths.

location: core inlet to core bypass

component no. (ccc): 122 component type: sngljun (i.e., single-junction [SJ])

from ccc-vv	to ccc-vv	junct. area	forward flow coeff.	reverse flow coeff.	junct. hydraulic dia.
120-01	121-01	0.067481 m^2	0.0	0.0	0.0696 m

***Note*:** The single-junction component no. 122 indicates that the branch component no. 120 for core inlet is connected to the pipe component no. 121 for core bypass. A proper junction area between the two components no. 120 and 121 is provided to better fit the specified core bypass

flow rate (shown in **Table 2-1**).

location: core bypass to upper plenum
component no. (ccc): 123 component type: sngljun (i.e., single-junction [SJ])

from ccc-vv	to ccc-vv	junct. area	forward flow coeff.	reverse flow coeff.	junct. hydraulic dia.
121-10	132-01	0.2006437 m^2	0.0	0.0	0.0696 m

***Note*:** The single-junction component no. 123 indicates that the pipe component no. 121 for core bypass is connected to the branch component no. 132 for upper plenum. A proper junction area between the two components no. 121 and 132 is provided to better fit the specified core bypass flow rate (shown in **Table 2-1**).

location: core exit
component no. (ccc): 128 component type: branch (i.e., branch [B]) number of junct.: 1

length	volume	inclination	elevation chg.	wall roughness	hydraulic dia.
0.385 m	1.9694 m^3	90.0 deg	0.385 m	3.33d-5	0.1044 m

from ccc-vv	to ccc-vv	junct. area	forward flow coeff.	reverse flow coeff.	junct. hydraulic dia.
124-09	128-01	3.7 m^2	1.375	1.375	0.01131 m

***Note*:** The branch component no. 128 for core exit is conjunctive with the pipe component no. 124 for core.

location: upper plenum
component no. (ccc): 132 component type: branch (i.e., branch [B]) number of junct.: 1

length	volume	inclination	elevation chg.	wall roughness	hydraulic dia.
0.27 m	2.8742 m^3	90.0 deg	0.27 m	3.33d-5	0.6798 m

from ccc-vv	to ccc-vv	junct. area	forward flow coeff.	reverse flow coeff.	junct. hydraulic dia.
128-01	132-01	4.187 m^2	1.18	1.18	0.1044 m

***Note*:** The branch component no. 132 for upper plenum is conjunctive with the branch component no. 128 for core exit.

location: upper plenum
component no. (ccc): 133 component type: branch (i.e., branch [B]) number of junct.: 2

length	volume	inclination	elevation chg.	wall roughness	hydraulic dia.
0.2699 m	2.8731 m^3	90.0 deg	0.2699 m	3.33d-5	0.6798 m

from ccc-vv	to ccc-vv	junct. area	forward flow coeff.	reverse flow coeff.	junct. hydraulic dia.
132-01	133-01	9.209 m^2	1.18	1.18	0.6798 m
156-02	133-01	1.435 m^2	0.0	0.0	0.6798 m

***Note*:** The branch component no. 133 for upper plenum is conjunctive with the branch component no. 132 for upper plenum and the pipe component no. 156 for CRGT.

location: CRGT to upper plenum
component no. (ccc): 998 component type: sngljun (i.e., single-junction [SJ])

from ccc-vv	to ccc-vv	junct. area	forward flow coeff.	reverse flow coeff.	junct. hydraulic dia.
156-02	134-01	1.435 m^2	0.0	0.0	0.0575 m

***Note*:** The single-junction component no. 998 indicates that the pipe component no. 156 for CRGT is connected to the branch component no. 134 for upper plenum.

location: upper plenum
component no. (ccc): 134 component type: branch (i.e., branch [B]) number of junct.: 1

length	volume	inclination	elevation chg.	wall roughness	hydraulic dia.
0.24085 m	2.2102 m^3	90.0 deg	0.24085 m	3.33d-5	0.6798 m

from ccc-vv	to ccc-vv	junct. area	forward flow coeff.	reverse flow coeff.	junct. hydraulic dia.
133-01	134-01	9.209 m^2	1.18	1.18	0.6798 m

***Note*:** The branch component no. 134 for upper plenum is conjunctive with the branch component no. 133 for upper plenum.

location: upper plenum
component no. (ccc): 136 component type: branch (i.e., branch [B]) number of junct.: 4

length	volume	inclination	elevation chg.	wall roughness	hydraulic dia.
0.8245 m	7.5929 m^3	90.0 deg	0.8245 m	3.33d-5	0.6798 m

from ccc-vv	to ccc-vv	junct. area	forward flow coeff.	reverse flow coeff.	junct. hydraulic dia.
136-01	200-01	0.0 m^2	0.0	0.0	0.7366 m
136-01	400-01	0.0 m^2	0.0	0.0	0.7366 m
134-01	136-01	0.0 m^2	0.0	0.0	0.6798 m
140-01	136-01	0.0 m^2	0.0	0.0	0.6798 m

***Note*:** The branch component no. 136 for upper plenum is conjunctive with the two branch components no. 200 and 400 for hot legs in both loops, the branch component no. 134 for upper plenum, and the single-volume component no. 140 for upper plenum.

location: upper plenum
component no. (ccc): 140 component type: snglvol (i.e., single-volume [SV])

length	volume	inclination	elevation chg.	wall roughness	hydraulic dia.
0.8248 m	5.4384 m^3	90.0 deg	0.8248 m	3.33d-5	0.6798 m

***Note*:** The single-volume component no. 140 is part of modeled upper plenum.

location: upper head
component no. (ccc): 144 component type: snglvol (i.e., single-volume [SV])

length	volume	inclination	elevation chg.	wall roughness	hydraulic dia.
0.897 m	7.3657 m^3	90.0 deg	0.897 m	3.33d-5	0.682 m

***Note*:** The single-volume component no. 144 is part of modeled upper head.

location: upper head
component no. (ccc): 148 component type: branch (i.e., branch [B]) number of junct.: 2

length	volume	inclination	elevation chg.	wall roughness	hydraulic dia.
0.463 m	5.4219 m^3	90.0 deg	0.463 m	3.33d-5	0.9385 m

from ccc-vv	to ccc-vv	junct. area	forward flow coeff.	reverse flow coeff.	junct. hydraulic dia.
100-01	148-01	0.0065 m^2	20.1	20.1	0.09097 m
144-01	148-01	0.0065 m^2	0.0	0.0	0.682 m

***Note*:** The branch component no. 148 for upper head is conjunctive with the single-volume component no. 100 for vessel DC and the single-volume component no. 144 for upper head. A relatively large energy loss coefficient of 20.1 for both forward and reverse flow in the junction between the two components no. 100 and 148 is given to better match the specified bypass flow rate between vessel DC and upper head (shown in **Table 2-1**).

location: upper head
component no. (ccc): 149 component type: branch (i.e., branch [B]) number of junct.: 2

length	volume	inclination	elevation chg.	wall roughness	hydraulic dia.
0.262 m	2.8318 m^3	90.0 deg	0.262 m	3.33d-5	0.8733 m

from ccc-vv	to ccc-vv	junct. area	forward flow coeff.	reverse flow coeff.	junct. hydraulic dia.
148-01	149-01	0.0 m^2	0.0	0.0	0.8733 m
149-01	152-01	0.0 m^2	0.0	0.0	0.8733 m

***Note*:** The branch component no. 149 for upper head is conjunctive with the branch component no. 148 for upper head and the pipe component no. 152 for upper head.

location: upper head to CRGT
component no. (ccc): 154 component type: sngljun (i.e., single-junction [SJ])

from ccc-vv	to ccc-vv	junct. area	forward flow coeff.	reverse flow coeff.	junct. hydraulic dia.
152-01	156-01	0.95 m^2	1.66	1.66	0.0696 m

***Note*:** The single-junction component no. 154 indicates that the pipe component no. 152 for upper head is joined to the pipe component no. 156 for CRGT.

location: upper head

component no. (ccc): 152 component type: pipe (i.e., pipe [P]) number of volumes: 3

ccc-vv	length	volume	inclination	elevation chg.	wall roughness	hydraulic dia.
152-01	0.458 m	4.9503 m^3	90.0 deg	0.458 m	3.33d-5	2.1 m
152-02	0.458 m	3.3911 m^3	90.0 deg	0.458 m	3.33d-5	1.6 m
152-03	0.4575 m	1.2703 m^3	90.0 deg	0.4575 m	3.33d-5	1.15 m

forward flow coeff.	reverse flow coeff.	junction hydraulic dia.	junction no.
1.9	1.9	1.6 m	01
1.9	1.9	1.15 m	02

***Note*:** The pipe component no. 152 for upper head consists of three vertically divided volumes with different lengths.

location: CRGT

component no. (ccc): 156 component type: pipe (i.e., pipe [P]) number of volumes: 2

ccc-vv	length	volume	inclination	elevation chg.	wall roughness	hydraulic dia.
156-01	1.62195 m	2.7825 m^3	-90.0 deg	-1.62195 m	3.33d-5	0.0696 m
156-02	1.89015 m	2.8018 m^3	-90.0 deg	-1.89015 m	3.33d-5	0.0575 m

forward flow coeff.	reverse flow coeff.	junction hydraulic dia.	junction no.
18.2	18.2	0.0575 m	01

***Note*:** The pipe component no. 156 for CRGT consists of two vertically divided volumes with different lengths. Similar to the LSTF input data, a relatively large energy loss coefficient of 18.2 for both forward and reverse flow in the pipe component no. 156 for CRGT is given to better simulate the flow in the CRGT.

location: bypass flow path between vessel DC and hot leg in loop-A

component no. (ccc): 402 component type: branch (i.e., branch [B]) number of junct.: 2

length	volume	inclination	elevation chg.	wall roughness	hydraulic dia.
0.41225 m	0.078 m^3	90.0 deg	0.41225 m	3.33d-5	0.2834 m

from ccc-vv	to ccc-vv	junct. area	forward flow coeff.	reverse flow coeff.	junct. hydraulic dia.
108-01	402-01	0.004251 m^2	0.0	0.0	0.04248 m
402-01	400-01	0.004251 m^2	0.0	0.0	0.04248 m

***Note*:** In loop-A, the branch component no. 402 for bypass flow path between vessel DC and hot leg is conjunctive with the annulus component no. 108 for vessel DC and the pipe component no. 400 for hot leg. A proper junction area between the two components no. 402 and 108 or 400 is provided to better fit the specified bypass flow rate (shown in **Table 2-1**).

location: bypass flow path between vessel DC and hot leg in loop-B

component no. (ccc): 202 component type: branch (i.e., branch [B]) number of junct.: 2

length	volume	inclination	elevation chg.	wall roughness	hydraulic dia.
0.41225 m	0.026 m^3	90.0 deg	0.41225 m	3.33d-5	0.2834 m

from ccc-vv	to ccc-vv	junct. area	forward flow coeff.	reverse flow coeff.	junct. hydraulic dia.
108-01	202-01	0.001417 m^2	0.0	0.0	0.04248 m
202-01	200-01	0.001417 m^2	0.0	0.0	0.04248 m

***Note*:** In loop-B, the branch component no. 202 for bypass flow path between vessel DC and hot leg is conjunctive with the annulus component no. 108 for vessel DC and the pipe component no. 200 for hot leg. A proper junction area between the two components no. 202 and 108 or 200 is provided to better fit the specified bypass flow rate (shown in **Table 2-1**).

location: hot leg in loop-A

component no. (ccc): 400 component type: pipe (i.e., pipe [P]) number of volumes: 2

ccc-vv	length	vol. flow area	inclination	elevation chg.	wall roughness	hydraulic dia.
400-01	1.27 m	1.2783 m^2	0.0 deg	0.0 m	3.33d-5	0.7366 m
400-02	2.098 m	1.2783 m^2	0.0 deg	0.0 m	3.33d-5	0.7366 m

forward flow coeff.	reverse flow coeff.	junction hydraulic dia.	junction no.
0.0	0.0	0.7366 m	01

***Note*:** The pipe component no. 400 for hot leg in loop-A consists of two horizontally divided volumes with different lengths.

location: hot leg in loop-B

component no. (ccc): 200 component type: pipe (i.e., pipe [P]) number of volumes: 2

ccc-vv	length	vol. flow area	inclination	elevation chg.	wall roughness	hydraulic dia.
200-01	1.27 m	0.4261 m^2	0.0 deg	0.0 m	3.33d-5	0.7366 m
200-02	2.098 m	0.4261 m^2	0.0 deg	0.0 m	3.33d-5	0.7366 m

forward flow coeff.	reverse flow coeff.	junction hydraulic dia.	junction no.
0.0	0.0	0.7366 m	01

***Note*:** The pipe component no. 200 for hot leg in loop-B consists of two horizontally divided volumes with different lengths.

location: hot leg in loop-A

component no. (ccc): 406 component type: branch (i.e., branch [B]) number of junct.: 3

length	vol. flow area	inclination	elevation chg.	wall roughness	hydraulic dia.
2.0 m	1.2783 m^2	0.0 deg	0.0 m	3.33d-5	0.7366 m

from ccc-vv	to ccc-vv	junct. area	forward flow coeff.	reverse flow coeff.	junct. hydraulic dia.
400-02	406-01	1.2783 m^2	0.0	0.0	0.7366 m
406-01	408-01	1.2783 m^2	0.0	0.0	0.7366 m
600-09	406-01	0.06344 m^2	1.0	0.5	0.2842 m

***Note*:** In loop-A, the branch component no. 406 for hot leg is conjunctive with the two pipe components no. 400 and 408 for hot leg, and the pipe component no. 600 for PZR surge line.

location: hot leg in loop-B

component no. (ccc): 206 component type: branch (i.e., branch [B]) number of junct.: 2

length	vol. flow area	inclination	elevation chg.	wall roughness	hydraulic dia.
2.0 m	0.4261 m^2	0.0 deg	0.0 m	3.33d-5	0.7366 m

from ccc-vv	to ccc-vv	junct. area	forward flow coeff.	reverse flow coeff.	junct. hydraulic dia.
200-02	206-01	0.4261 m^2	0.0	0.0	0.7366 m
206-01	208-01	0.4261 m^2	0.0	0.0	0.7366 m

***Note*:** In loop-B, the branch component no. 206 for hot leg is conjunctive with the two pipe components no. 200 and 208 for hot leg.

location: hot leg in loop-A

component no. (ccc): 408 component type: pipe (i.e., pipe [P]) number of volumes: 2

ccc-vv	length	vol. flow area	inclination	elevation chg.	wall roughness	hydraulic dia.
408-01	0.769 m	1.2783 m^2	16.84 deg	0.2318 m	3.33d-5	0.7366 m
408-02	0.856 m	1.2783 m^2	35.42 deg	0.4782 m	3.33d-5	0.7366 m

forward flow coeff.	reverse flow coeff.	junction hydraulic dia.	junction no.
0.0	0.0	0.7366 m	01

***Note*:** The pipe component no. 408 for hot leg in loop-A consists of two divided volumes with different inclination angles and lengths.

location: hot leg in loop-B

component no. (ccc): 208 component type: pipe (i.e., pipe [P]) number of volumes: 2

ccc-vv	length	vol. flow area	inclination	elevation chg.	wall roughness	hydraulic dia.
208-01	0.769 m	0.4261 m^2	16.84 deg	0.2318 m	3.33d-5	0.7366 m
208-02	0.856 m	0.4261 m^2	35.42 deg	0.4782 m	3.33d-5	0.7366 m

forward flow coeff.	reverse flow coeff.	junction hydraulic dia.	junction no.
0.0	0.0	0.7366 m	01

***Note*:** The pipe component no. 208 for hot leg in loop-B consists of two divided volumes with different inclination angles and lengths.

location: hot leg to SG inlet in loop-A
component no. (ccc): 409 component type: sngljun (i.e., single-junction [SJ])

from ccc-vv	to ccc-vv	junct. area	forward flow coeff.	reverse flow coeff.	junct. hydraulic dia.
408-02	412-01	1.2783 m^2	0.0	0.0	0.7366 m

***Note*:** In loop-A, the single-junction component no. 409 indicates that the pipe component no. 408 for hot leg is joined to the single-volume component no. 412 for SG inlet.

location: hot leg to SG inlet in loop-B
component no. (ccc): 209 component type: sngljun (i.e., single-junction [SJ])

from ccc-vv	to ccc-vv	junct. area	forward flow coeff.	reverse flow coeff.	junct. hydraulic dia.
208-02	212-01	0.4261 m^2	0.0	0.0	0.7366 m

***Note*:** In loop-B, the single-junction component no. 209 indicates that the pipe component no. 208 for hot leg is joined to the single-volume component no. 212 for SG inlet.

location: SG inlet in loop-A
component no. (ccc): 412 component type: snglvol (i.e., single-volume [SV])

length	volume	inclination	elevation chg.	wall roughness	hydraulic dia.
0.73 m	5.601 m^3	90.0 deg	0.73 m	3.33d-5	2.08 m

***Note*:** The single-volume component no. 412 is part of modeled SG inlet in loop-A.

location: SG inlet in loop-B
component no. (ccc): 212 component type: snglvol (i.e., single-volume [SV])

length	volume	inclination	elevation chg.	wall roughness	hydraulic dia.
0.73 m	1.867 m^3	90.0 deg	0.73 m	3.33d-5	2.08 m

***Note*:** The single-volume component no. 212 is part of modeled SG inlet in loop-B.

location: SG inlet to SG inlet plenum in loop-A
component no. (ccc): 413 component type: sngljun (i.e., single-junction [SJ])

from ccc-vv	to ccc-vv	junct. area	forward flow coeff.	reverse flow coeff.	junct. hydraulic dia.
412-01	416-01	2.457 m^2	0.0	0.0	1.02117 m

***Note*:** In loop-A, the single-junction component no. 413 indicates that the single-volume component no. 412 for SG inlet is joined to the pipe component no. 416 for SG inlet plenum.

location: SG inlet to SG inlet plenum in loop-B
component no. (ccc): 213 component type: sngljun (i.e., single-junction [SJ])

from ccc-vv	to ccc-vv	junct. area	forward flow coeff.	reverse flow coeff.	junct. hydraulic dia.
212-01	216-01	0.819 m^2	0.0	0.0	1.02117 m

***Note*:** In loop-B, the single-junction component no. 213 indicates that the single-volume component no. 212 for SG inlet is joined to the pipe component no. 216 for SG inlet plenum.

location: SG inlet plenum in loop-A
component no. (ccc): 416 component type: pipe (i.e., pipe [P]) number of volumes: 2

ccc-vv	length	volume	inclination	elevation chg.	wall roughness	hydraulic dia.
416-01	0.6 m	6.939 m^3	90.0 deg	0.6 m	3.33d-5	2.415 m

ccc-vv	length	vol. flow area	inclination	elevation chg.	wall roughness	hydraulic dia.
416-02	0.545 m	3.0612 m^2	90.0 deg	0.545 m	3.33d-5	0.0196 m

forward flow coeff.	reverse flow coeff.	junction hydraulic dia.	junction no.
0.40628	0.40628	0.0196 m	01

***Note*:** The pipe component no. 416 for SG inlet plenum in loop-A consists of two vertically divided volumes with different lengths.

location: SG inlet plenum in loop-B

component no. (ccc): 216 component type: pipe (i.e., pipe [P]) number of volumes: 2

ccc-vv	length	volume	inclination	elevation chg.	wall roughness	hydraulic dia.
216-01	0.6 m	2.313 m^3	90.0 deg	0.6 m	3.33d-5	2.415 m
ccc-vv	length	vol. flow area	inclination	elevation chg.	wall roughness	hydraulic dia.
216-02	0.545 m	1.0204 m^2	90.0 deg	0.545 m	3.33d-5	0.0196 m

forward flow coeff.	reverse flow coeff.	junction hydraulic dia.	junction no.
0.40628	0.40628	0.0196 m	01

***Note*:** The pipe component no. 216 for SG inlet plenum in loop-B consists of two vertically divided volumes with different lengths.

location: SG inlet plenum to SG U-tube in loop-A

component no. (ccc): 417 component type: sngljun (i.e., single-junction [SJ])

from ccc-vv	to ccc-vv	junct. area	forward flow coeff.	reverse flow coeff.	junct. hydraulic dia.
416-02	420-01	3.0612 m^2	0.0	0.0	0.0196 m

***Note*:** In loop-A, the single-junction component no. 417 indicates that the pipe component no. 416 for SG inlet plenum is joined to the pipe component no. 420 for SG U-tube.

location: SG inlet plenum to SG U-tube in loop-B

component no. (ccc): 217 component type: sngljun (i.e., single-junction [SJ])

from ccc-vv	to ccc-vv	junct. area	forward flow coeff.	reverse flow coeff.	junct. hydraulic dia.
216-02	220-01	1.0204 m^2	0.0	0.0	0.0196 m

***Note*:** In loop-B, the single-junction component no. 217 indicates that the pipe component no. 216 for SG inlet plenum is joined to the pipe component no. 220 for SG U-tube.

location: SG U-tube in loop-A

component no. (ccc): 420 component type: pipe (i.e., pipe [P]) number of volumes: 10

ccc-vv	length	vol. flow area	inclination	elevation chg.	wall roughness	hydraulic dia.
420-01	2.258 m	3.0612 m^2	90.0 deg	2.258 m	3.33d-5	0.0196 m
420-02	2.258 m	3.0612 m^2	90.0 deg	2.258 m	3.33d-5	0.0196 m
420-03	2.258 m	3.0612 m^2	90.0 deg	2.258 m	3.33d-5	0.0196 m
420-04	2.258 m	3.0612 m^2	90.0 deg	2.258 m	3.33d-5	0.0196 m
420-05	1.178 m	3.0612 m^2	39.54 deg	0.75 m	3.33d-5	0.0196 m
420-06	1.178 m	3.0612 m^2	-39.54 deg	-0.75 m	3.33d-5	0.0196 m
420-07	2.258 m	3.0612 m^2	-90.0 deg	-2.258 m	3.33d-5	0.0196 m
420-08	2.258 m	3.0612 m^2	-90.0 deg	-2.258 m	3.33d-5	0.0196 m
420-09	2.258 m	3.0612 m^2	-90.0 deg	-2.258 m	3.33d-5	0.0196 m
420-10	2.258 m	3.0612 m^2	-90.0 deg	-2.258 m	3.33d-5	0.0196 m

forward flow coeff.	reverse flow coeff.	junction hydraulic dia.	junction no.
0.0	0.0	0.0196 m	01-09

***Note*:** The pipe component no. 420 for SG U-tube in loop-A consists of ten divided volumes with different inclination angles and lengths.

location: SG U-tube in loop-B

component no. (ccc): 220 component type: pipe (i.e., pipe [P]) number of volumes: 10

ccc-vv	length	vol. flow area	inclination	elevation chg.	wall roughness	hydraulic dia.
220-01	2.258 m	1.0204 m^2	90.0 deg	2.258 m	3.33d-5	0.0196 m
220-02	2.258 m	1.0204 m^2	90.0 deg	2.258 m	3.33d-5	0.0196 m
220-03	2.258 m	1.0204 m^2	90.0 deg	2.258 m	3.33d-5	0.0196 m
220-04	2.258 m	1.0204 m^2	90.0 deg	2.258 m	3.33d-5	0.0196 m
220-05	1.178 m	1.0204 m^2	39.54 deg	0.75 m	3.33d-5	0.0196 m
220-06	1.178 m	1.0204 m^2	-39.54 deg	-0.75 m	3.33d-5	0.0196 m
220-07	2.258 m	1.0204 m^2	-90.0 deg	-2.258 m	3.33d-5	0.0196 m
220-08	2.258 m	1.0204 m^2	-90.0 deg	-2.258 m	3.33d-5	0.0196 m
220-09	2.258 m	1.0204 m^2	-90.0 deg	-2.258 m	3.33d-5	0.0196 m
220-10	2.258 m	1.0204 m^2	-90.0 deg	-2.258 m	3.33d-5	0.0196 m

forward flow coeff.	reverse flow coeff.	junction hydraulic dia.	junction no.
0.0	0.0	0.0196 m	01-09

***Note*:** The pipe component no. 220 for SG U-tube in loop-B consists of ten divided volumes with different inclination angles and lengths.

location: SG U-tube to SG outlet plenum in loop-A

component no. (ccc): 421 component type: sngljun (i.e., single-junction [SJ])

from ccc-vv	to ccc-vv	junct. area	forward flow coeff.	reverse flow coeff.	junct. hydraulic dia.
420-10	424-01	3.0612 m^2	0.0	0.0	0.0196 m

***Note*:** In loop-A, the single-junction component no. 421 indicates that the pipe component no. 420 for SG U-tube is joined to the pipe component no. 424 for SG outlet plenum.

location: SG U-tube to SG outlet plenum in loop-B

component no. (ccc): 221 component type: sngljun (i.e., single-junction [SJ])

from ccc-vv	to ccc-vv	junct. area	forward flow coeff.	reverse flow coeff.	junct. hydraulic dia.
220-10	224-01	1.0204 m^2	0.0	0.0	0.0196 m

***Note*:** In loop-B, the single-junction component no. 221 indicates that the pipe component no. 220 for SG U-tube is joined to the pipe component no. 224 for SG outlet plenum.

location: SG outlet plenum in loop-A

component no. (ccc): 424 component type: pipe (i.e., pipe [P]) number of volumes: 2

ccc-vv	length	vol. flow area	inclination	elevation chg.	wall roughness	hydraulic dia.
424-01	0.545 m	3.0612 m^2	-90.0 deg	-0.545 m	3.33d-5	0.0196 m
ccc-vv	length	volume	inclination	elevation chg.	wall roughness	hydraulic dia.
424-02	0.6 m	6.939 m^3	-90.0 deg	-0.6 m	3.33d-5	2.415 m

forward flow coeff.	reverse flow coeff.	junction hydraulic dia.	junction no.
0.40628	0.40628	0.0196 m	01

***Note*:** The pipe component no. 424 for SG outlet plenum in loop-A consists of two vertically divided volumes with different lengths.

location: SG outlet plenum in loop-B

component no. (ccc): 224 component type: pipe (i.e., pipe [P]) number of volumes: 2

ccc-vv	length	vol. flow area	inclination	elevation chg.	wall roughness	hydraulic dia.
224-01	0.545 m	1.0204 m^2	-90.0 deg	-0.545 m	3.33d-5	0.0196 m
ccc-vv	length	volume	inclination	elevation chg.	wall roughness	hydraulic dia.
224-02	0.6 m	2.313 m^3	-90.0 deg	-0.6 m	3.33d-5	2.415 m

forward flow coeff.	reverse flow coeff.	junction hydraulic dia.	junction no.
0.40628	0.40628	0.0196 m	01

***Note*:** The pipe component no. 224 for SG outlet plenum in loop-B consists of two vertically divided volumes with different lengths.

location: SG outlet plenum to SG outlet in loop-A

component no. (ccc): 425 component type: sngljun (i.e., single-junction [SJ])

from ccc-vv	to ccc-vv	junct. area	forward flow coeff.	reverse flow coeff.	junct. hydraulic dia.
424-02	428-01	2.457 m^2	0.0	0.0	1.02117 m

***Note*:** In loop-A, the single-junction component no. 425 indicates that the pipe component no. 424 for SG outlet plenum is joined to the single-volume component no. 428 for SG outlet.

location: SG outlet plenum to SG outlet in loop-B

component no. (ccc): 225 component type: sngljun (i.e., single-junction [SJ])

from ccc-vv	to ccc-vv	junct. area	forward flow coeff.	reverse flow coeff.	junct. hydraulic dia.
224-02	228-01	0.819 m^2	0.0	0.0	1.02117 m

***Note*:** In loop-B, the single-junction component no. 225 indicates that the pipe component no. 224 for SG outlet plenum is joined to the single-volume component no. 228 for SG outlet.

location: SG outlet in loop-A
component no. (ccc): 428 component type: snglvol (i.e., single-volume [SV])

length	volume	inclination	elevation chg.	wall roughness	hydraulic dia.
0.73 m	5.601 m^3	-90.0 deg	-0.73 m	3.33d-5	2.08 m

***Note*:** The single-volume component no. 428 is part of modeled SG outlet in loop-A.

location: SG outlet in loop-B
component no. (ccc): 228 component type: snglvol (i.e., single-volume [SV])

length	volume	inclination	elevation chg.	wall roughness	hydraulic dia.
0.73 m	1.867 m^3	-90.0 deg	-0.73 m	3.33d-5	2.08 m

***Note*:** The single-volume component no. 228 is part of modeled SG outlet in loop-B.

location: SG outlet to COL downflow side in loop-A
component no. (ccc): 429 component type: sngljun (i.e., single-junction [SJ])

from ccc-vv	to ccc-vv	junct. area	forward flow coeff.	reverse flow coeff.	junct. hydraulic dia.
428-01	432-01	1.4607 m^2	0.0	0.0	0.7874 m

***Note*:** In loop-A, the single-junction component no. 429 indicates that the single-volume component no. 428 for SG outlet is joined to the pipe component no. 432 for COL downflow side.

location: SG outlet to COL downflow side in loop-B
component no. (ccc): 229 component type: sngljun (i.e., single-junction [SJ])

from ccc-vv	to ccc-vv	junct. area	forward flow coeff.	reverse flow coeff.	junct. hydraulic dia.
228-01	232-01	0.4869 m^2	0.0	0.0	0.7874 m

***Note*:** In loop-B, the single-junction component no. 229 indicates that the single-volume component no. 228 for SG outlet is joined to the pipe component no. 232 for COL downflow side.

location: COL downflow side in loop-A
component no. (ccc): 432 component type: pipe (i.e., pipe [P]) number of volumes: 5

ccc-vv	length	vol. flow area	inclination	elevation chg.	wall roughness	hydraulic dia.
432-01	0.543 m	1.4607 m^2	-35.42 deg	-0.45 m	3.33d-5	0.7874 m
432-02	1.08 m	1.4607 m^2	-90.0 deg	-1.08 m	3.33d-5	0.7874 m
432-03	1.08 m	1.4607 m^2	-90.0 deg	-1.08 m	3.33d-5	0.7874 m
432-04	0.95 m	1.4607 m^2	-60.0 deg	-0.824 m	3.33d-5	0.7874 m
432-05	0.95 m	1.4607 m^2	-30.0 deg	-0.476 m	3.33d-5	0.7874 m

forward flow coeff.	reverse flow coeff.	junction hydraulic dia.	junction no.
0.0	0.0	0.7874 m	01-04

***Note*:** The pipe component no. 432 for COL downflow side in loop-A consists of five divided volumes with different inclination angles and lengths.

location: COL downflow side in loop-B
component no. (ccc): 232 component type: pipe (i.e., pipe [P]) number of volumes: 5

ccc-vv	length	vol. flow area	inclination	elevation chg.	wall roughness	hydraulic dia.
232-01	0.543 m	0.4869 m^2	-35.42 deg	-0.45 m	3.33d-5	0.7874 m
232-02	1.08 m	0.4869 m^2	-90.0 deg	-1.08 m	3.33d-5	0.7874 m
232-03	1.08 m	0.4869 m^2	-90.0 deg	-1.08 m	3.33d-5	0.7874 m
232-04	0.95 m	0.4869 m^2	-60.0 deg	-0.824 m	3.33d-5	0.7874 m
232-05	0.95 m	0.4869 m^2	-30.0 deg	-0.476 m	3.33d-5	0.7874 m

forward flow coeff.	reverse flow coeff.	junction hydraulic dia.	junction no.
0.0	0.0	0.7874 m	01-04

***Note*:** The pipe component no. 232 for COL downflow side in loop-B consists of five divided volumes with different inclination angles and lengths.

location: COL valve in loop-A

component no. (ccc): 433 component type: valve (i.e., valve junction [motor valve: MTR])

from ccc-vv	to ccc-vv	junct. area	forward flow coeff.	reverse flow coeff.	junct. hydraulic dia.
432-05	436-01	1.4607 m^2	0.0	0.0	0.7874 m

valve type	open trip card no.	close trip card no.	valve chg. rate	initial position
mtrvlv (i.e., motor valve)	538	539	1.42 s^{-1}	1.0

***Note*:** In loop-A, the pipe component no. 432 for COL downflow side is joined to the pipe component no. 436 for COL upflow side through the valve junction component no. 433 for COL valve. The COL valve is virtually modeled due to its mounting for the experiment on the LSTF, which is used as a reference for noding. In loop-A, a motor valve employed for COL valve is always controlled to be open because the initial position is set to 1.0 according to two trip cards no. 538 and 539.

location: COL valve in loop-B

component no. (ccc): 233 component type: valve (i.e., valve junction [motor valve: MTR])

from ccc-vv	to ccc-vv	junct. area	forward flow coeff.	reverse flow coeff.	junct. hydraulic dia.
232-05	236-01	0.4869 m^2	0.0	0.0	0.7874 m

valve type	open trip card no.	close trip card no.	valve chg. rate	initial position
mtrvlv (i.e., motor valve)	536	537	1.42 s^{-1}	1.0

***Note*:** In loop-B, the pipe component no. 232 for COL downflow side is joined to the pipe component no. 236 for COL upflow side through the valve junction component no. 233 for COL valve. The COL valve is virtually modeled due to its mounting for the experiment on the LSTF, which is used as a reference for noding. In loop-B, a motor valve employed for COL valve is always controlled to be open because the initial position is set to 1.0 according to two trip cards no. 536 and 537.

location: COL upflow side in loop-A

component no. (ccc): 436 component type: pipe (i.e., pipe [P]) number of volumes: 4

ccc-vv	length	vol. flow area	inclination	elevation chg.	wall roughness	hydraulic dia.
436-01	1.843 m	1.4607 m^2	0.0 deg	0.0 m	3.33d-5	0.7874 m
436-02	0.95 m	1.4607 m^2	30.0 deg	0.476 m	3.33d-5	0.7874 m
436-03	0.95 m	1.4607 m^2	60.0 deg	0.824 m	3.33d-5	0.7874 m
436-04	1.4 m	1.4607 m^2	90.0 deg	1.4 m	3.33d-5	0.7874 m

forward flow coeff.	reverse flow coeff.	junction hydraulic dia.	junction no.
0.0	0.0	0.7874 m	01-03

***Note*:** The pipe component no. 436 for COL upflow side in loop-A consists of four divided volumes with different inclination angles and lengths.

location: COL upflow side in loop-B

component no. (ccc): 236 component type: pipe (i.e., pipe [P]) number of volumes: 4

ccc-vv	length	vol. flow area	inclination	elevation chg.	wall roughness	hydraulic dia.
236-01	1.843 m	0.4869 m^2	0.0 deg	0.0 m	3.33d-5	0.7874 m
236-02	0.95 m	0.4869 m^2	30.0 deg	0.476 m	3.33d-5	0.7874 m
236-03	0.95 m	0.4869 m^2	60.0 deg	0.824 m	3.33d-5	0.7874 m
236-04	1.4 m	0.4869 m^2	90.0 deg	1.4 m	3.33d-5	0.7874 m

forward flow coeff.	reverse flow coeff.	junction hydraulic dia.	junction no.
0.0	0.0	0.7874 m	01-03

***Note*:** The pipe component no. 236 for COL upflow side in loop-B consists of four divided volumes with different inclination angles and lengths.

location: reactor coolant pump in loop-A

component no. (ccc): 440 component type: pump (i.e., pump [PMP])

length	volume	inclination angle	elevation change
1.74 m	5.0907 m^3	90.0 deg	0.5 m

ccc-vv	junction area	forward flow coeff.	reverse flow coeff.	junction hydraulic dia.
436-04	1.4607 m^2	0.0	0.0	0.7874 m
444-01	1.155 m^2	0.0	0.0	0.6985 m

rated velocity	ratio of initial to rated velocity		rated volume flow rate
124.6 rad/s	1.0		16.749 m^3/s
rated head	rated torque	moment of inertia	rated density
84.0 m	97212.0 N·m	10380.0 kg·m^2	744.6 kg/m^3

***Note*:** In loop-A, the pump component no. 440 for reactor coolant pump is conjunctive with the pipe component no. 436 for COL upflow side and the branch component no. 444 for cold leg.

location: reactor coolant pump in loop-B

component no. (ccc): 240 component type: pump (i.e., pump [PMP])

length	volume	inclination angle	elevation change
1.74 m	1.6969 m^3	90.0 deg	0.5 m

ccc-vv	junction area	forward flow coeff.	reverse flow coeff.	junction hydraulic dia.
236-04	0.4869 m^2	0.0	0.0	0.7874 m
244-01	0.385 m^2	0.0	0.0	0.6985 m

rated velocity	ratio of initial to rated velocity		rated volume flow rate
124.6 rad/s	1.0		5.583 m^3/s
rated head	rated torque	moment of inertia	rated density
84.0 m	32404.0 N·m	3460.0 kg·m^2	744.6 kg/m^3

***Note*:** In loop-B, the pump component no. 240 for reactor coolant pump is conjunctive with the pipe component no. 236 for COL upflow side and the branch component no. 244 for cold leg.

Regarding PWR reactor coolant pump, the pump characteristic data involving single-phase homologous curve, two-phase multiplier table, and two-phase difference table for the USNRC's Semiscale test facility integrated into the RELAP5 code are converted into the input format of the RELAP5 code and are applied.

Each PWR reactor coolant pump curve is denoted by three letters in the following.
1st letter; H: curve for dynamic head. B: curve for hydraulic torque.
2nd letter; A: abscissa is v/α, and ordinate is h/α^2 or β/α^2. V: abscissa is α/v, and ordinate is h/v^2 or β/v^2. Here, α: rotation ratio. v: volumetric flow ratio. h: head ratio. β: torque ratio.
3rd letter; N: normal pump. D: energy dissipation. T: normal turbine. R: reverse pump.

For example, HAN means curve for dynamic head, and abscissa is v/α, and ordinate is h/α^2 or β/α^2, as well as normal pump.

item: single-phase homologous curve

curve type: head curve

curve regime no.: 1 (i.e., HAN BAN normal regime for v/α versus h/α^2)

v/α	h/α^2	v/α	h/α^2	v/α	h/α^2	v/α	h/α^2	v/α	h/α^2
0.0	1.73	0.1	1.6	0.2	1.5	0.5	1.23	0.7	1.23
v/α	h/α^2	v/α	h/α^2						
0.9	1.1	1.0	1.0						

curve regime no.: 2 (i.e., HVN BVN pump regime for α/v versus h/v^2)

α/v	h/v^2	α/v	h/v^2	α/v	h/v^2	α/v	h/v^2	α/v	h/v^2
0.0	-0.96	0.1	-0.9	0.2	-0.81	0.3	-0.7	0.4	-0.54
α/v	h/v^2	α/v	h/v^2	α/v	h/v^2				
0.8	1.4	0.9	0.68	1.0	1.0				

curve regime no.: 3 (i.e., HAD BAD energy regime for v/α versus h/α²)

v/α	h/α²	v/α	h/α²	v/α	h/α²	v/α	h/α²	v/α	h/α²
-1.0	3.55	-0.9	3.3	-0.8	3.21	-0.7	2.92	-0.6	2.73
v/α	h/α²	v/α	h/α²	v/α	h/α²	v/α	h/α²	v/α	h/α²
-0.5	2.53	-0.4	2.34	-0.25	2.1	-0.1	1.86	-0.6	2.73

curve regime no.: 4 (i.e., HVD BVD dissipation regime for α/v versus h/v²)

α/v	h/v²	α/v	h/v²	α/v	h/v²	α/v	h/v²	α/v	h/v²
-1.0	3.55	-0.9	3.22	-0.8	2.95	-0.7	2.7	-0.6	2.47
α/v	h/v²	α/v	h/v²	α/v	h/v²	α/v	h/v²	α/v	h/v²
-0.5	2.24	-0.35	1.98	-0.2	1.73	-0.1	1.56	0.0	1.4

curve regime no.: 5 (i.e., HAT BAT normal regime for v/α versus h/α²)

v/α	h/α²	v/α	h/α²	v/α	h/α²	v/α	h/α²	v/α	h/α²
0.0	-0.16	0.2	-0.06	0.4	0.09	0.6	0.31	0.8	0.5
v/α	h/α²								
1.0	0.59								

curve regime no.: 6 (i.e., HVT BVT turbine regime for α/v versus h/v²)

α/v	h/v²	α/v	h/v²	α/v	h/v²	α/v	h/v²	α/v	h/v²
0.0	1.4	0.1	1.18	0.25	0.95	0.4	0.78	0.5	0.68
α/v	h/v²	α/v	h/v²	α/v	h/v²	α/v	h/v²	α/v	h/v²
0.6	0.63	0.7	0.61	0.8	0.59	0.9	0.59	1.0	0.59

curve regime no.: 7 (i.e., HAR BAR reverse regime for v/α versus h/α²)

v/α	h/a²	v/α	h/a²
-1.0	0.0	0.0	0.0

curve regime no.: 8 (i.e., HVR BVR pump regime for α/v versus h/v²)

α/v	h/v²	α/v	h/v²
-1.0	0.0	0.0	0.0

curve type: torque curve

curve regime no.: 1 (i.e., HAN BAN normal regime for v/α versus β/α²)

v/α	β/α²	v/α	β/α²	v/α	β/α²	v/α	β/α²	v/α	β/α²
0.0	1.01	0.1	0.96	0.2	0.92	0.3	0.9	0.4	0.89
v/α	β/α²	v/α	β/α²	v/α	β/α²	v/α	β/α²	v/α	β/α²
0.5	0.91	0.7	0.99	0.8	1.02	0.9	1.02	1.0	1.0

curve regime no.: 2 (i.e., HVN BVN pump regime for α/v versus β/v²)

α/v	β/v²	α/v	β/v²	α/v	β/v²	α/v	β/v²	α/v	β/v²
0.0	-0.87	0.1	-0.76	0.2	-0.63	0.3	-0.48	0.4	-0.31
α/v	h/v²	α/v	h/v²						
0.74	0.4	1.0	1.0						

curve regime no.: 3 (i.e., HAD BAD energy regime for v/α versus β/α²)

v/α	β/α²	v/α	β/α²	v/α	β/α²	v/α	β/α²	v/α	β/α²
-1.0	2.98	-0.82	2.4	-0.6	1.87	-0.46	1.6	-0.34	1.4
v/α	β/α²	v/α	β/α²	v/α	β/α²				
-0.2	1.21	-0.1	1.1	0.0	1.01				

curve regime no.: 4 (i.e., HVD BVD dissipation regime for α/v versus β/v²)

α/v	β/v²	α/v	β/v²	α/v	β/v²	α/v	β/v²	α/v	β/v²
-1.0	2.98	-0.91	2.8	-0.8	2.6	-0.7	2.42	-0.6	2.25
α/v	β/v²	α/v	β/v²						
-0.42	2.0	0.0	1.42						

curve regime no.: 5 (i.e., HAT BAT normal regime for v/α versus β/α²)

v/α	β/α²	v/α	β/α²	v/α	β/α²	v/α	β/α²	v/α	β/α²
0.0	-1.0	0.25	-0.6	0.4	-0.37	0.5	-0.25	0.6	-0.16
v/α	β/α²	v/α	β/α²						
0.8	-0.01	1.0	0.11						

curve regime no.: 6 (i.e., HVT BVT turbine regime for α/v versus β/v²)

α/v	β/v²	α/v	β/v²	α/v	β/v²	α/v	β/v²
0.0	1.42	0.6	0.61	0.8	0.35	1.0	0.11

curve regime no.: 7 (i.e., HAR BAR reverse regime for v/α versus β/α^2)

v/α	β/α^2	v/α	β/α^2
-1.0	0.0	0.0	0.0

curve regime no.: 8 (i.e., HVR BVR pump regime for α/v versus β/v^2)

α/v	β/v^2	α/v	β/v^2
-1.0	0.0	0.0	0.0

item: two-phase multiplier tables

table type: head multiplier table (i.e., table for void fraction versus head multiplier)

void	multiplier	void	multiplier	void	multiplier	void	multiplier	void	multiplier
0.0	0.0	0.1	0.0	0.15	0.05	0.24	0.80	0.3	0.96
void	multiplier	void	multiplier	void	multiplier	void	multiplier	void	multiplier
0.4	0.98	0.6	0.97	0.8	0.90	0.9	0.80	0.96	0.50
void	multiplier								
1.0	0.0								

table type: torque multiplier table (i.e., table for void fraction versus torque multiplier)

void	multiplier	void	multiplier	void	multiplier	void	multiplier	void	multiplier
0.0	0.0	0.1	0.0	0.15	0.05	0.24	0.56	0.8	0.56
void	multiplier	void	multiplier						
0.96	0.45	1.0	0.0						

item: two-phase difference tables

curve type: head difference curve

curve regime no.: 1 (i.e., HAN BAN normal regime for v/α versus head difference)

v/α	difference	v/α	difference	v/α	difference	v/α	difference	v/α	difference
0.0	0.0	0.1	0.83	0.2	1.09	0.5	1.02	0.7	1.01
v/α	difference	v/α	difference						
0.9	0.94	1.0	1.0						

curve regime no.: 2 (i.e., HVN BVN pump regime for α/v versus head difference)

α/v	difference	α/v	difference	α/v	difference	α/v	difference	α/v	difference
0.0	0.0	0.1	-0.04	0.2	0.0	0.3	0.1	0.4	0.21
α/v	difference	α/v	difference	α/v	difference				
0.8	0.67	0.9	0.8	1.0	1.0				

curve regime no.: 3 (i.e., HAD BAD energy regime for v/α versus head difference)

v/α	difference	v/α	difference	v/α	difference	v/α	difference	v/α	difference
-1.0	-1.16	-0.9	-1.24	-0.8	-1.77	-0.7	-2.36	-0.6	-2.79
v/α	difference	v/α	difference	v/α	difference	v/α	difference	v/α	difference
-0.5	-2.91	-0.4	-2.67	-0.25	-1.69	-0.1	-0.5	0.0	0.0

curve regime no.: 4 (i.e., HVD BVD dissipation regime for α/v versus head difference)

α/v	difference	α/v	difference	α/v	difference	α/v	difference	α/v	difference
-1.0	-1.16	-0.9	-0.78	-0.8	-0.5	-0.7	-0.31	-0.6	-0.17
α/v	difference	α/v	difference	α/v	difference	α/v	difference	α/v	difference
-0.5	-0.08	-0.35	0.0	-0.2	0.05	-0.1	0.08	0.0	0.11

curve regime no.: 5 (i.e., HAT BAT normal regime for v/α versus head difference)

v/α	difference	v/α	difference	v/α	difference	v/α	difference	v/α	difference
0.0	0.0	0.2	-0.34	0.4	-0.65	0.6	-0.93	0.8	-1.19
v/α	difference								
1.0	-1.47								

curve regime no.: 6 (i.e., HVT BVT turbine regime for α/v versus head difference)

α/v	difference	α/v	difference	α/v	difference	α/v	difference	α/v	difference
0.0	0.11	0.1	0.13	0.25	0.15	0.4	0.13	0.5	0.07
α/v	difference	α/v	difference	α/v	difference	α/v	difference	α/v	difference
0.6	-0.04	0.7	-0.23	0.8	-0.51	0.9	-0.91	1.0	-1.47

curve regime no.: 7 (i.e., HAR BAR reverse regime for v/α versus head difference)

v/α	difference	v/α	difference
-1.0	0.0	0.0	0.0

curve regime no.: 8 (i.e., HVR BVR pump regime for α/v versus head difference)

α/v	difference	α/v	difference
-1.0	0.0	0.0	0.0

curve type: torque difference curve

curve regime no.: 1 (i.e., HAN BAN normal regime for v/α versus torque difference)

v/α	difference	v/α	difference
0.0	0.0	0.0	0.0

curve regime no.: 2 (i.e., HVN BVN pump regime for α/v versus torque difference)

α/v	difference	α/v	difference
0.	0.0	0.0	0.0

curve regime no.: 3 (i.e., HAD BAD energy regime for v/α versus torque difference)

v/α	difference	v/α	difference
0.0	0.0	0.0	0.0

curve regime no.: 4 (i.e., HVD BVD dissipation regime for α/v versus torque difference)

α/v	difference	α/v	difference
0.	0.0	0.0	0.0

curve regime no.: 5 (i.e., HAT BAT normal regime for v/α versus torque difference)

v/α	difference	v/α	difference
0.0	0.0	0.0	0.0

curve regime no.: 6 (i.e., HVT BVT turbine regime for α/v versus torque difference)

α/v	difference	α/v	difference
0.	0.0	0.0	0.0

curve regime no.: 7 (i.e., HAR BAR reverse regime for v/α versus torque difference)

v/α	difference	v/α	difference
0.0	0.0	0.0	0.0

curve regime no.: 8 (i.e., HVR BVR pump regime for α/v versus torque difference)

α/v	difference	α/v	difference
0.	0.0	0.0	0.0

item: time-dependent pump velocity trip card no.: 501

component no. (ccc): 440 (reactor coolant pump in loop-A)

time	pump velocity	time	pump velocity	time	pump velocity
0.0 s	124.6 rad/s	12.0 s	64.61756 rad/s	15.0 s	49.29176 rad/s
time	pump velocity	time	pump velocity	time	pump velocity
22.0 s	43.59754 rad/s	32.0 s	33.52986 rad/s	42.0 s	26.92606 rad/s
time	pump velocity	time	pump velocity	time	pump velocity
52.0 s	22.40308 rad/s	62.0 s	19.41268 rad/s	72.0 s	17.0079 rad/s
time	pump velocity	time	pump velocity	time	pump velocity
82.0 s	15.05168 rad/s	92.0 s	13.34466 rad/s	102.0 s	12.11112 rad/s
time	pump velocity	time	pump velocity	time	pump velocity
112.0 s	11.06448 rad/s	122.0 s	10.25458 rad/s	132.0 s	9.7188 rad/s
time	pump velocity	time	pump velocity	time	pump velocity
143.0 s	8.39804 rad/s	248.0 s	7.7875 rad/s	251.0 s	0.04984 rad/s
time	pump velocity	time	pump velocity		
412.0 s	0.0 rad/s	1.0d+8 s	0.0 rad/s		

***Note*:** In loop-A, the pump component no. 440 indicates that the reactor coolant pump velocity is defined as a function of time following a reactor scram signal according to a trip card no. 501.

item: time-dependent pump velocity trip card no.: 501

component no. (ccc): 240 (reactor coolant pump in loop-B)

time	pump velocity	time	pump velocity	time	pump velocity
0.0 s	124.6 rad/s	12.0 s	64.61756 rad/s	15.0 s	49.29176 rad/s
time	pump velocity	time	pump velocity	time	pump velocity
22.0 s	43.59754 rad/s	32.0 s	33.52986 rad/s	42.0 s	26.92606 rad/s

time	pump velocity	time	pump velocity	time	pump velocity
52.0 s	22.40308 rad/s	62.0 s	19.41268 rad/s	72.0 s	17.0079 rad/s
time	pump velocity	time	pump velocity	time	pump velocity
82.0 s	15.05168 rad/s	92.0 s	13.34466 rad/s	102.0 s	12.11112 rad/s
time	pump velocity	time	pump velocity	time	pump velocity
112.0 s	11.06448 rad/s	122.0 s	10.25458 rad/s	132.0 s	9.7188 rad/s
time	pump velocity	time	pump velocity	time	pump velocity
143.0 s	8.39804 rad/s	248.0 s	7.7875 rad/s	251.0 s	0.04984 rad/s
time	pump velocity	time	pump velocity		
412.0 s	0.0 rad/s	1.0d+8 s	0.0 rad/s		

***Note*:** In loop-B, the pump component no. 240 indicates the reactor coolant pump velocity is defined as a function of time following a reactor scram signal according to a trip card no. 501.

location: cold leg in loop-A

component no. (ccc): 444 component type: branch (i.e., branch [B]) number of junct.: 1

length	vol. flow area	inclination	elevation chg.	wall roughness	hydraulic dia.
2.098 m	1.1496 m^2	0.0 deg	0.0 m	3.33d-5	0.6985 m

from ccc-vv	to ccc-vv	junct. area	forward flow coeff.	reverse flow coeff.	junct. hydraulic dia.
444-01	448-01	1.1496 m^2	0.0	0.0	0.6985 m

***Note*:** In loop-A, the branch component no. 444 for cold leg is conjunctive with the branch component no. 448 for cold leg.

location: cold leg in loop-B

component no. (ccc): 244 component type: branch (i.e., branch [B]) number of junct.: 1

length	vol. flow area	inclination	elevation chg.	wall roughness	hydraulic dia.
2.098 m	0.3832 m^2	0.0 deg	0.0 m	3.33d-5	0.6985 m

from ccc-vv	to ccc-vv	junct. area	forward flow coeff.	reverse flow coeff.	junct. hydraulic dia.
244-01	248-01	0.3832 m^2	0.0	0.0	0.6985 m

***Note*:** In loop-B, the branch component no. 244 for cold leg is conjunctive with the branch component no. 248 for cold leg.

location: cold leg in loop-A

component no. (ccc): 448 component type: branch (i.e., branch [B]) number of junct.: 1

length	vol. flow area	inclination	elevation chg.	wall roughness	hydraulic dia.
2.098 m	1.1496 m^2	0.0 deg	0.0 m	3.33d-5	0.6985 m

from ccc-vv	to ccc-vv	junct. area	forward flow coeff.	reverse flow coeff.	junct. hydraulic dia.
448-01	452-01	1.1496 m^2	0.0	0.0	0.6985 m

***Note*:** In loop-A, the branch component no. 448 for cold leg is conjunctive with the pipe component no. 452 for cold leg.

location: cold leg in loop-B

component no. (ccc): 248 component type: branch (i.e., branch [B]) number of junct.: 1

length	vol. flow area	inclination	elevation chg.	wall roughness	hydraulic dia.
2.098 m	0.3832 m^2	0.0 deg	0.0 m	3.33d-5	0.6985 m

from ccc-vv	to ccc-vv	junct. area	forward flow coeff.	reverse flow coeff.	junct. hydraulic dia.
248-01	252-01	0.3832 m^2	0.0	0.0	0.6985 m

***Note*:** In loop-B, the branch component no. 248 for cold leg is conjunctive with the pipe component no. 252 for cold leg.

location: cold leg in loop-A

component no. (ccc): 452 component type: pipe (i.e., pipe [P]) number of volumes: 2

ccc-vv	length	vol. flow area	inclination	elevation chg.	wall roughness	hydraulic dia.
452-01	2.098 m	1.1496 m^2	0.0 deg	0.0 m	3.33d-5	0.6985 m
452-02	0.953 m	1.1496 m^2	0.0 deg	0.0 m	3.33d-5	0.6985 m

forward flow coeff.	reverse flow coeff.	junction hydraulic dia.	junction no.
0.0	0.0	0.6985 m	01

***Note*:** The pipe component no. 452 for cold leg in loop-A consists of two horizontally divided volumes with different lengths.

location: cold leg in loop-B

component no. (ccc): 252 component type: pipe (i.e., pipe [P]) number of volumes: 2

ccc-vv	length	vol. flow area	inclination	elevation chg.	wall roughness	hydraulic dia.
252-01	2.098 m	0.3832 m^2	0.0 deg	0.0 m	3.33d-5	0.6985 m
252-02	0.953 m	0.3832 m^2	0.0 deg	0.0 m	3.33d-5	0.6985 m

forward flow coeff.	reverse flow coeff.	junction hydraulic dia.	junction no.
0.0	0.0	0.6985 m	01

***Note*:** The pipe component no. 252 for cold leg in loop-B consists of two horizontally divided volumes with different lengths.

location: SG DC in loop-A

component no. (ccc): 500 component type: annulus (i.e., annulus [AN]) number of vol.: 5

ccc-vv	length	volume	inclination	elevation chg.	wall roughness	hydraulic dia.
500-01	1.916 m	17.07 m^3	-90.0 deg	-1.916 m	3.33d-5	0.131 m

ccc-vv	length	vol. flow area	inclination	elevation chg.	wall roughness	hydraulic dia.
500-02	2.258 m	1.9881 m^2	-90.0 deg	-2.258 m	3.33d-5	0.131 m
500-03	2.258 m	1.9881 m^2	-90.0 deg	-2.258 m	3.33d-5	0.131 m
500-04	2.258 m	1.9881 m^2	-90.0 deg	-2.258 m	3.33d-5	0.131 m
500-05	2.258 m	1.9881 m^2	-90.0 deg	-2.258 m	3.33d-5	0.131 m

forward flow coeff.	reverse flow coeff.	junction hydraulic dia.	junction no.
0.0	0.0	0.131 m	01-04

***Note*:** The annulus component no. 500 for SG DC in loop-A consists of five vertically divided volumes with different lengths.

location: SG DC in loop-B

component no. (ccc): 300 component type: annulus (i.e., annulus [AN]) number of vol.: 5

ccc-vv	length	volume	inclination	elevation chg.	wall roughness	hydraulic dia.
300-01	1.916 m	5.69 m^3	-90.0 deg	-1.916 m	3.33d-5	0.131 m

ccc-vv	length	vol. flow area	inclination	elevation chg.	wall roughness	hydraulic dia.
300-02	2.258 m	0.6627 m^2	-90.0 deg	-2.258 m	3.33d-5	0.131 m
300-03	2.258 m	0.6627 m^2	-90.0 deg	-2.258 m	3.33d-5	0.131 m
300-04	2.258 m	0.6627 m^2	-90.0 deg	-2.258 m	3.33d-5	0.131 m
300-05	2.258 m	0.6627 m^2	-90.0 deg	-2.258 m	3.33d-5	0.131 m

forward flow coeff.	reverse flow coeff.	junction hydraulic dia.	junction no.
0.0	0.0	0.131 m	01-04

***Note*:** The annulus component no. 300 for SG DC in loop-B consists of five vertically divided volumes with different lengths.

location: SG DC to SG riser in loop-A

component no. (ccc): 501 component type: sngljun (i.e., single-junction [SJ])

from ccc-vv	to ccc-vv	junct. area	forward flow coeff.	reverse flow coeff.	junct. hydraulic dia.
500-05	504-01	0.0 m^2	1.5	1.5	0.0423 m

***Note*:** In loop-A, the single-junction component no. 501 indicates that the annulus component no. 500 for SG DC is joined to the pipe component no. 504 for SG riser.

location: SG DC to SG riser in loop-B

component no. (ccc): 301 component type: sngljun (i.e., single-junction [SJ])

from ccc-vv	to ccc-vv	junct. area	forward flow coeff.	reverse flow coeff.	junct. hydraulic dia.
300-05	304-01	0.0 m^2	1.5	1.5	0.0423 m

***Note*:** In loop-B, the single-junction component no. 301 indicates that the annulus component no. 300 for SG DC is joined to the pipe component no. 304 for SG riser.

location: SG riser in loop-A

component no. (ccc): 504 component type: pipe (i.e., pipe [P]) number of volumes: 5

ccc-vv	length	volume	inclination	elevation chg.	wall roughness	hydraulic dia.
504-01	2.258 m	34.203 m^3	90.0 deg	2.258 m	3.33d-5	0.0423 m
ccc-vv	length	vol. flow area	inclination	elevation chg.	wall roughness	hydraulic dia.
504-02	2.258 m	15.303 m^2	90.0 deg	2.258 m	3.33d-5	0.0423 m
504-03	2.258 m	15.303 m^2	90.0 deg	2.258 m	3.33d-5	0.0423 m
504-04	2.258 m	15.303 m^2	90.0 deg	2.258 m	3.33d-5	0.0423 m
504-05	1.916 m	15.303 m^2	90.0 deg	1.916 m	3.33d-5	0.0423 m

forward flow coeff.	reverse flow coeff.	junction hydraulic dia.	junction no.
1.5	1.5	0.0423 m	01-04

***Note*:** The pipe component no. 504 for SG riser in loop-A consists of five vertically divided volumes with different lengths.

location: SG riser in loop-B

component no. (ccc): 304 component type: pipe (i.e., pipe [P]) number of volumes: 5

ccc-vv	length	volume	inclination	elevation chg.	wall roughness	hydraulic dia.
304-01	2.258 m	11.401 m^3	90.0 deg	2.258 m	3.33d-5	0.0423 m
ccc-vv	length	vol. flow area	inclination	elevation chg.	wall roughness	hydraulic dia.
304-02	2.258 m	5.101 m^2	90.0 deg	2.258 m	3.33d-5	0.0423 m
304-03	2.258 m	5.101 m^2	90.0 deg	2.258 m	3.33d-5	0.0423 m
304-04	2.258 m	5.101 m^2	90.0 deg	2.258 m	3.33d-5	0.0423 m
304-05	1.916 m	5.101 m^2	90.0 deg	1.916 m	3.33d-5	0.0423 m

forward flow coeff.	reverse flow coeff.	junction hydraulic dia.	junction no.
1.5	1.5	0.0423 m	01-04

***Note*:** The pipe component no. 304 for SG riser in loop-B consists of five vertically divided volumes with different lengths.

location: SG steam dome in loop-A

component no. (ccc): 506 component type: branch (i.e., branch [B]) number of junct.: 1

length	volume	inclination	elevation chg.	wall roughness	hydraulic dia.
1.051 m	13.3305 m^3	90.0 deg	1.051 m	3.33d-5	1.43 m

from ccc-vv	to ccc-vv	junct. area	forward flow coeff.	reverse flow coeff.	junct. hydraulic dia.
504-05	506-01	13.107 m^2	0.0	0.0	0.0423 m

***Note*:** In loop-A, the branch component no. 506 for SG steam dome is conjunctive with the pipe component no. 504 for SG riser.

location: SG steam dome in loop-B

component no. (ccc): 306 component type: branch (i.e., branch [B]) number of junct.: 1

length	volume	inclination	elevation chg.	wall roughness	hydraulic dia.
1.051 m	4.4435 m^3	90.0 deg	1.051 m	3.33d-5	1.43 m

from ccc-vv	to ccc-vv	junct. area	forward flow coeff.	reverse flow coeff.	junct. hydraulic dia.
304-05	306-01	4.369 m^2	0.0	0.0	0.0423 m

***Note*:** In loop-B, the branch component no. 306 for SG steam dome is conjunctive with the pipe component no. 304 for SG riser.

location: SG separator in loop-A

component no. (ccc): 508 component type: separatr (i.e., separator [SP]) number of junct.:3

length	volume	inclination	elevation chg.	wall roughness	hydraulic dia.
2.949 m	26.661 m^3	90.0 deg	2.949 m	3.33d-5	1.43 m

from ccc-vv	to ccc-vv	junct. area	forward flow coeff.	reverse flow coeff.	junct. hydraulic dia.
508-01	516-01	4.719 m^2	0.0	0.0	1.43 m
508-01	512-01	2.6163 m^2	1.0	1.0	1.05375 m
506-01	508-01	13.107 m^2	0.0	0.0	1.43 m

***Note*:** In loop-A, the separator component no. 508 for SG separator is conjunctive with the single-volume component no. 516 for SG steam dome, the pipe component no. 512 for SG riser, and

the branch component no. 506 for SG steam dome.

location: SG separator in loop-B

component no. (ccc): 308 component type: separatr (i.e., separator [SP]) number of junct.:3

length	volume	inclination	elevation chg.	wall roughness	hydraulic dia.
2.949 m	8.887 m^3	90.0 deg	2.949 m	3.33d-5	1.43 m

from ccc-vv	to ccc-vv	junct. area	forward flow coeff.	reverse flow coeff.	junct. hydraulic dia.
308-01	316-01	1.573 m^2	0.0	0.0	1.43 m
308-01	312-01	0.8721 m^2	1.0	1.0	1.05375 m
306-01	308-01	4.369 m^2	0.0	0.0	1.43 m

***Note*:** In loop-B, the separator component no. 308 for SG separator is conjunctive with the single-volume component no. 316 for SG steam dome, the pipe component no. 312 for SG riser, and the branch component no. 306 for SG steam dome.

location: SG riser in loop-A

component no. (ccc): 512 component type: pipe (i.e., pipe [P]) number of volumes: 3

ccc-vv	length	volume	inclination	elevation chg.	wall roughness	hydraulic dia.
512-01	1.051 m	27.849 m^3	90.0 deg	1.051 m	3.33d-5	1.195 m
512-02	1.051 m	27.849 m^3	90.0 deg	1.051 m	3.33d-5	1.195 m
512-03	1.898 m	27.849 m^3	90.0 deg	1.898 m	3.33d-5	1.195 m

forward flow coeff.	reverse flow coeff.	junction hydraulic dia.	junction no.
0.0	0.0	1.195 m	01-02

***Note*:** The pipe component no. 512 for SG riser in loop-A consists of three vertically divided volumes with different lengths.

location: SG riser in loop-B

component no. (ccc): 312 component type: pipe (i.e., pipe [P]) number of volumes: 3

ccc-vv	length	volume	inclination	elevation chg.	wall roughness	hydraulic dia.
312-01	1.051 m	9.283 m^3	90.0 deg	1.051 m	3.33d-5	1.195 m
312-02	1.051 m	9.283 m^3	90.0 deg	1.051 m	3.33d-5	1.195 m
312-03	1.898 m	9.283 m^3	90.0 deg	1.898 m	3.33d-5	1.195 m

forward flow coeff.	reverse flow coeff.	junction hydraulic dia.	junction no.
0.0	0.0	1.195 m	01-02

***Note*:** The pipe component no. 312 for SG riser in loop-B consists of three vertically divided volumes with different lengths.

location: SG DC to SG riser in loop-A

component no. (ccc): 513 component type: sngljun (i.e., single-junction [SJ])

from ccc-vv	to ccc-vv	junct. area	forward flow coeff.	reverse flow coeff.	junct. hydraulic dia.
500-01	512-01	20.883 m^2	0.0	0.0	0.131 m

***Note*:** In loop-A, the single-junction component no. 513 indicates that the annulus component no. 500 for SG DC is joined to the pipe component no. 512 for SG riser.

location: SG DC to SG riser in loop-B

component no. (ccc): 313 component type: sngljun (i.e., single-junction [SJ])

from ccc-vv	to ccc-vv	junct. area	forward flow coeff.	reverse flow coeff.	junct. hydraulic dia.
300-01	312-01	6.961 m^2	0.0	0.0	0.131 m

***Note*:** In loop-B, the single-junction component no. 313 indicates that the annulus component no. 300 for SG DC is joined to the pipe component no. 312 for SG riser.

location: SG riser to SG steam dome in loop-A

component no. (ccc): 514 component type: sngljun (i.e., single-junction [SJ])

from ccc-vv	to ccc-vv	junct. area	forward flow coeff.	reverse flow coeff.	junct. hydraulic dia.
512-03	516-01	2.5872 m^2	1.5	1.5	1.04787 m

***Note*:** In loop-A, the single-junction component no. 514 indicates that the pipe component no. 512 for SG riser is joined to the single-volume component no. 516 for SG steam dome.

location: SG riser to SG steam dome in loop-B
component no. (ccc): 314 component type: sngljun (i.e., single-junction [SJ])

from ccc-vv	to ccc-vv	junct. area	forward flow coeff.	reverse flow coeff.	junct. hydraulic dia.
312-03	316-01	0.8624 m^2	1.5	1.5	1.04787 m

***Note*:** In loop-B, the single-junction component no. 314 indicates that the pipe component no. 312 for SG riser is joined to the single-volume component no. 316 for SG steam dome.

location: SG steam dome in loop-A
component no. (ccc): 516 component type: snglvol (i.e., single-volume [SV])

length	volume	inclination	elevation chg.	wall roughness	hydraulic dia.
3.372 m	158.721 m^3	90.0 deg	3.372 m	3.33d-5	3.9958 m

***Note*:** The single-volume component no. 516 is part of modeled SG steam dome in loop-A.

location: SG steam dome in loop-B
component no. (ccc): 316 component type: snglvol (i.e., single-volume [SV])

length	volume	inclination	elevation chg.	wall roughness	hydraulic dia.
3.372 m	52.907 m^3	90.0 deg	3.372 m	3.33d-5	3.9958 m

***Note*:** The single-volume component no. 316 is part of modeled SG steam dome in loop-B.

location: SG steam line in loop-A
component no. (ccc): 520 component type: branch (i.e., branch [B]) number of junct.: 2

length	vol. flow area	inclination	elevation chg.	wall roughness	hydraulic dia.
24.7 m	0.9747 m^2	3.48 deg	1.5 m	3.33d-5	0.643 m

from ccc-vv	to ccc-vv	junct. area	forward flow coeff.	reverse flow coeff.	junct. hydraulic dia.
516-01	520-01	0.9747 m^2	0.0	0.0	0.643 m
520-01	524-01	0.9747 m^2	0.0	0.0	0.643 m

***Note*:** In loop-A, the branch component no. 520 for SG steam line is conjunctive with the single-volume component no. 516 for SG steam dome and the branch component no. 524 for SG steam line.

location: SG steam line in loop-B
component no. (ccc): 320 component type: branch (i.e., branch [B]) number of junct.: 2

length	vol. flow area	inclination	elevation chg.	wall roughness	hydraulic dia.
24.7 m	0.3249 m^2	3.48 deg	1.5 m	3.33d-5	0.643 m

from ccc-vv	to ccc-vv	junct. area	forward flow coeff.	reverse flow coeff.	junct. hydraulic dia.
316-01	320-01	0.3249 m^2	0.0	0.0	0.643 m
320-01	324-01	0.3249 m^2	0.0	0.0	0.643 m

***Note*:** In loop-B, the branch component no. 320 for SG steam line is conjunctive with the single-volume component no. 316 for SG steam dome and the branch component no. 324 for SG steam line.

location: SG steam line in loop-A
component no. (ccc): 524 component type: branch (i.e., branch [B]) number of junct.: 1

length	vol. flow area	inclination	elevation chg.	wall roughness	hydraulic dia.
39.0 m	0.9747 m^2	0.0 deg	0.0 m	3.33d-5	0.643 m

from ccc-vv	to ccc-vv	junct. area	forward flow coeff.	reverse flow coeff.	junct. hydraulic dia.
524-01	528-01	0.9747 m^2	0.0	0.0	0.643 m

***Note*:** In loop-A, the branch component no. 524 for SG steam line is conjunctive with the single-volume component no. 528 for SG steam line.

location: SG steam line in loop-B
component no. (ccc): 324 component type: branch (i.e., branch [B]) number of junct.: 1

length	vol. flow area	inclination	elevation chg.	wall roughness	hydraulic dia.
39.0 m	0.3249 m^2	0.0 deg	0.0 m	3.33d-5	0.643 m

from ccc-vv	to ccc-vv	junct. area	forward flow coeff.	reverse flow coeff.	junct. hydraulic dia.
324-01	328-01	0.3249 m^2	0.0	0.0	0.643 m

***Note*:** In loop-B, the branch component no. 324 for SG steam line is conjunctive with the single-volume component no. 328 for SG steam line.

location: SG steam line in loop-A
component no. (ccc): 528 component type: snglvol (i.e., single-volume [SV])

length	vol. flow area	inclination	elevation chg.	wall roughness	hydraulic dia.
31.0 m	0.9747 m^2	0.0 deg	0.0 m	3.33d-5	0.643 m

***Note*:** The single-volume component no. 528 is part of modeled SG steam line in loop-A.

location: SG steam line in loop-B
component no. (ccc): 328 component type: snglvol (i.e., single-volume [SV])

length	vol. flow area	inclination	elevation chg.	wall roughness	hydraulic dia.
31.0 m	0.3249 m^2	0.0 deg	0.0 m	3.33d-5	0.643 m

***Note*:** The single-volume component no. 328 is part of modeled SG steam line in loop-B.

location: SG MSIV in loop-A
component no. (ccc): 529 component type: valve (i.e., valve junction [motor valve: MTR])

from ccc-vv	to ccc-vv	junct. area	forward flow coeff.	reverse flow coeff.	junct. hydraulic dia.
528-01	532-01	0.9747 m^2	0.0	0.0	0.643 m

valve type	open trip card no.	close trip card no.	valve chg. rate	initial position
mtrvlv (i.e., motor valve)	597	501	1.0 s^{-1}	1.0

***Note*:** In loop-A, the single-volume component no. 528 for SG steam line is joined to the single-volume component no. 532 for SG steam line through the valve junction component no. 529 for SG MSIV. In loop-A, a motor valve employed for SG MSIV is controlled not to reopen after being closed following a reactor scram signal because the initial position is set to 1.0 according to two trip cards no. 597 and 501.

location: SG MSIV in loop-B
component no. (ccc): 329 component type: valve (i.e., valve junction [motor valve: MTR])

from ccc-vv	to ccc-vv	junct. area	forward flow coeff.	reverse flow coeff.	junct. hydraulic dia.
328-01	332-01	0.3249 m^2	0.0	0.0	0.643 m

valve type	open trip card no.	close trip card no.	valve chg. rate	initial position
mtrvlv (i.e., motor valve)	597	501	1.0 s^{-1}	1.0

***Note*:** In loop-B, the single-volume component no. 328 for SG steam line is joined to the single-volume component no. 332 for SG steam line through the valve junction component no. 329 for SG MSIV. In loop-B, a motor valve employed for SG MSIV is controlled not to reopen after being closed following a reactor scram signal because the initial position is set to 1.0 according to two trip cards no. 597 and 501.

location: SG steam line in loop-A
component no. (ccc): 532 component type: snglvol (i.e., single-volume [SV])

length	vol. flow area	inclination	elevation chg.	wall roughness	hydraulic dia.
31.8 m	0.9747 m^2	-79.83 deg	-31.3 m	3.33d-5	0.643 m

***Note*:** The single-volume component no. 532 is part of modeled SG steam line in loop-A.

location: SG steam line in loop-B
component no. (ccc): 332 component type: snglvol (i.e., single-volume [SV])

length	vol. flow area	inclination	elevation chg.	wall roughness	hydraulic dia.
31.8 m	0.3249 m^2	-79.83 deg	-31.3 m	3.33d-5	0.643 m

***Note*:** The single-volume component no. 332 is part of modeled SG steam line in loop-B.

location: SG steam line valve in loop-A
component no. (ccc): 533 component type: valve (i.e., valve junction [motor valve: MTR])

from ccc-vv	to ccc	junct. area	forward flow coeff.	reverse flow coeff.	junct. hydraulic dia.
532-01	816	0.9747 m^2	0.0	0.0	0.643 m

valve type	open trip card no.	close trip card no.	valve chg. rate	initial position
mtrvlv (i.e., motor valve)	597	501	1.0 s^{-1}	1.0

***Note*:** In loop-A, the single-volume component no. 532 for SG steam line is joined to the time-dependent volume component no. 816 for the connection to SG steam line through the valve junction component no. 533 for SG steam line valve. In loop-A, a motor valve employed for SG main steam line valve is controlled not to reopen after being closed following a reactor scram signal because the initial position is set to 1.0 according to two trip cards no. 597 and 501.

location: SG steam line valve in loop-B

component no. (ccc): 333 component type: valve (i.e., valve junction [motor valve: MTR])

from ccc-vv	to ccc	junct. area	forward flow coeff.	reverse flow coeff.	junct. hydraulic dia.
332-01	820	0.3249 m^2	0.0	0.0	0.643 m

valve type	open trip card no.	close trip card no.	valve chg. rate	initial position
mtrvlv (i.e., motor valve)	597	501	1.0 s^{-1}	1.0

***Note*:** In loop-B, the single-volume component no. 332 for SG steam line is joined to the time-dependent volume component no. 820 for the connection to SG steam line through the valve junction component no. 333 for SG steam line valve. In loop-B, a motor valve employed for SG main steam line valve is controlled not to reopen after being closed following a reactor scram signal because the initial position is set to 1.0 according to two trip cards no. 597 and 501.

location: connection to SG steam line in loop-A

component no. (ccc): 816 component type: tmdpvol (i.e., time-dependent volume [TDV])

length	vol. flow area	inclination	elevation chg.	wall roughness	hydraulic dia.
10.0 m	3.0d+8 m^2	0.0 deg	0.0 m	0.0	0.643 m

time	pressure	quality
0.0 s	5.99d+6 Pa	1.0

***Note*:** The time-dependent volume component no. 816 models the connection to SG steam line in loop-A.

location: connection to SG steam line in loop-B

component no. (ccc): 820 component type: tmdpvol (i.e., time-dependent volume [TDV])

length	vol. flow area	inclination	elevation chg.	wall roughness	hydraulic dia.
10.0 m	1.0d+8 m^2	0.0 deg	0.0 m	0.0	0.643 m

time	pressure	quality
0.0 s	5.99d+6 Pa	1.0

***Note*:** The time-dependent volume component no. 820 models the connection to SG steam line in loop-B.

location: connection to SG AFW line in loop-A

component no. (ccc): 550 component type: tmdpvol (i.e., time-dependent volume [TDV])

length	volume	inclination	elevation chg.	wall roughness	hydraulic dia.
10.0 m	300.0 m^3	0.0 deg	0.0 m	0.0	3.568 m

time	pressure	temperature
0.0 s	6.1d+6 Pa	493.17 K

***Note*:** The time-dependent volume component no. 550 models the connection to SG AFW line in loop-A.

location: connection to SG AFW line in loop-B

component no. (ccc): 350 component type: tmdpvol (i.e., time-dependent volume [TDV])

length	volume	inclination	elevation chg.	wall roughness	hydraulic dia.
10.0 m	100.0 m^3	0.0 deg	0.0 m	0.0	3.568 m

time	pressure	temperature
0.0 s	6.1d+6 Pa	493.17 K

***Note*:** The time-dependent volume component no. 350 models the connection to SG AFW line in loop-B.

location: SG AFW line in loop-A

component no. (ccc): 551 component type: tmdpjun (i.e., time-dependent junction [TDJ])

from ccc	to ccc-vv	junction area	trip card no.
550	512-01	0.201 m^2	644
time	mass flow rate	time	mass flow rate
0.0 s	91.5 kg/s	1.0d+4 s	91.5 kg/s

***Note*:** In loop-A, the time-dependent junction component no. 551 indicates that the time-dependent volume component no. 550 for the connection to SG AFW line is joined to the pipe component no. 512 for SG riser. The mass flow rate of SG AFW line in loop-A is given as constant value, relying on a trip card no. 644.

location: SG AFW line in loop-B

component no. (ccc): 351 component type: tmdpjun (i.e., time-dependent junction [TDJ])

from ccc	to ccc-vv	junction area	trip card no.
350	312-01	0.067 m^2	648
time	mass flow rate	time	mass flow rate
0.0 s	30.5 kg/s	1.0d+4 s	30.5 kg/s

***Note*:** In loop-B, the time-dependent junction component no. 351 indicates that the time-dependent volume component no. 350 for the connection to SG AFW line is joined to the pipe component no. 312 for SG riser. The mass flow rate of SG AFW line in loop-B is given as constant value, relying on a trip card no. 648.

location: connection to SG main feedwater line in loop-A

component no. (ccc): 560 component type: tmdpvol (i.e., time-dependent volume [TDV])

length	volume	inclination	elevation chg.	wall roughness	hydraulic dia.
10.0 m	300.0 m^3	0.0 deg	0.0 m	0.0	3.568 m
time	pressure	temperature			
0.0 s	6.1d+6 Pa	493.17 K			

***Note*:** The time-dependent volume component no. 560 models the connection to SG main feedwater line in loop-A.

location: connection to SG main feedwater line in loop-B

component no. (ccc): 360 component type: tmdpvol (i.e., time-dependent volume [TDV])

length	volume	inclination	elevation chg.	wall roughness	hydraulic dia.
10.0 m	100.0 m^3	0.0 deg	0.0 m	0.0	3.568 m
time	pressure	temperature			
0.0 s	6.1d+6 Pa	493.17 K			

***Note*:** The time-dependent volume component no. 360 models the connection to SG main feedwater line in loop-B.

location: SG main feedwater line in loop-A

component no. (ccc): 561 component type: tmdpjun (i.e., time-dependent junction [TDJ])

from ccc	to ccc-vv	junction area	trip card no.	variable parameter
560	512-01	0.201 m^2	0	cntrlvar 531
control value	liquid mass flow rate	control value	liquid mass flow rate	
-1.0 (-)	0.0 kg/s	0.0 (-)	1399.7 kg/s	
control value	liquid mass flow rate			
1.0 (-)	2799.6 kg/s			

***Note*:** In loop-A, the time-dependent junction component no. 561 indicates that the time-dependent volume component no. 560 for the connection to SG main feedwater line is joined to the pipe component no. 512 for SG riser. A set of data consist of the control value as the search variable, followed by the liquid mass flow rate. Setting a trip card no. to zero means no trip. To control the liquid mass flow rate of SG main feedwater line in loop-A, the opening degree of SG main feedwater valve computed in the 'cntrlvar 531' is determined by the difference between SG reference secondary liquid level and SG secondary narrow-range liquid level. Here, SG main feedwater system in loop-A is stopped when the control value is set to -1.0.

location: SG main feedwater line in loop-B

component no. (ccc): 361 component type: tmdpjun (i.e., time-dependent junction [TDJ])

from ccc	to ccc-vv	junction area	trip card no.	variable parameter
360	312-01	0.067 m^2	0	cntrlvar 331

control value	liquid mass flow rate	control value	liquid mass flow rate
-1.0 (-)	0.0 kg/s	0.0 (-)	466.6 kg/s
control value	liquid mass flow rate		
1.0 (-)	933.2 kg/s		

***Note*:** In loop-B, the time-dependent junction component no. 361 indicates that the time-dependent volume component no. 360 for the connection to SG main feedwater line is joined to the pipe component no. 312 for SG riser. A set of data consist of the control value as the search variable, followed by the liquid mass flow rate. Setting a trip card no. to zero means no trip. To control the liquid mass flow rate of SG main feedwater line in loop-B, the opening degree of SG main feedwater valve computed in the 'cntrlvar 331' is determined by the difference between SG reference secondary liquid level and SG secondary narrow-range liquid level. Here, SG main feedwater system in loop-B is stopped when the control value is set to -1.0.

location: SG relief valve in loop-A

component no. (ccc): 569 component type: valve (i.e., valve junction [trip valve: TRP])

from ccc-vv	to ccc	junct. area	forward flow coeff.	reverse flow coeff.	junct. hydraulic dia.
520-01	570	11.7375d-3 m^2	0.0149	0.0	0.07058 m

valve type	trip card no.
tripvlv (i.e., trip valve)	633

***Note*:** In loop-A, the branch component no. 520 for SG steam line is joined to the time-dependent volume component no. 570 for the connection to SG relief valve through the valve junction component no. 569 for SG relief valve. In loop-A, a trip valve employed for SG relief valve is open or closed, relying on a trip card no. 633.

location: SG relief valve in loop-B

component no. (ccc): 369 component type: valve (i.e., valve junction [trip valve: TRP])

from ccc-vv	to ccc	junct. area	forward flow coeff.	reverse flow coeff.	junct. hydraulic dia.
320-01	370	3.9125d-3 m^2	0.0149	0.0	0.07058 m

valve type	trip card no.
tripvlv (i.e., trip valve)	639

***Note*:** In loop-B, the branch component no. 320 for SG steam line is joined to the time-dependent volume component no. 370 for the connection to SG relief valve through the valve junction component no. 369 for SG relief valve. In loop-B, a trip valve employed for SG relief valve is open or closed, relying on a trip card no. 639.

location: connection to SG relief valve in loop-A

component no. (ccc): 570 component type: tmdpvol (i.e., time-dependent volume [TDV])

length	vol. flow area	inclination	elevation chg.	wall roughness	hydraulic dia.
10.0 m	3.0d+8 m^2	0.0 deg	0.0 m	0.0	0.0 m

time	pressure	temperature
0.0 s	1.01325d+5 Pa	293.15 K

***Note*:** The time-dependent volume component no. 570 models the connection to SG relief valve in loop-A.

location: connection to SG relief valve in loop-B

component no. (ccc): 370 component type: tmdpvol (i.e., time-dependent volume [TDV])

length	vol. flow area	inclination	elevation chg.	wall roughness	hydraulic dia.
10.0 m	1.0d+8 m^2	0.0 deg	0.0 m	0.0	0.0 m

time	pressure	temperature
0.0 s	1.01325d+5 Pa	293.15 K

***Note*:** The time-dependent volume component no. 370 models the connection to SG relief valve in loop-B.

location: SG safety valve in loop-A

component no. (ccc): 579 component type: valve (i.e., valve junction [trip valve: TRP])

from ccc-vv	to ccc	junct. area	forward flow coeff.	reverse flow coeff.	junct. hydraulic dia.
524-01	580	11.0077d-2 m^2	0.0149	0.0	0.21614 m

valve type	trip card no.
tripvlv (i.e., trip valve)	653

***Note*:** In loop-A, the branch component no. 524 for SG steam line is joined to the time-dependent volume component no. 580 for the connection to SG safety valve through the valve junction component no. 579 for SG safety valve. In loop-A, a trip valve employed for SG safety valve is open or closed, relying on a trip card no. 653.

location: SG safety valve in loop-B

component no. (ccc): 379 component type: valve (i.e., valve junction [trip valve: TRP])

from ccc-vv	to ccc	junct. area	forward flow coeff.	reverse flow coeff.	junct. hydraulic dia.
324-01	380	3.66992d-2 m^2	0.0149	0.0	0.21614 m

valve type	trip card no.
tripvlv (i.e., trip valve)	659

***Note*:** In loop-B, the branch component no. 324 for SG steam line is joined to the time-dependent volume component no. 380 for the connection to SG safety valve through the valve junction component no. 379 for SG safety valve. In loop-B, a trip valve employed for SG safety valve is open or closed, relying on a trip card no. 659.

location: connection to SG safety valve in loop-A

component no. (ccc): 580 component type: tmdpvol (i.e., time-dependent volume [TDV])

length	vol. flow area	inclination	elevation chg.	wall roughness	hydraulic dia.
10.0 m	3.0d+8 m^2	0.0 deg	0.0 m	0.0	0.0 m

time	pressure	temperature
0.0 s	1.01325d+5 Pa	293.15 K

***Note*:** The time-dependent volume component no. 580 models the connection to SG safety valve in loop-A.

location: connection to SG safety valve in loop-B

component no. (ccc): 380 component type: tmdpvol (i.e., time-dependent volume [TDV])

length	vol. flow area	inclination	elevation chg.	wall roughness	hydraulic dia.
10.0 m	1.0d+8 m^2	0.0 deg	0.0 m	0.0	0.0 m

time	pressure	temperature
0.0 s	1.01325d+5 Pa	293.15 K

***Note*:** The time-dependent volume component no. 380 models the connection to SG safety valve in loop-B.

location: PZR surge line

component no. (ccc): 600 component type: pipe (i.e., pipe [P]) number of volumes: 9

ccc-vv	length	vol. flow area	inclination	elevation chg.	wall roughness	hydraulic dia.
600-01	0.76 m	0.063436 m^2	-90.0 deg	-0.76 m	4.57d-5	0.0 m
600-02	1.3577 m	0.063436 m^2	-45.0 deg	-0.96 m	4.57d-5	0.0 m
600-03	1.74 m	0.063436 m^2	-1.068 deg	-0.0324 m	4.57d-5	0.0 m
600-04	4.6 m	0.063436 m^2	-1.068 deg	-0.0857 m	4.57d-5	0.0 m
600-05	5.1 m	0.063436 m^2	-1.068 deg	-0.0951 m	4.57d-5	0.0 m
600-06	3.585 m	0.063436 m^2	-1.068 deg	-0.0668 m	4.57d-5	0.0 m
600-07	1.3576 m	0.063436 m^2	-45.0 deg	-0.96 m	4.57d-5	0.0 m
600-08	1.24 m	0.063436 m^2	-90.0 deg	-1.24 m	4.57d-5	0.0 m
600-09	0.5657 m	0.063436 m^2	-45.0 deg	-0.4 m	4.57d-5	0.0 m

forward flow coeff.	reverse flow coeff.	junction hydraulic dia.	junction no.
0.061	0.061	0.2842 m	01-02
0.122	0.122	0.2842 m	03-04
0.061	0.061	0.2842 m	05-08

***Note*:** The pipe component no. 600 for PZR surge line consists of nine divided volumes with different inclination angles and lengths.

location: PZR to its surge line

component no. (ccc): 603 component type: sngljun (i.e., single-junction [SJ])

from ccc-vv	to ccc-vv	junct. area	forward flow coeff.	reverse flow coeff.	junct. hydraulic dia.
610-10	600-01	0.0 m^2	0.0	0.0	0.2842 m

***Note*:** The single-junction component no. 603 indicates that the pipe component no. 610 for PZR is joined to the pipe component no. 600 for PZR surge line.

location: PZR

component no. (ccc): 610 component type: pipe (i.e., pipe [P]) number of volumes: 10

ccc-vv	length	volume	inclination	elevation chg.	wall roughness	hydraulic dia.
610-01	1.05 m	2.4382 m^3	-90.0 deg	-1.05 m	4.57d-5	0.0 m
610-02	1.61 m	5.5764 m^3	-90.0 deg	-1.61 m	4.57d-5	0.0 m
610-03	1.61 m	5.5764 m^3	-90.0 deg	-1.61 m	4.57d-5	0.0 m
610-04	1.61 m	5.5764 m^3	-90.0 deg	-1.61 m	4.57d-5	0.0 m
610-05	1.61 m	5.5764 m^3	-90.0 deg	-1.61 m	4.57d-5	0.0 m
610-06	1.61 m	5.5764 m^3	-90.0 deg	-1.61 m	4.57d-5	0.0 m
610-07	1.61 m	5.5764 m^3	-90.0 deg	-1.61 m	4.57d-5	0.0 m
610-08	1.61 m	5.5764 m^3	-90.0 deg	-1.61 m	4.57d-5	0.0 m
610-09	1.61 m	5.5764 m^3	-90.0 deg	-1.61 m	4.57d-5	0.0 m
610-10	1.57 m	4.1564 m^3	-90.0 deg	-1.57 m	4.57d-5	0.0 m

forward flow coeff.	reverse flow coeff.	junction hydraulic dia.	junction no.
0.0	0.0	1.719 m	01
0.0	0.0	2.1 m	02-08
0.0	0.0	1.836 m	09

***Note*:** The pipe component no. 610 for PZR consists of ten vertically divided volumes with different lengths.

location: PZR spray line valve

component no. (ccc): 621 component type: valve (i.e., valve junction [trip valve: TRP])

from ccc-vv	to ccc-vv	junct. area	forward flow coeff.	reverse flow coeff.	junct. hydraulic dia.
444-01	620-01	0.00599 m^2	0.0	0.0	0.0873 m

valve type	trip card no.
tripvlv (i.e., trip valve)	598

***Note*:** In loop-A, the branch component no. 444 for cold leg is joined to the pipe component no. 620 for PZR spray line through the valve junction component no. 621 for PZR spray line valve. A trip valve employed for PZR spray line valve is always controlled to be closed according to a trip card no. 598.

location: PZR spray line

component no. (ccc): 620 component type: pipe (i.e., pipe [P]) number of volumes: 2

ccc-vv	length	vol. flow area	inclination	elevation chg.	wall roughness	hydraulic dia.
620-01	20.12 m	0.00599 m^2	90.0 deg	20.12 m	3.33d-5	0.0873 m
620-02	6.7 m	0.00599 m^2	0.0 deg	0.0 m	3.33d-5	0.0873 m

forward flow coeff.	reverse flow coeff.	junction hydraulic dia.	junction no.
0.0	0.0	0.0873 m	01

***Note*:** The pipe component no. 620 for PZR spray line consists of two divided volumes with different inclination angles and lengths.

location: PZR spray line valve

component no. (ccc): 622 component type: valve (i.e., valve junction [servo valve: SRV])

from ccc-vv	to ccc-vv	junct. area	forward flow coeff.	reverse flow coeff.	junct. hydraulic dia.
620-02	610-01	0.00599 m^2	0.0	0.0	0.0873 m

valve type	valve table no.
srvvlv (i.e., servo valve)	670

***Note*:** The pipe component no. 620 for PZR spray line is joined to the pipe component no. 610 for PZR through the valve junction component no. 622 for PZR spray line valve. The valve table no. 670 (i.e., the 'cntrlvar 670') presents the opening degree of the valve junction component no. 622. Regarding the control of the opening degree of PZR spray line valve, the 'cntrlvar 670' involves the 'cntrlvar 669' which concerns the control of the valve opening degree. The 'cntrlvar 666' concerning a reactor scram occurs or not. A servo valve employed for PZR spray line valve is always controlled to be closed through these control variable commands of 'cntrlvar 670', 'cntrlvar 669', and 'cntrlvar 666'.

location: connection to PZR PORV

component no. (ccc): 650 component type: tmdpvol (i.e., time-dependent volume [TDV])

length	vol. flow area	inclination	elevation chg.	wall roughness	hydraulic dia.
10.0 m	10.0 m^2	0.0 deg	0.0 m	0.0	0.0 m

time	pressure	temperature
0.0 s	1.01325d+5 Pa	293.15 K

***Note*:** The time-dependent volume component no. 650 models the connection to PZR PORV.

location: PZR PORV

component no. (ccc): 651 component type: valve (i.e., valve junction [trip valve: TRP])

from ccc-vv	to ccc	junct. area	forward flow coeff.	reverse flow coeff.	junct. hydraulic dia.
610-01	650	0.0029279 m^2	0.0251	0.0	0.06106 m

valve type	trip card no.
tripvlv (i.e., trip valve)	626

***Note*:** The pipe component no. 610 for PZR is joined to the time-dependent volume component no. 650 for the connection to PZR PORV through the valve junction component no. 651 for PZR PORV. A trip valve employed for PZR PORV is open or closed, relying on a trip card no. 626.

location: connection to PZR safety valve

component no. (ccc): 660 component type: tmdpvol (i.e., time-dependent volume [TDV])

length	vol. flow area	inclination	elevation chg.	wall roughness	hydraulic dia.
10.0 m	1.0d+8 m^2	0.0 deg	0.0 m	0.0	0.0 m

time	pressure	temperature
0.0 s	1.01325d+5 Pa	293.15 K

***Note*:** The time-dependent volume component no. 660 models the connection to PZR safety valve.

location: PZR safety valve

component no. (ccc): 661 component type: valve (i.e., valve junction [trip valve: TRP])

from ccc-vv	to ccc	junct. area	forward flow coeff.	reverse flow coeff.	junct. hydraulic dia.
610-01	660	0.005393 m^2	0.2052	0.0	0.08286 m

valve type	trip card no.
tripvlv (i.e., trip valve)	615

***Note*:** The pipe component no. 610 for PZR is joined to the time-dependent volume component no. 660 for the connection to PZR safety valve through the valve junction component no. 661 for PZR safety valve. A trip valve employed for PZR safety valve is open or closed, relying on a trip card no. 615.

location: ACC tank in loop-A

component no. (ccc): 700 component type: accum (i.e., ACC [ACC])

length	volume	inclination	elevation chg.	wall roughness	hydraulic dia.
4.81 m	114.0 m^3	90.0 deg	4.81 m	3.33d-5	1.5865 m

pressure	temperature	to ccc	forward flow coeff.	reverse flow coeff.	junction area
4.51d+6 Pa	320.0 K	710	0.0	0.0	0.13257 m^2

liquid volume	liquid level	length of surgeline and standpipe	elevation drop	thickness
75.9 m^3	0.0 m	20.0 m	3.5 m	5.0d-2 m
heat transfer flag	density	specific heat capacity	trip card no.	
0	7820.0 kg/m^3	493.73 J/kg･K	505	

***Note*:** In loop-A, the ACC component no. 700 for ACC tank is connected to the single-volume component no. 710 for ACC system. In loop-A, the liquid level in the ACC tank is computed from the liquid volume and the length of the surgeline and standpipe because it is set to zero. The heat transfer is calculated because the heat transfer flag is set to zero. The pressure and temperature of ACC tank in loop-A are 4.51 MPa and 320 K, respectively.

location: ACC tank in loop-B

component no. (ccc): 705 component type: accum (i.e., ACC [ACC])

length	volume	inclination	elevation chg.	wall roughness	hydraulic dia.
4.81 m	38.0 m^3	90.0 deg	4.81 m	3.33d-5	1.5865 m
pressure	temperature	to ccc	forward flow coeff.	reverse flow coeff.	junction area
4.51d+6 Pa	320.0 K	715	0.0	0.0	0.04419 m^2
liquid volume	liquid level	length of surgeline and standpipe	elevation drop	thickness	
25.3 m^3	0.0 m	20.0 m	3.5 m	5.0d-2 m	
heat transfer flag	density	specific heat capacity	trip card no.		
0	7820.0 kg/m^3	493.73 J/kg･K	505		

***Note*:** In loop-B, the ACC component no. 705 for ACC tank is connected to the single-volume component no. 715 for ACC system. In loop-B, the liquid level in the ACC tank is computed from the liquid volume and the length of the surgeline and standpipe because it is set to zero. The heat transfer is calculated because the heat transfer flag is set to zero. The pressure and temperature of ACC tank in loop-B are 4.51 MPa and 320 K, respectively.

location: ACC system in loop-A

component no. (ccc): 710 component type: snglvol (i.e., single-volume [SV])

length	vol. flow area	inclination	elevation chg.	wall roughness	hydraulic dia.
15.0 m	0.13257 m^2	0.0 deg	0.0 m	3.33d-5	0.2372 m

***Note*:** The single-volume component no. 710 is part of modeled ACC system in loop-A.

location: ACC system in loop-B

component no. (ccc): 715 component type: snglvol (i.e., single-volume [SV])

length	vol. flow area	inclination	elevation chg.	wall roughness	hydraulic dia.
15.0 m	0.04419 m^2	0.0 deg	0.0 m	3.33d-5	0.2372 m

***Note*:** The single-volume component no. 715 is part of modeled ACC system in loop-B.

location: ACC tank outlet valve in loop-A

component no. (ccc): 712 component type: valve (i.e., valve junction [trip valve: TRP])

from ccc-vv	to ccc-vv	junct. area	forward flow coeff.	reverse flow coeff.	junct. hydraulic dia.
710-01	726-01	0.13257 m^2	10.0	10.0	0.2372 m
valve type		trip card no.			
tripvlv (i.e., trip valve)		618			

***Note*:** In loop-A, the single-volume component no. 710 for ACC system is joined to the branch component no. 726 for ACC system through the valve junction component no. 712 for ACC tank outlet valve. In loop-A, a trip valve employed for ACC tank outlet valve is open or closed, relying on a trip card no. 618.

location: ACC tank outlet valve in loop-B

component no. (ccc): 711 component type: valve (i.e., valve junction [trip valve: TRP])

from ccc-vv	to ccc-vv	junct. area	forward flow coeff.	reverse flow coeff.	junct. hydraulic dia.
715-01	725-01	0.04419 m^2	10.0	10.0	0.2372 m
valve type		trip card no.			
tripvlv (i.e., trip valve)		619			

***Note*:** In loop-B, the single-volume component no. 715 for ACC system is joined to the branch component no. 725 for ACC system through the valve junction component no. 711 for ACC tank outlet valve. In loop-B, a trip valve employed for ACC tank outlet valve is open or closed, relying on a trip card no. 619.

location: ACC system in loop-A

component no. (ccc): 726 component type: branch (i.e., branch [B]) number of junct.: 1

length	vol. flow area	inclination	elevation chg.	wall roughness	hydraulic dia.
5.0 m	0.13257 m^2	0.0 deg	0.0 m	3.33d-5	0.2372 m

from ccc-vv	to ccc-vv	junct. area	forward flow coeff.	reverse flow coeff.	junct. hydraulic dia.
726-01	448-01	0.13257 m^2	0.0	0.0	0.2372 m

***Note*:** In loop-A, the branch component no. 726 for ACC system is conjunctive with the branch component no. 448 for cold leg.

location: ACC system in loop-B

component no. (ccc): 725 component type: branch (i.e., branch [B]) number of junct.: 1

length	vol. flow area	inclination	elevation chg.	wall roughness	hydraulic dia.
5.0 m	0.04419 m^2	0.0 deg	0.0 m	3.33d-5	0.2372 m

from ccc-vv	to ccc-vv	junct. area	forward flow coeff.	reverse flow coeff.	junct. hydraulic dia.
725-01	248-01	0.04419 m^2	0.0	0.0	0.2372 m

***Note*:** In loop-B, the branch component no. 725 for ACC system is conjunctive with the branch component no. 248 for cold leg.

location: connection to HPI system in loop-A

component no. (ccc): 720 component type: tmdpvol (i.e., time-dependent volume [TDV])

length	volume	inclination	elevation chg.	wall roughness	hydraulic dia.
10.0 m	300.0 m^3	0.0 deg	0.0 m	0.0	0.2372 m

time	pressure	temperature
0.0 s	1.01325d+5 Pa	310.0 K

***Note*:** The time-dependent volume component no. 720 models the connection to HPI system in loop-A. The temperature of HPI system in loop-A is 310 K.

location: connection to HPI system in loop-B

component no. (ccc): 770 component type: tmdpvol (i.e., time-dependent volume [TDV])

length	volume	inclination	elevation chg.	wall roughness	hydraulic dia.
10.0 m	100.0 m^3	0.0 deg	0.0 m	0.0	0.2372 m

time	pressure	temperature
0.0 s	1.01325d+5 Pa	310.0 K

***Note*:** The time-dependent volume component no. 770 models the connection to HPI system in loop-B. The temperature of HPI system in loop-B is 310 K.

location: HPI system in loop-A

component no. (ccc): 721 component type: tmdpjun (i.e., time-dependent junction [TDJ])

from ccc	to ccc-vv	junction area	trip card no.	variable parameter
720	745-01	0.13257 m^2	683	p 116010000

pressure	mass flow rate	pressure	mass flow rate
0.101325d+6 Pa	66.993 kg/s	0.493591d+6 Pa	66.009 kg/s
pressure	mass flow rate	pressure	mass flow rate
0.691649d+6 Pa	65.472 kg/s	0.925084d+6 Pa	64.989 kg/s
pressure	mass flow rate	pressure	mass flow rate
1.08199d+6 Pa	64.878 kg/s	2.06266d+6 Pa	61.68 kg/s
pressure	mass flow rate	pressure	mass flow rate
4.02399d+6 Pa	54.705 kg/s	5.98532d+6 Pa	46.62 kg/s
pressure	mass flow rate	pressure	mass flow rate
7.94665d+6 Pa	36.369 kg/s	9.90798d+6 Pa	19.59 kg/s

pressure	mass flow rate	pressure	mass flow rate
11.8693d+6 Pa	16.713 kg/s	13.8306d+6 Pa	13.338 kg/s

***Note*:** In loop-A, the time-dependent junction component no. 721 indicates that the time-dependent volume component no. 720 for the connection to HPI system is joined to the single-volume component no. 745 for ECCS line. The mass flow rate of HPI system in loop-A changes in response to pressure of the branch component no. 116 for lower plenum, relying on a trip card no. 683. The HPI flow rate in loop-A is set referring to the previous study's calculation for the loss of ECCS recirculation functions event, as the base case. The HPI system in loop-A is stopped 1140 s after break. Next, the HPI system in loop-A is restarted 440 s after stopping, for the alternative recirculation water injection.

location: HPI system in loop-B

component no. (ccc): 771 component type: tmdpjun (i.e., time-dependent junction [TDJ])

from ccc	to ccc-vv	junction area	trip card no.	variable parameter
770	775-01	0.04419 m^2	683	p 116010000

pressure	mass flow rate	pressure	mass flow rate
0.101325d+6 Pa	22.331 kg/s	0.493591d+6 Pa	22.003 kg/s
pressure	mass flow rate	pressure	mass flow rate
0.691649d+6 Pa	21.824 kg/s	0.925084d+6 Pa	21.663 kg/s
pressure	mass flow rate	pressure	mass flow rate
1.08199d+6 Pa	21.626 kg/s	2.06266d+6 Pa	20.56 kg/s
pressure	mass flow rate	pressure	mass flow rate
4.02399d+6 Pa	18.235 kg/s	5.98532d+6 Pa	15.54 kg/s
pressure	mass flow rate	pressure	mass flow rate
7.94665d+6 Pa	12.123 kg/s	9.90798d+6 Pa	6.53 kg/s
pressure	mass flow rate	pressure	mass flow rate
11.8693d+6 Pa	5.571 kg/s	13.8306d+6 Pa	4.446 kg/s

***Note*:** In loop-B, the time-dependent junction component no. 771 indicates that the time-dependent volume component no. 770 for the connection to HPI system is joined to the single-volume component no. 775 for ECCS line. The mass flow rate of HPI system in loop-B changes in response to pressure of the branch component no. 116 for lower plenum, relying on a trip card no. 683. The HPI flow rate in loop-B is set referring to the previous study's calculation for the loss of ECCS recirculation functions event, as the base case. The HPI system in loop-B is stopped 1140 s after break. Next, the HPI system in loop-B is restarted 440 s after stopping, for the alternative recirculation water injection.

location: connection to LPI system in loop-A

component no. (ccc): 750 component type: tmdpvol (i.e., time-dependent volume [TDV])

length	volume	inclination	elevation chg.	wall roughness	hydraulic dia.
10.0 m	300.0 m^3	0.0 deg	0.0 m	0.0	0.2372 m
time	pressure		temperature		
0.0 s	1.01325d+5 Pa		310.0 K		

***Note*:** The time-dependent volume component no. 750 models the connection to LPI system in loop-A. The temperature of LPI system in loop-A is 310 K.

location: connection to LPI system in loop-B

component no. (ccc): 760 component type: tmdpvol (i.e., time-dependent volume [TDV])

length	volume	inclination	elevation chg.	wall roughness	hydraulic dia.
10.0 m	100.0 m^3	0.0 deg	0.0 m	0.0	0.2372 m
time	pressure		temperature		
0.0 s	1.01325d+5 Pa		310.0 K		

***Note*:** The time-dependent volume component no. 760 models the connection to LPI system in loop-B. The temperature of LPI system in loop-B is 310 K.

location: LPI system in loop-A

component no. (ccc): 751 component type: tmdpjun (i.e., time-dependent junction [TDJ])

from ccc	to ccc-vv	junction area	trip card no.	variable parameter
750	745-01	0.13257 m^2	684	p 116010000
pressure	mass flow rate	pressure	mass flow rate	
0.0 Pa	300.0 kg/s	0.99d+6 Pa	300.0 kg/s	
pressure	mass flow rate	pressure	mass flow rate	
1.15d+6 Pa	180.0 kg/s	1.22d+6 Pa	0.0 kg/s	

***Note*:** In loop-A, the time-dependent junction component no. 751 indicates that the time-dependent volume component no. 750 for the connection to LPI system is joined to the single-volume component no. 745 for ECCS line. The mass flow rate of LPI system in loop-A changes in response to pressure of the branch component no. 116 for lower plenum, relying on a trip card no. 684. The LPI flow rate in loop-A is set referring to the previous study's calculation for the loss of ECCS recirculation functions event, as the base case. The LPI system in loop-A is stopped 1140 s after break. Next, the LPI system in loop-A is restarted 440 s after stopping, for the alternative recirculation water injection.

location: LPI system in loop-B

component no. (ccc): 761 component type: tmdpjun (i.e., time-dependent junction [TDJ])

from ccc	to ccc-vv	junction area	trip card no.	variable parameter
760	775-01	0.04419 m^2	684	p 116010000
pressure	mass flow rate	pressure	mass flow rate	
0.0 Pa	100.0 kg/s	0.99d+6 Pa	100.0 kg/s	
pressure	mass flow rate	pressure	mass flow rate	
1.15d+6 Pa	60.0 kg/s	1.22d+6 Pa	0.0 kg/s	

***Note*:** In loop-B, the time-dependent junction component no. 761 indicates that the time-dependent volume component no. 760 for the connection to LPI system is joined to the single-volume component no. 775 for ECCS line. The mass flow rate of LPI system in loop-B changes in response to pressure of the branch component no. 116 for lower plenum, relying on a trip card no. 684. The LPI flow rate in loop-B is set referring to the previous study's calculation for the loss of ECCS recirculation functions event, as the base case. The LPI system in loop-B is stopped 1140 s after break. Next, the LPI system in loop-B is restarted 440 s after stopping, for the alternative recirculation water injection.

location: ECCS line in loop-A

component no. (ccc): 745 component type: snglvol (i.e., single-volume [SV])

length	vol. flow area	inclination	elevation chg.	wall roughness	hydraulic dia.
5.0 m	0.13257 m^2	0.0 deg	0.0 m	3.33d-5	0.2372 m

***Note*:** The single-volume component no. 745 is part of modeled ECCS line in loop-A.

location: ECCS line in loop-B

component no. (ccc): 775 component type: snglvol (i.e., single-volume [SV])

length	vol. flow area	inclination	elevation chg.	wall roughness	hydraulic dia.
5.0 m	0.04419 m^2	0.0 deg	0.0 m	3.33d-5	0.2372 m

***Note*:** The single-volume component no. 775 is part of modeled ECCS line in loop-B.

location: ECCS line in loop-A

component no. (ccc): 740 component type: branch (i.e., branch [B]) number of junct.: 2

length	vol. flow area	inclination	elevation chg.	wall roughness	hydraulic dia.
5.0 m	0.13257 m^2	0.0 deg	0.0 m	3.33d-5	0.2372 m

from ccc-vv	to ccc-vv	junct. area	forward flow coeff.	reverse flow coeff.	junct. hydraulic dia.
745-01	740-01	0.13257 m^2	0.0	0.0	0.2372 m
740-01	444-01	0.13257 m^2	0.0	0.0	0.2372 m

***Note*:** In loop-A, the branch component no. 740 for ECCS line is conjunctive with the single-volume component no. 745 for ECCS line and the branch component no. 444 for cold leg.

location: ECCS line in loop-B

component no. (ccc): 790 component type: branch (i.e., branch [B]) number of junct.: 2

length	vol. flow area	inclination	elevation chg.	wall roughness	hydraulic dia.
5.0 m	0.04419 m^2	0.0 deg	0.0 m	3.33d-5	0.2372 m

from ccc-vv	to ccc-vv	junct. area	forward flow coeff.	reverse flow coeff.	junct. hydraulic dia.
775-01	790-01	0.04419 m^2	0.0	0.0	0.2372 m
790-01	244-01	0.04419 m^2	0.0	0.0	0.2372 m

***Note*:** In loop-B, the branch component no. 790 for ECCS line is conjunctive with the single-volume component no. 775 for ECCS line and the branch component no. 244 for cold leg.

location: connection to environment

component no. (ccc): 900 component type: tmdpvol (i.e., time-dependent volume [TDV])

length	vol. flow area	inclination	elevation chg.	wall roughness	hydraulic dia.
100.0 m	2000.0 m^2	0.0 deg	0.0 m	0.0	0.0 m

time	pressure	temperature	quality
0.0 s	1.01325d+5 Pa	300.0 K	1.0

***Note*:** The time-dependent volume component no. 900 models the connection to environment (containment).

location: environment

component no. (ccc): 901 component type: sngljun (i.e., single-junction [SJ])

from ccc-vv	to ccc-vv	junct. area	forward flow coeff.	reverse flow coeff.	junct. hydraulic dia.
900-01	910-01	0.00741 m^2	0.0	0.0	0.09713 m

***Note*:** The single-junction component no. 901 indicates that the time-dependent volume component no. 900 for environment (containment) is joined to the single-volume component no. 910 for environment (containment).

location: environment

component no. (ccc): 910 component type: snglvol (i.e., single-volume [SV])

length	vol. flow area	inclination	elevation chg.	wall roughness	hydraulic dia.
1.0 m	10.0 m^2	0.0 deg	0.0 m	0.0	0.0 m

***Note*:** The single-volume component no. 910 is part of modeled environment (containment).

location: cold leg in loop-B

component no. (ccc): 249 component type: valve (i.e., valve junction [trip valve: TRP])

from ccc-vv	to ccc-vv	junct. area	forward flow coeff.	reverse flow coeff.	junct. hydraulic dia.
248-01	252-01	0.3832 m^2	0.0	0.0	0.6985 m

valve type	trip card no.
tripvlv (i.e., trip valve)	630

***Note*:** In loop-B, the branch component no. 248 for cold leg is joined to the pipe component no. 252 for cold leg through the valve junction component no. 249 for cold leg. In loop-B, a trip valve employed for cold leg is closed at time zero according to a trip card no. 630.

location: break at cold leg in loop-B

component no. (ccc): 941 component type: valve (i.e., valve junction [trip valve: TRP])

from ccc-vv	to ccc	junct. area	forward flow coeff.	reverse flow coeff.	junct. hydraulic dia.
248-01	942	0.3832 m^2	0.0	1.0d+6	0.6985 m

valve type	trip card no.	subcooled coeff.	two-phase coeff.	superheated coeff.
tripvlv (i.e., trip valve)	530	1.0	1.0	1.0

***Note*:** In loop-B, the branch component no. 248 for cold leg is joined to the time-dependent volume component no. 942 for the connection to break at cold leg through the valve junction component no. 941 for break. In loop-B, a trip valve employed for break at cold leg is open at time zero according to a trip card no. 530. All the subcooled, two-phase, and superheated coefficients are fixed to 1.0. A Cd through break is reflected in the junction area of the valve junction component no. 941. This junction area is used for the base case (i.e., Cd = 1.0). A large energy loss coefficient of 10^6 for the reverse flow in the junction between the two components

no. 248 and 942 is given to prevent the reverse flow in the junction between the two components.

location: break at cold leg in loop-B
component no. (ccc): 951 component type: valve (i.e., valve junction [trip valve: TRP])

from ccc-vv	to ccc	junct. area	forward flow coeff.	reverse flow coeff.	junct. hydraulic dia.
252-01	952	0.3832 m^2	0.0	1.0d+6	0.6985 m
valve type		trip card no.	subcooled coeff.	two-phase coeff.	superheated coeff.
tripvlv (i.e., trip valve)		530	1.0	1.0	1.0

***Note*:** In loop-B, the branch component no. 252 for cold leg is joined to the time-dependent volume component no. 952 for the connection to break at cold leg through the valve junction component no. 951 for break. In loop-B, a trip valve employed for break at cold leg is open at time zero according to a trip card no. 530. All the subcooled, two-phase, and superheated coefficients are fixed to 1.0. A Cd through break is reflected in the junction area of the valve junction component no. 951. This junction area is used for the base case (i.e., Cd = 1.0). A large energy loss coefficient of 10^6 for the reverse flow in the junction between the two components no. 252 and 952 is given to prevent the reverse flow in the junction between the two components.

location: connection to break at cold leg in loop-B
component no. (ccc): 942 component type: tmdpvol (i.e., time-dependent volume [TDV])

length	vol. flow area	inclination	elevation chg.	wall roughness	hydraulic dia.
10.0 m	1.0d+8 m^2	0.0 deg	0.0 m	0.0	0.0 m
time	pressure		temperature		
0.0 s	1.01325d+5 Pa		293.15 K		

***Note*:** The time-dependent volume component no. 942 models the connection to break at cold leg in loop-B, associated with the valve junction component no. 941 for the cold leg break.

location: connection to break at cold leg in loop-B
component no. (ccc): 952 component type: tmdpvol (i.e., time-dependent volume [TDV])

length	vol. flow area	inclination	elevation chg.	wall roughness	hydraulic dia.
10.0 m	1.0d+8 m^2	0.0 deg	0.0 m	0.0	0.0 m
time	pressure		temperature		
0.0 s	1.01325d+5 Pa		293.15 K		

***Note*:** The time-dependent volume component no. 952 models the connection to break at cold leg in loop-B, associated with the valve junction component no. 951 for the cold leg break.

E. Heat structure input (cards 1cccgxnn)

The heat structure card numbers are divided into fields, where ccc is the heat structure number, g is the geometry number, x is the card type, and nn is the card number within card type. Here, each of left and right boundary numbers of heat structure geometry number is represented by 'ppp-vv', 'ppp' or 'zero', where ppp is the component number and vv is the volume number.

Setting the boundary volume number to zero means a symmetry or insulated boundary condition (i.e., zero temperature gradient at the boundary).

The boundary condition for each heat structure geometry number is chosen length, surface area, or factor. The boundary condition for cylindrical and rectangular geometry is selected either the length or the surface area, while the boundary condition for spherical geometry is chosen the factor.

As for left and right boundary numbers of heat structure geometry number, the length, surface area, and factor for loop-A are three times as large as those for loop-B. This is because loop-A and loop-B simulate three loops and one loop, respectively.

The number of fuel rods in the PWR is 50952. On the other hand, the number of electric heater rods in the LSTF is 360, 180, and 468 for high-power, mean-power, and low-power heater rods, respectively. The radial power peaking factors in the LSTF are 1.51, 1.00, and 0.66 for high-power,

mean-power, and low-power heater rods, respectively.

The following base factor for the heat structure geometry no. for each fuel rod in the PWR is set referring to the number of electric heater rods and the radial power peaking factor in the LSTF.

A. The base factor for the heat structure geometry no. 1241 for high-power fuel rods is 0.5265. This value is calculated as (1.51*360)/(1.51*360+1.00*180+0.66*468).
B. The base factor for the heat structure geometry no. 1242 for mean-power fuel rods is 0.1743. This value is calculated as (1.00*180)/(1.51*360+1.00*180+0.66*468).
C. The base factor for the heat structure geometry no. 1243 for low-power fuel rods is 0.2992. This value is calculated as (0.66*468)/(1.51*360+1.00*180+0.66*468).

The following reference coefficient for axial heat structure end no. for each fuel rod in the PWR is set considering the axial power peaking factor in the LSTF.

a. The reference coefficient for each of axial structure end no. 1 and 9 is 0.04032. This value is calculated as 0.3633/(0.3633*2+0.8135*2+1.1736*2+1.4071*2+1.4945).
b. The reference coefficient for each of axial structure end no. 2 and 8 is 0.090294. This value is calculated as 0.8135/(0.3633*2+0.8135*2+1.1736*2+1.4071*2+1.4945).
c. The reference coefficient for each of axial structure end no. 3 and 7 is 0.130262. This value is calculated as 1.1736/(0.3633*2+0.8135*2+1.1736*2+1.4071*2+1.4945).
d. The reference coefficient for each of axial structure end no. 4 and 6 is 0.15618. This value is calculated as 1.4071/(0.3633*2+0.8135*2+1.1736*2+1.4071*2+1.4945).
e. The reference coefficient for axial structure end no. 5 is 0.16588. This value is calculated as 1.4945/(0.3633*2+0.8135*2+1.1736*2+1.4071*2+1.4945).

The internal source multiplier for each heat structure geometry no. for high-power, mean-power, and low-power fuel rods in the PWR shown below is obtained by multiplying the above base factor by the above reference coefficient.

heat structure geometry no. (cccg): 1241 (high-power fuel rods)

The number of high-power fuel rods is estimated to be 18197. This value is calculated as 360/(360+180+468)*50952. By multiplying 18197 by the length per each high-power fuel rod of 0.406666 m, the length of high-power fuel rods is 7400.101 m.

number of axial heat structures: 9 number of radial (r-) mesh points: 8
geometry type: 2 (i.e., cylindrical) left bound. coordinate: 0.0 m
reflood condition flag: 599 maximum number of axial intervals: 64
boundary volume indicator: 1 (Namely, reflood heat transfer applies to right boundary.)

number of r-intervals	right bound. coordinate	r-composition no.	temperature
4	0.004095 m	15 (i.e., uranium dioxide)	614.6 K
1	0.00418 m	16 (i.e., helium gas in gap)	614.6 K
2	0.00475 m	17 (i.e., zirconium)	614.6 K

left bound. no.	length [left bound.]	right bound. no.	length [right bound.]	inter. source multiplier
0	7400.101 m	124-01	7400.101 m	0.021230
0	7400.101 m	124-02	7400.101 m	0.047540
0	7400.101 m	124-03	7400.101 m	0.068583
0	7400.101 m	124-04	7400.101 m	0.082229
0	7400.101 m	124-05	7400.101 m	0.087336
0	7400.101 m	124-06	7400.101 m	0.082229
0	7400.101 m	124-07	7400.101 m	0.068583
0	7400.101 m	124-08	7400.101 m	0.047540
0	7400.101 m	124-09	7400.101 m	0.021230

***Note*:** The heat structure geometry no. 1241 for high-power fuel rods is cylindrical, being composed of uranium dioxide, helium gas in gap, and zirconium. Thus, for each of nine axial heat structures, the length of the left boundary no. zero is consistent with that of the right boundary no. 124 for core. The maximum number of the axial intervals is chosen 64 (i.e., 2 to the power of 6), considering the RELAP5 code's computational load and accuracy. The reflood

condition flag of 599 means that reflood model built into the RELAP5 code is used because the time is set to zero. Specifically, the reflood model is applied to the right boundary condition of heat structure geometry of high-power fuel rods.

heat structure geometry no. (cccg): 1242 (mean-power fuel rods)

The number of mean-power fuel rods is estimated to be 9099. This value is calculated as 180/(360+180+468)*50952. By multiplying 9099 by the length per each mean-power fuel rod of 0.406666 m, the length of mean-power fuel rods is 3700.254 m.

number of axial heat structures: 9 number of radial (r-) mesh points: 8
geometry type: 2 (i.e., cylindrical) left bound. coordinate: 0.0 m
reflood condition flag: 599 maximum number of axial intervals: 64
boundary volume indicator: 1 (Namely, reflood heat transfer applies to right boundary.)

number of r-intervals	right bound. coordinate	r-composition no.	temperature
4	0.004095 m	15 (i.e., uranium dioxide)	614.6 K
1	0.00418 m	16 (i.e., helium gas in gap)	614.6 K
2	0.00475 m	17 (i.e., zirconium)	614.6 K

left bound. no.	length [left bound.]	right bound. no.	length [right bound.]	inter. source multiplier
0	3700.254 m	124-01	3700.254 m	0.007028
0	3700.254 m	124-02	3700.254 m	0.015738
0	3700.254 m	124-03	3700.254 m	0.022705
0	3700.254 m	124-04	3700.254 m	0.027222
0	3700.254 m	124-05	3700.254 m	0.028913
0	3700.254 m	124-06	3700.254 m	0.027222
0	3700.254 m	124-07	3700.254 m	0.022705
0	3700.254 m	124-08	3700.254 m	0.015738
0	3700.254 m	124-09	3700.254 m	0.007028

***Note*:** The heat structure geometry no. 1242 for mean-power fuel rods is cylindrical, being composed of uranium dioxide, helium gas in gap, and zirconium. Thus, for each of nine axial heat structures, the length of the left boundary no. zero is consistent with that of the right boundary no. 124 for core. The maximum number of the axial intervals is chosen 64 (i.e., 2 to the power of 6), considering the RELAP5 code's computational load and accuracy. The reflood condition flag of 599 means that reflood model built into the RELAP5 code is used because the time is set to zero. Specifically, the reflood model is applied to the right boundary condition of heat structure geometry of mean-power fuel rods.

heat structure geometry no. (cccg): 1243 (low-power fuel rods)

The number of low-power fuel rods is estimated to be 23656. This value is calculated as 468/(360+180+468)*50952. By multiplying 23656 by the length per each low-power fuel rod of 0.406666 m, the length of low-power fuel rods is 9620.091 m.

number of axial heat structures: 9 number of radial (r-) mesh points: 8
geometry type: 2 (i.e., cylindrical) left bound. coordinate: 0.0 m
reflood condition flag: 599 maximum number of axial intervals: 64
boundary volume indicator: 1 (Namely, reflood heat transfer applies to right boundary.)

number of r-intervals	right bound. coordinate	r-composition no.	temperature
4	0.004095 m	15 (i.e., uranium dioxide)	614.6 K
1	0.00418 m	16 (i.e., helium gas in gap)	614.6 K
2	0.00475 m	17 (i.e., zirconium)	614.6 K

left bound. no.	length [left bound.]	right bound. no.	length [right bound.]	inter. source multiplier
0	9620.091 m	124-01	9620.091 m	0.012065
0	9620.091 m	124-02	9620.091 m	0.027016
0	9620.091 m	124-03	9620.091 m	0.038974
0	9620.091 m	124-04	9620.091 m	0.046729
0	9620.091 m	124-05	9620.091 m	0.049631
0	9620.091 m	124-06	9620.091 m	0.046729

0	9620.091 m	124-07	9620.091 m	0.038974
0	9620.091 m	124-08	9620.091 m	0.027016
0	9620.091 m	124-09	9620.091 m	0.012065

***Note*:** The heat structure geometry no. 1243 for low-power fuel rods is cylindrical, being composed of uranium dioxide, helium gas in gap, and zirconium. Thus, for each of nine axial heat structures, the length of the left boundary no. zero is consistent with that of the right boundary no. 124 for core. The maximum number of the axial intervals is chosen 64 (i.e., 2 to the power of 6), considering the RELAP5 code's computational load and accuracy. The reflood condition flag of 599 means that reflood model built into the RELAP5 code is used because the time is set to zero. Specifically, the reflood model is applied to the right boundary condition of heat structure geometry of low-power fuel rods.

heat structure geometry no. (cccg): 1081 (vessel DC wall)

number of axial heat structures: 15		number of radial (r-) mesh points: 8	
geometry type: 2 (i.e., cylindrical)		left bound. coordinate: 2.197 m	
number of r-intervals	right bound. coordinate	r-composition no.	temperature
1	2.201 m	5 (i.e., stainless steel)	562.0 K
4	2.417 m	6 (i.e., carbon steel)	562.0 K
2	2.617 m	12 (i.e., calcium silicate)	562.0 K
left bound. no.	length [left bound.]	right bound. no.	length [right bound.]
100-01	0.89695 m	900-01	0.89695 m
101-01	0.8248 m	900-01	0.8248 m
104-01	0.8245 m	900-01	0.8245 m
108-01	0.51075 m	900-01	0.51075 m
108-02	0.655 m	900-01	0.655 m
108-03	0.406666 m	900-01	0.406666 m
108-04	0.406666 m	900-01	0.406666 m
108-05	0.406666 m	900-01	0.406666 m
108-06	0.406666 m	900-01	0.406666 m
108-07	0.406666 m	900-01	0.406666 m
108-08	0.406666 m	900-01	0.406666 m
108-09	0.406666 m	900-01	0.406666 m
108-10	0.406666 m	900-01	0.406666 m
108-11	0.406666 m	900-01	0.406666 m
108-12	1.2588 m	900-01	1.2588 m

***Note*:** The heat structure geometry no. 1081 for vessel DC wall is cylindrical, being composed of stainless steel, carbon steel, and calcium silicate. Thus, for each of fifteen axial heat structures, the length of the left boundary no. 100, 101, 104, or 108 for vessel DC is consistent with that of the right boundary no. 900 for environment (containment).

heat structure geometry no. (cccg): 1161 (lower plenum shell)

number of axial heat structures: 1		number of radial (r-) mesh points: 8	
geometry type: 3 (i.e., spherical)		left bound. coordinate: 2.2316 m	
number of r-intervals	right bound. coordinate	r-composition no.	temperature
1	2.2356 m	5 (i.e., stainless steel)	562.0 K
4	2.3771 m	6 (i.e., carbon steel)	562.0 K
2	2.577 m	12 (i.e., calcium silicate)	562.0 K
left bound. no.	factor [left bound.]	right bound. no.	factor [right bound.]
116-01	0.2689	900-01	0.2689

***Note*:** The heat structure geometry no. 1161 for lower plenum shell is spherical, being composed of stainless steel, carbon steel, and calcium silicate. The factor is defined as the surface area of spherical zone divided by the surface area of hemisphere. Thus, for a single heat structure, the factor for the left boundary no. 116 for lower plenum is consistent with that for the right boundary no. 900 for environment (containment).

heat structure geometry no. (cccg): 1121 (lower plenum shell)

number of axial heat structures: 1		number of radial (r-) mesh points: 8	
geometry type: 3 (i.e., spherical)		left bound. coordinate: 2.2316 m	
number of r-intervals	right bound. coordinate	r-composition no.	temperature
1	2.2356 m	5 (i.e., stainless steel)	562.0 K
4	2.3771 m	6 (i.e., carbon steel)	562.0 K
2	2.577 m	12 (i.e., calcium silicate)	562.0 K
left bound. no.	factor [left bound.]	right bound. no.	factor [right bound.]
112-1	0.1434	900-01	0.1434

***Note*:** The heat structure geometry no. 1121 for lower plenum shell is spherical, being composed of stainless steel, carbon steel, and calcium silicate. The factor is defined as the surface area of spherical zone divided by the surface area of hemisphere. Thus, for a single heat structure, the factor for the left boundary no. 112 for lower plenum is consistent with that for the right boundary no. 900 for environment (containment).

heat structure geometry no. (cccg): 1481 (upper head wall)

number of axial heat structures: 1		number of radial (r-) mesh points: 8	
geometry type: 2 (i.e., cylindrical)		left bound. coordinate: 2.0903 m	
number of r-intervals	right bound. coordinate	r-composition no.	temperature
1	2.0943 m	5 (i.e., stainless steel)	562.0 K
4	2.611 m	6 (i.e., carbon steel)	562.0 K
2	2.811 m	12 (i.e., calcium silicate)	562.0 K
left bound. no.	length [left bound.]	right bound. no.	length [right bound.]
148-1	0.463 m	900-01	0.463 m

***Note*:** The heat structure geometry no. 1481 for upper head wall is cylindrical, being composed of stainless steel, carbon steel, and calcium silicate. Thus, for a single heat structure, the length of the left boundary no. 148 for upper head is consistent with that of the right boundary no. 900 for environment (containment).

heat structure geometry no. (cccg): 1491 (upper head wall)

number of axial heat structures: 1		number of radial (r-) mesh points: 8	
geometry type: 2 (i.e., cylindrical)		left bound. coordinate: 2.037 m	
number of r-intervals	right bound. coordinate	r-composition no.	temperature
1	2.041 m	5 (i.e., stainless steel)	562.0 K
4	2.611 m	6 (i.e., carbon steel)	562.0 K
2	2.811 m	12 (i.e., calcium silicate)	562.0 K
left bound. no.	length [left bound.]	right bound. no.	length [right bound.]
149-1	0.197 m	900-01	0.197 m

***Note*:** The heat structure geometry no. 1491 for upper head wall is cylindrical, being composed of stainless steel, carbon steel, and calcium silicate. Thus, for a single heat structure, the length of the left boundary no. 149 for upper head is consistent with that of the right boundary no. 900 for environment (containment).

heat structure geometry no. (cccg): 1521 (upper head wall)

number of axial heat structures: 4		number of radial (r-) mesh points: 8	
geometry type: 3 (i.e., spherical)		left bound. coordinate: 2.0985 m	
number of r-intervals	right bound. coordinate	r-composition no.	temperature
1	2.1025 m	5 (i.e., stainless steel)	562.0 K
4	2.3771 m	6 (i.e., carbon steel)	562.0 K
2	2.577 m	12 (i.e., calcium silicate)	562.0 K
left bound. no.	factor [left bound.]	right bound. no.	factor [right bound.]
149-01	0.031	900-01	0.031
152-01	0.2182	900-01	0.2182
152-02	0.2183	900-01	0.2183
152-03	0.224	900-01	0.224

***Note*:** The heat structure geometry no. 1521 for upper head wall is spherical, being composed of stainless steel, carbon steel, and calcium silicate. The factor is defined as the surface area of spherical zone divided by the surface area of hemisphere. Thus, for each of four axial heat structures, the factor for the left boundary no. 149 or 152 for upper head is consistent with that for the right boundary no. 900 for environment (containment).

heat structure geometry no. (cccg): 1482 (upper core support plate)

number of axial heat structures: 1		number of radial (r-) mesh points: 5	
geometry type: 1 (i.e., rectangular)		left bound. coordinate: 1.7945 m	
number of r-intervals	right bound. coordinate	r-composition no.	temperature
4	1.9215 m	5 (i.e., stainless steel)	562.0 K
left bound. no.	surface area [left bound.]	right bound. no.	surface area [right bound.]
0	3.718 m^2	148-01	3.718 m^2

***Note*:** The heat structure geometry no. 1482 for upper core support plate is rectangular, being composed of stainless steel. Thus, for a single heat structure, the surface area of the left boundary no. zero is consistent with that of the right boundary no. 148 for upper head.

heat structure geometry no. (cccg): 1441 (upper core support plate)

number of axial heat structures: 1		number of radial (r-) mesh points: 5	
geometry type: 2 (i.e., cylindrical)		left bound. coordinate: 1.7945 m	
number of r-intervals	right bound. coordinate	r-composition no.	temperature
4	1.8705 m	5 (i.e., stainless steel)	562.0 K
left bound. no.	length [left bound.]	right bound. no.	length [right bound.]
0	0.897 m	144-01	0.897 m

***Note*:** The heat structure geometry no. 1441 for upper core support plate is cylindrical, being composed of stainless steel. Thus, for a single heat structure, the length of the left boundary no. zero is consistent with that of the right boundary no. 144 for upper head.

heat structure geometry no. (cccg): 1442 (upper core support plate)

number of axial heat structures: 1		number of radial (r-) mesh points: 5	
geometry type: 1 (i.e., rectangular)		left bound. coordinate: 0.0 m	
number of r-intervals	right bound. coordinate	r-composition no.	temperature
4	0.304 m	5 (i.e., stainless steel)	562.0 K
left bound. no.	surface area [left bound.]	right bound. no.	surface area [right bound.]
144-01	6.731 m^2	140-01	6.731 m^2

***Note*:** The heat structure geometry no. 1442 for upper core support plate is rectangular, being composed of stainless steel. Thus, for a single heat structure, the surface area of the left boundary no. 144 for upper head is consistent with that of the right boundary no. 140 for upper plenum.

heat structure geometry no. (cccg): 1211 (core barrel)

number of axial heat structures: 11		number of radial (r-) mesh points: 5	
geometry type: 2 (i.e., cylindrical)		left bound. coordinate: 1.8795 m	
number of r-intervals	right bound. coordinate	r-composition no.	temperature
4	1.937 m	5 (i.e., stainless steel)	562.0 K
left bound. no.	length [left bound.]	right bound. no.	length [right bound.]
120-01	0.7508 m	108-12	0.7508 m
121-01	0.406666 m	108-11	0.406666 m
121-02	0.406666 m	108-10	0.406666 m
121-03	0.406666 m	108-09	0.406666 m
121-04	0.406666 m	108-08	0.406666 m
121-05	0.406666 m	108-07	0.406666 m
121-06	0.406666 m	108-06	0.406666 m
121-07	0.406666 m	108-05	0.406666 m
121-08	0.406666 m	108-04	0.406666 m
121-09	0.406666 m	108-03	0.406666 m

121-10	0.385 m	108-02	0.385 m

***Note*:** The heat structure geometry no. 1211 for core barrel is cylindrical, being composed of stainless steel. Thus, for each of eleven axial heat structures, the length of the left boundary no. 121 for core bypass is consistent with that of the right boundary no. 108 for vessel DC.

heat structure geometry no. (cccg): 1361 (core barrel)

number of axial heat structures: 5		number of radial (r-) mesh points: 5	
geometry type: 2 (i.e., cylindrical)		left bound. coordinate: 1.8795 m	
number of r-intervals	right bound. coordinate	r-composition no.	temperature
4	1.937 m	5 (i.e., stainless steel)	598.0 K
left bound. no.	length [left bound.]	right bound. no.	length [right bound.]
132-01	0.27 m	108-02	0.27 m
133-01	0.2699 m	108-01	0.2699 m
134-01	0.24085 m	108-01	0.24085 m
136-01	0.8245 m	104-01	0.8245 m
140-01	0.8248 m	101-01	0.8248 m

***Note*:** The heat structure geometry no. 1361 for core barrel is cylindrical, being composed of stainless steel. Thus, for each of five axial heat structures, the length of the left boundary no. 132, 133, 134, 136, or 140 for upper plenum is consistent with that of the right boundary no. 108, 104, or 101 for vessel DC.

heat structure geometry no. (cccg): 1201 (lower core support plate)

number of axial heat structures: 1		number of radial (r-) mesh points: 5	
geometry type: 1 (i.e., rectangular)		left bound. coordinate: 0.0 m	
number of r-intervals	right bound. coordinate	r-composition no.	temperature
4	0.0235 m	5 (i.e., stainless steel)	562.0 K
left bound. no.	surface area [left bound.]	right bound. no.	surface area [right bound.]
0	118.34 m^2	120-01	118.34 m^2

***Note*:** The heat structure geometry no. 1201 for lower core support plate is rectangular, being composed of stainless steel. Thus, for a single heat structure, the surface area of the left boundary no. zero is consistent with that of the right boundary no. 120 for core inlet.

heat structure geometry no. (cccg): 1082 (lower core support plate)

number of axial heat structures: 1		number of radial (r-) mesh points: 5	
geometry type: 1 (i.e., rectangular)		left bound. coordinate: 0.0 m	
number of r-intervals	right bound. coordinate	r-composition no.	temperature
4	0.0575 m	5 (i.e., stainless steel)	562.0 K
left bound. no.	surface area [left bound.]	right bound. no.	surface area [right bound.]
0	6.087 m^2	108-12	6.087 m^2

***Note*:** The heat structure geometry no. 1082 for lower core support plate is rectangular, being composed of stainless steel. Thus, for a single heat structure, the surface area of the left boundary no. zero is consistent with that of the right boundary no. 108 for vessel DC.

heat structure geometry no. (cccg): 1083 (vessel DC internals)

number of axial heat structures: 9		number of radial (r-) mesh points: 5	
geometry type: 2 (i.e., cylindrical)		left bound. coordinate: 1.937 m	
number of r-intervals	right bound. coordinate	r-composition no.	temperature
4	1.972 m	5 (i.e., stainless steel)	562.0 K
left bound. no.	surface area [left bound.]	right bound. no.	surface area [right bound.]
0	4.475 m^2	108-03	4.556 m^2
0	4.475 m^2	108-04	4.556 m^2
0	4.475 m^2	108-05	4.556 m^2
0	4.475 m^2	108-06	4.556 m^2
0	4.475 m^2	108-07	4.556 m^2
0	4.475 m^2	108-08	4.556 m^2
0	4.475 m^2	108-09	4.556 m^2

0	4.475 m^2	108-10	4.556 m^2
0	4.475 m^2	108-11	4.556 m^2

***Note*:** The heat structure geometry no. 1083 for vessel DC internals is cylindrical, being composed of stainless steel. The left and right boundary coordinates are 1.937 m and 1.972 m, respectively, away from the center. Thus, for each of nine axial heat structures, the surface area of the left boundary no. zero is smaller than that of the right boundary no. 108 for vessel DC.

heat structure geometry no. (cccg): 1122 (lower plenum support)

number of axial heat structures: 1		number of radial (r-) mesh points: 5	
geometry type: 2 (i.e., cylindrical)		left bound. coordinate: 0.0 m	
number of r-intervals	right bound. coordinate	r-composition no.	temperature
4	0.1396 m	5 (i.e., stainless steel)	562.0 K
left bound. no.	surface area [left bound.]	right bound. no.	surface area [right bound.]
0	0.0 m^2	112-01	3.721 m^2

***Note*:** The heat structure geometry no. 1122 for lower plenum support is cylindrical, being composed of stainless steel. The left boundary coordinate corresponding to the cylindrical center is zero. Thus, for a single heat structure, the surface area of the left boundary no. zero is smaller than that of the right boundary no. 112 for lower plenum.

heat structure geometry no. (cccg): 1162 (lower plenum support)

number of axial heat structures: 1		number of radial (r-) mesh points: 5	
geometry type: 2 (i.e., cylindrical)		left bound. coordinate: 0.0 m	
number of r-intervals	right bound. coordinate	r-composition no.	temperature
4	0.1072 m	5 (i.e., stainless steel)	562.0 K
left bound. no.	surface area [left bound.]	right bound. no.	surface area [right bound.]
0	0.0 m^2	116-01	27.256 m^2

***Note*:** The heat structure geometry no. 1162 for lower plenum support is cylindrical, being composed of stainless steel. The left boundary coordinate corresponding to the cylindrical center is zero. Thus, for a single heat structure, the surface area of the left boundary no. zero is smaller than that of the right boundary no. 116 for lower plenum.

heat structure geometry no. (cccg): 1202 (lower plenum support)

number of axial heat structures: 1		number of radial (r-) mesh points: 5	
geometry type: 2 (i.e., cylindrical)		left bound. coordinate: 0.0 m	
number of r-intervals	right bound. coordinate	r-composition no.	temperature
4	0.0298 m	5 (i.e., stainless steel)	562.0 K
left bound. no.	surface area [left bound.]	right bound. no.	surface area [right bound.]
0	0.0 m^2	120-01	55.886 m^2

***Note*:** The heat structure geometry no. 1202 for lower plenum support is cylindrical, being composed of stainless steel. The left boundary coordinate corresponding to the cylindrical center is zero. Thus, for a single heat structure, the surface area of the left boundary no. zero is smaller than that of the right boundary no. 120 for core inlet.

heat structure geometry no. (cccg): 1212 (core baffle plate)

number of axial heat structures: 9		number of radial (r-) mesh points: 3	
geometry type: 1 (i.e., rectangular)		left bound. coordinate: 0.01 m	
number of r-intervals	right bound. coordinate	r-composition no.	temperature
4	0.0298 m	5 (i.e., stainless steel)	562.0 K
left bound. no.	surface area [left bound.]	right bound. no.	surface area [right bound.]
0	6.796 m^2	121-01	6.796 m^2
0	6.796 m^2	121-02	6.796 m^2
0	6.796 m^2	121-03	6.796 m^2
0	6.796 m^2	121-04	6.796 m^2
0	6.796 m^2	121-05	6.796 m^2
0	6.796 m^2	121-06	6.796 m^2
0	6.796 m^2	121-07	6.796 m^2

0	6.796 m^2	121-08	6.796 m^2
0	5.913 m^2	121-09	5.913 m^2

***Note*:** The heat structure geometry no. 1212 for core baffle plate is rectangular, being composed of stainless steel. Thus, for each of nine axial heat structures, the surface area of the left boundary no. zero is consistent with that of the right boundary no. 121 for core bypass.

heat structure geometry no. (cccg): 1281 (core exit internals)

number of axial heat structures: 1		number of radial (r-) mesh points: 3	
geometry type: 2 (i.e., cylindrical)		left bound. coordinate: 0.0 m	
number of r-intervals	right bound. coordinate	r-composition no.	temperature
2	0.01326 m	5 (i.e., stainless steel)	598.0 K
left bound. no.	surface area [left bound.]	right bound. no.	surface area [right bound.]
0	0.0 m^2	128-01	371.15 m^2

***Note*:** The heat structure geometry no. 1281 for core exit internals is cylindrical, being composed of stainless steel. The left boundary coordinate corresponding to the cylindrical center is zero. Thus, for a single heat structure, the surface area of the left boundary no. zero is smaller than that of the right boundary no. 128 for core exit.

heat structure geometry no. (cccg): 1321 (CRGT)

number of axial heat structures: 3		number of radial (r-) mesh points: 3	
geometry type: 2 (i.e., cylindrical)		left bound. coordinate: 0.1025 m	
number of r-intervals	right bound. coordinate	r-composition no.	temperature
2	0.108 m	5 (i.e., stainless steel)	594.4 K
left bound. no.	surface area [left bound.]	right bound. no.	surface area [right bound.]
156-02	28.272 m^2	134-01	29.789 m^2
156-02	29.89 m^2	136-01	31.494 m^2
156-02	29.901 m^2	140-01	31.505 m^2

***Note*:** The heat structure geometry no. 1321 for CRGT is cylindrical, being composed of stainless steel. The left and right boundary coordinates are 0.1025 m and 0.108 m, respectively, away from the center. Thus, for each of three axial heat structures, the surface area of the left boundary no. 156 for CRGT is smaller than that of the right boundary no. 134, 136, or 140 for upper plenum.

heat structure geometry no. (cccg): 1322 (upper plenum support)

number of axial heat structures: 5		number of radial (r-) mesh points: 3	
geometry type: 2 (i.e., cylindrical)		left bound. coordinate: 0.0 m	
number of r-intervals	right bound. coordinate	r-composition no.	temperature
2	0.08 m	5 (i.e., stainless steel)	598.0 K
left bound. no.	surface area [left bound.]	right bound. no.	surface area [right bound.]
0	0.0 m^2	132-01	3.257 m^2
0	0.0 m^2	133-01	3.256 m^2
0	0.0 m^2	134-01	2.895 m^2
0	0.0 m^2	136-01	9.947 m^2
0	0.0 m^2	140-01	9.95 m^2

***Note*:** The heat structure geometry no. 1322 for upper plenum support is cylindrical, being composed of stainless steel. The left boundary coordinate corresponding to the cylindrical center is zero. Thus, for each of five axial heat structures, the surface area of the left boundary no. zero is smaller than that of the right boundary no. 132, 133, 134, 136, or 140 for upper plenum.

heat structure geometry no. (cccg): 1483 (CRGT)

number of axial heat structures: 3		number of radial (r-) mesh points: 3	
geometry type: 2 (i.e., cylindrical)		left bound. coordinate: 0.098 m	
number of r-intervals	right bound. coordinate	r-composition no.	temperature
2	0.103 m	5 (i.e., stainless steel)	594.4 K
left bound. no.	surface area [left bound.]	right bound. no.	surface area [right bound.]
156-01	31.483 m^2	144-01	33.089 m^2
156-01	9.196 m^2	148-01	9.665 m^2

156-01	16.25 m^2	149-01	17.079 m^2

***Note*:** The heat structure geometry no. 1483 for CRGT is cylindrical, being composed of stainless steel. The left and right boundary coordinates are 0.098 m and 0.103 m, respectively, away from the center. Thus, for each of three axial heat structures, the surface area of the left boundary no. 156 for CRGT is smaller than that of the right boundary no. 144, 148, or 149 for upper head.

heat structure geometry no. (cccg): 1522 (control rod)

number of axial heat structures: 3		number of radial (r-) mesh points: 3	
geometry type: 2 (i.e., cylindrical)		left bound. coordinate: 0.0 m	
number of r-intervals	right bound. coordinate	r-composition no.	temperature
2	0.025 m	5 (i.e., stainless steel)	594.4 K
left bound. no.	surface area [left bound.]	right bound. no.	surface area [right bound.]
0	0.0 m^2	152-01	4.101 m^2
0	0.0 m^2	152-02	4.101 m^2
0	0.0 m^2	152-03	4.096 m^2

***Note*:** The heat structure geometry no. 1522 for control rod is cylindrical, being composed of stainless steel. The left boundary coordinate corresponding to the cylindrical center is zero. Thus, for each of three axial heat structures, the surface area of the left boundary no. zero is smaller than that of the right boundary no. 152 for upper head.

heat structure geometry no. (cccg): 4001 (hot leg in loop-A)

number of axial heat structures: 5		number of radial (r-) mesh points: 5	
geometry type: 2 (i.e., cylindrical)		left bound. coordinate: 0.3683 m	
number of r-intervals	right bound. coordinate	r-composition no.	temperature
2	0.4413 m	5 (i.e., stainless steel)	598.0 K
2	0.6113 m	12 (i.e., calcium silicate)	598.0 K
left bound. no.	length [left bound.]	right bound. no.	length [right bound.]
400-01	3.81 m	900-01	3.81 m
400-02	6.294 m	900-01	6.294 m
406-01	6.0 m	900-01	6.0 m
408-01	2.307 m	900-01	2.307 m
408-02	2.568 m	900-01	2.568 m

***Note*:** In loop-A, the heat structure geometry no. 4001 for hot leg is cylindrical, being composed of stainless steel and calcium silicate. Thus, for each of five axial heat structures, the length of the left boundary no. 400, 406, or 408 for hot leg is consistent with that of the right boundary no. 900 for environment (containment).

heat structure geometry no. (cccg): 2001 (hot leg in loop-B)

number of axial heat structures: 5		number of radial (r-) mesh points: 5	
geometry type: 2 (i.e., cylindrical)		left bound. coordinate: 0.3683 m	
number of r-intervals	right bound. coordinate	r-composition no.	temperature
2	0.4413 m	5 (i.e., stainless steel)	598.0 K
2	0.6113 m	12 (i.e., calcium silicate)	598.0 K
left bound. no.	length [left bound.]	right bound. no.	length [right bound.]
200-01	1.27 m	900-01	1.27 m
200-02	2.098 m	900-01	2.098 m
206-01	2.0 m	900-01	2.0 m
208-01	0.769 m	900-01	0.769 m
208-02	0.856 m	900-01	0.856 m

***Note*:** In loop-B, the heat structure geometry no. 2001 for hot leg is cylindrical, being composed of stainless steel and calcium silicate. Thus, for each of five axial heat structures, the length of the left boundary no. 200, 206, or 208 for hot leg is consistent with that of the right boundary no. 900 for environment (containment).

heat structure geometry no. (cccg): 4121 (SG inlet in loop-A)

number of axial heat structures: 1		number of radial (r-) mesh points: 8	
geometry type: 3 (i.e., spherical)		left bound. coordinate: 1.6 m	
number of r-intervals	right bound. coordinate	r-composition no.	temperature
1	1.604 m	5 (i.e., stainless steel)	598.0 K
4	1.7 m	6 (i.e., carbon steel)	598.0 K
2	1.9 m	12 (i.e., calcium silicate)	598.0 K
left bound. no.	factor [left bound.]	right bound. no.	factor [right bound.]
412-01	0.4635	900-01	0.4635

***Note*:** In loop-A, the heat structure geometry no. 4121 for SG inlet plenum is spherical, being composed of stainless steel, carbon steel, and calcium silicate. The factor is defined as the surface area of spherical zone divided by the surface area of hemisphere. Thus, for a single heat structure, the factor for the left boundary no. 412 for SG inlet is consistent with that for the right boundary no. 900 for environment (containment).

heat structure geometry no. (cccg): 2121 (SG inlet in loop-B)

number of axial heat structures: 1		number of radial (r-) mesh points: 8	
geometry type: 3 (i.e., spherical)		left bound. coordinate: 1.6 m	
number of r-intervals	right bound. coordinate	r-composition no.	temperature
1	1.604 m	5 (i.e., stainless steel)	598.0 K
4	1.7 m	6 (i.e., carbon steel)	598.0 K
2	1.9 m	12 (i.e., calcium silicate)	598.0 K
left bound. no.	factor [left bound.]	right bound. no.	factor [right bound.]
212-01	0.1545	900-01	0.1545

***Note*:** In loop-B, the heat structure geometry no. 2121 for SG inlet plenum is spherical, being composed of stainless steel, carbon steel, and calcium silicate. The factor is defined as the surface area of spherical zone divided by the surface area of hemisphere. Thus, for a single heat structure, the factor for left right boundary no. 212 for SG inlet is consistent with that for the right boundary no. 900 for environment (containment).

heat structure geometry no. (cccg): 4122 (SG plate in loop-A)

number of axial heat structures: 1		number of radial (r-) mesh points: 5	
geometry type: 1 (i.e., rectangular)		left bound. coordinate: 0.0 m	
number of r-intervals	right bound. coordinate	r-composition no.	temperature
4	0.06 m	5 (i.e., stainless steel)	598.0 K
left bound. no.	surface area [left bound.]	right bound. no.	surface area [right bound.]
412-01	3.222 m^2	428-01	3.222 m^2

***Note*:** In loop-A, the heat structure geometry no. 4122 for SG plate is rectangular, being composed of stainless steel. Thus, for a single heat structure, the surface area of the left boundary no. 412 for SG inlet is consistent with that of the right boundary no. 428 for SG outlet.

heat structure geometry no. (cccg): 2122 (SG plate in loop-B)

number of axial heat structures: 1		number of radial (r-) mesh points: 5	
geometry type: 1 (i.e., rectangular)		left bound. coordinate: 0.0 m	
number of r-intervals	right bound. coordinate	r-composition no.	temperature
4	0.06 m	5 (i.e., stainless steel)	598.0 K
left bound. no.	surface area [left bound.]	right bound. no.	surface area [right bound.]
212-01	1.074 m^2	228-01	1.074 m^2

***Note*:** In loop-B, the heat structure geometry no. 2122 for SG plate is rectangular, being composed of stainless steel. Thus, for a single heat structure, the surface area of the left boundary no. 212 for SG inlet is consistent with that of the right boundary no. 228 for SG outlet.

heat structure geometry no. (cccg): 4161 (SG inlet plenum in loop-A)

number of axial heat structures: 1		number of radial (r-) mesh points: 8	
geometry type: 3 (i.e., spherical)		left bound. coordinate: 1.6 m	
number of r-intervals	right bound. coordinate	r-composition no.	temperature
1	1.604 m	5 (i.e., stainless steel)	598.0 K
4	1.7 m	6 (i.e., carbon steel)	598.0 K
2	1.9 m	12 (i.e., calcium silicate)	598.0 K
left bound. no.	factor [left bound.]	right bound. no.	factor [right bound.]
416-01	0.2796	900-01	0.2796

***Note*:** In loop-A, the heat structure geometry no. 4161 for SG inlet plenum is spherical, being composed of stainless steel, carbon steel, and calcium silicate. The factor is defined as the surface area of spherical zone divided by the surface area of hemisphere. Thus, for a single heat structure, the factor for the left boundary no. 416 for SG inlet plenum is consistent with that for the right boundary no. 900 for environment (containment).

heat structure geometry no. (cccg): 2161 (SG inlet plenum in loop-B)

number of axial heat structures: 1		number of radial (r-) mesh points: 8	
geometry type: 3 (i.e., spherical)		left bound. coordinate: 1.6 m	
number of r-intervals	right bound. coordinate	r-composition no.	temperature
1	1.604 m	5 (i.e., stainless steel)	598.0 K
4	1.7 m	6 (i.e., carbon steel)	598.0 K
2	1.9 m	12 (i.e., calcium silicate)	598.0 K
left bound. no.	factor [left bound.]	right bound. no.	factor [right bound.]
216-01	0.0932	900-01	0.0932

***Note*:** In loop-B, the heat structure geometry no. 2161 for SG inlet plenum is spherical, being composed of stainless steel, carbon steel, and calcium silicate. The factor is defined as the surface area of spherical zone divided by the surface area of hemisphere. Thus, for a single heat structure, the factor for the left boundary no. 216 for SG inlet plenum is consistent with that for the right boundary no. 900 for environment (containment).

heat structure geometry no. (cccg): 4162 (SG plate in loop-A)

number of axial heat structures: 1		number of radial (r-) mesh points: 5	
geometry type: 1 (i.e., rectangular)		left bound. coordinate: 0.0 m	
number of r-intervals	right bound. coordinate	r-composition no.	temperature
4	0.06 m	5 (i.e., stainless steel)	598.0 K
left bound. no.	surface area [left bound.]	right bound. no.	surface area [right bound.]
416-01	2.808 m^2	424-02	2.808 m^2

***Note*:** In loop-A, the heat structure geometry no. 4162 for SG plate is rectangular, being composed of stainless steel. Thus, for a single heat structure, the surface area of the left boundary no. 416 for SG inlet plenum is consistent with that of the right boundary no. 424 for SG outlet plenum.

heat structure geometry no. (cccg): 2162 (SG plate in loop-B)

number of axial heat structures: 1		number of radial (r-) mesh points: 5	
geometry type: 1 (i.e., rectangular)		left bound. coordinate: 0.0 m	
number of r-intervals	right bound. coordinate	r-composition no.	temperature
4	0.06 m	5 (i.e., stainless steel)	598.0 K
left bound. no.	surface area [left bound.]	right bound. no.	surface area [right bound.]
216-01	0.936 m^2	224-02	0.936 m^2

***Note*:** In loop-B, the heat structure geometry no. 2162 for SG plate is rectangular, being composed of stainless steel. Thus, for a single heat structure, the surface area of the left boundary no. 216 for SG inlet plenum is consistent with that of the right boundary no. 224 for SG outlet plenum.

heat structure geometry no. (cccg): 4163 (SG tube sheet in loop-A)

number of axial heat structures: 1		number of radial (r-) mesh points: 5	
geometry type: 2 (i.e., cylindrical)		left bound. coordinate: 0.0098 m	
number of r-intervals	right bound. coordinate	r-composition no.	temperature
2	0.01111 m	18 (i.e., Inconel 600)	598.0 K
2	0.04 m	6 (i.e., carbon steel)	598.0 K
left bound. no.	surface area [left bound.]	right bound. no.	surface area [right bound.]
416-02	340.47 m^2	0	1389.673 m^2

***Note*:** In loop-A, the heat structure geometry no. 4163 for SG tube sheet is cylindrical, being composed of Inconel 600 and carbon steel. The left boundary coordinate is 0.0098 m away from the center. The right boundary coordinate is 0.01111 m or 0.04 m away from the center. Thus, for a single heat structure, the surface area of the left boundary no. 416 for SG inlet plenum is smaller than that of the right boundary no. zero.

heat structure geometry no. (cccg): 2163 (SG tube sheet in loop-B)

number of axial heat structures: 1		number of radial (r-) mesh points: 5	
geometry type: 2 (i.e., cylindrical)		left bound. coordinate: 0.0098 m	
number of r-intervals	right bound. coordinate	r-composition no.	temperature
2	0.01111 m	18 (i.e., Inconel 600)	598.0 K
2	0.04 m	6 (i.e., carbon steel)	598.0 K
left bound. no.	surface area [left bound.]	right bound. no.	surface area [right bound.]
216-02	113.49 m^2	0	463.224 m^2

***Note*:** In loop-B, the heat structure geometry no. 2163 for SG tube sheet is cylindrical, being composed of Inconel 600 and carbon steel. The left boundary coordinate is 0.0098 m away from the center. The right boundary coordinate is 0.01111 m or 0.04 m away from the center. Thus, for a single heat structure, the surface area of the left boundary no. 216 for SG inlet plenum is smaller than that of the right boundary no. zero.

heat structure geometry no. (cccg): 4201 (SG U-tube in loop-A)

number of axial heat structures: 10		number of radial (r-) mesh points: 8	
geometry type: 2 (i.e., cylindrical)		left bound. coordinate: 0.0098 m	
number of r-intervals	right bound. coordinate	r-composition no.	temperature
7	0.01111 m	18 (i.e., Inconel 600)	580.0 K
left bound. no.	length [left bound.]	right bound. no.	length [right bound.]
420-01	30852.4499 m	504-01	30852.4499 m
420-02	30852.4499 m	504-02	30852.4499 m
420-03	30852.4499 m	504-03	30852.4499 m
420-04	30852.4499 m	504-04	30852.4499 m
420-05	16095.7422 m	504-05	16095.7422 m
420-06	16095.7422 m	504-05	16095.7422 m
420-07	30852.4499 m	504-04	30852.4499 m
420-08	30852.4499 m	504-03	30852.4499 m
420-09	30852.4499 m	504-02	30852.4499 m
420-10	30852.4499 m	504-01	30852.4499 m

***Note*:** In loop-A, the heat structure geometry no. 4201 for SG U-tube is cylindrical, being composed of Inconel 600. Thus, for each of ten axial heat structures, the length of the left boundary no. 420 for SG U-tube is consistent with that of the right boundary no. 504 for SG riser.

heat structure geometry no. (cccg): 2201 (SG U-tube in loop-B)

number of axial heat structures: 10		number of radial (r-) mesh points: 8	
geometry type: 2 (i.e., cylindrical)		left bound. coordinate: 0.0098 m	
number of r-intervals	right bound. coordinate	r-composition no.	temperature
7	0.01111 m	18 (i.e., Inconel 600)	580.0 K
left bound. no.	length [left bound.]	right bound. no.	length [right bound.]
220-01	10284.15 m	304-01	10284.15 m
220-02	10284.15 m	304-02	10284.15 m

220-03	10284.15 m	304-03	10284.15 m
220-04	10284.15 m	304-04	10284.15 m
220-05	5365.2471 m	304-05	5365.2471 m
220-06	5365.2471 m	304-05	5365.2471 m
220-07	10284.15 m	304-04	10284.15 m
220-08	10284.15 m	304-03	10284.15 m
220-09	10284.15 m	304-02	10284.15 m
220-10	10284.15 m	304-01	10284.15 m

***Note*:** In loop-B, the heat structure geometry no. 2201 for SG U-tube is cylindrical, being composed of Inconel 600. Thus, for each of ten axial heat structures, the length of the left boundary no. 220 for SG U-tube is consistent with that of the right boundary no. 304 for SG riser.

heat structure geometry no. (cccg): 4241 (SG tube sheet in loop-A)

number of axial heat structures: 1 — number of radial (r-) mesh points: 5
geometry type: 2 (i.e., cylindrical) — left bound. coordinate: 0.0098 m

number of r-intervals	right bound. coordinate	r-composition no.	temperature
2	0.01111 m	18 (i.e., Inconel 600)	562.0 K
2	0.04 m	6 (i.e., carbon steel)	562.0 K

left bound. no.	surface area [left bound.]	right bound. no.	surface area [right bound.]
424-01	340.47 m^2	0	1389.673 m^2

***Note*:** In loop-A, the heat structure geometry no. 4241 for SG tube sheet is cylindrical, being composed of Inconel 600 and carbon steel. The left boundary coordinate is 0.0098 m away from the center. The right boundary coordinate is 0.01111 m or 0.04 m away from the center. Thus, for a single heat structure, the surface area of the left boundary no. 424 for SG outlet plenum is smaller than that of the right boundary no. zero.

heat structure geometry no. (cccg): 2241 (SG tube sheet in loop-B)

number of axial heat structures: 1 — number of radial (r-) mesh points: 5
geometry type: 2 (i.e., cylindrical) — left bound. coordinate: 0.0098 m

number of r-intervals	right bound. coordinate	r-composition no.	temperature
2	0.01111 m	18 (i.e., Inconel 600)	562.0 K
2	0.04 m	6 (i.e., carbon steel)	562.0 K

left bound. no.	surface area [left bound.]	right bound. no.	surface area [right bound.]
224-01	113.49 m^2	0	463.224 m^2

***Note*:** In loop-B, the heat structure geometry no. 2241 for SG tube sheet is cylindrical, being composed of Inconel 600 and carbon steel. The left boundary coordinate is 0.0098 m away from the center. The right boundary coordinate is 0.01111 m or 0.04 m away from the center. Thus, for a single heat structure, the surface area of the left boundary no. 224 for SG outlet plenum is smaller than that of the right boundary no. zero.

heat structure geometry no. (cccg): 4242 (SG outlet plenum in loop-A)

number of axial heat structures: 1 — number of radial (r-) mesh points: 8
geometry type: 3 (i.e., spherical) — left bound. coordinate: 1.6 m

number of r-intervals	right bound. coordinate	r-composition no.	temperature
1	1.604 m	5 (i.e., stainless steel)	562.0 K
4	1.7 m	6 (i.e., carbon steel)	562.0 K
2	1.9 m	12 (i.e., calcium silicate)	562.0 K

left bound. no.	factor [left bound.]	right bound. no.	factor [right bound.]
424-02	0.2796	900-01	0.2796

***Note*:** In loop-A, the heat structure geometry no. 4242 for SG outlet plenum is spherical, being composed of stainless steel, carbon steel, and calcium silicate. The factor is defined as the surface area of spherical zone divided by the surface area of hemisphere. Thus, for a single heat structure, the factor for the left boundary no. 424 for SG outlet plenum is consistent with that for the right boundary no. 900 for environment (containment).

heat structure geometry no. (cccg): 2242 (SG outlet plenum in loop-B)

number of axial heat structures: 1		number of radial (r-) mesh points: 8	
geometry type: 3 (i.e., spherical)		left bound. coordinate: 1.6 m	
number of r-intervals	right bound. coordinate	r-composition no.	temperature
1	1.604 m	5 (i.e., stainless steel)	562.0 K
4	1.7 m	6 (i.e., carbon steel)	562.0 K
2	1.9 m	12 (i.e., calcium silicate)	562.0 K
left bound. no.	factor [left bound.]	right bound. no.	factor [right bound.]
224-02	0.0932	900-01	0.0932

***Note*:** In loop-B, the heat structure geometry no. 2242 for SG outlet plenum is spherical, being composed of stainless steel, carbon steel, and calcium silicate. The factor is defined as the surface area of spherical zone divided by the surface area of hemisphere. Thus, for a single heat structure, the factor for the left boundary no. 224 for SG outlet plenum is consistent with that for the right boundary no. 900 for environment (containment).

heat structure geometry no. (cccg): 4281 (SG outlet in loop-A)

number of axial heat structures: 1		number of radial (r-) mesh points: 8	
geometry type: 3 (i.e., spherical)		left bound. coordinate: 1.6 m	
number of r-intervals	right bound. coordinate	r-composition no.	temperature
1	1.604 m	5 (i.e., stainless steel)	562.0 K
4	1.7 m	6 (i.e., carbon steel)	562.0 K
2	1.9 m	12 (i.e., calcium silicate)	562.0 K
left bound. no.	factor [left bound.]	right bound. no.	factor [right bound.]
428-01	0.4635	900-01	0.4635

***Note*:** In loop-A, the heat structure geometry no. 4281 for SG outlet is spherical, being composed of stainless steel, carbon steel, and calcium silicate. The factor is defined as the surface area of spherical zone divided by the surface area of hemisphere. Thus, for a single heat structure, the factor for the left boundary no. 428 for SG outlet is consistent with that for the right boundary no. 900 for environment (containment).

heat structure geometry no. (cccg): 2281 (SG outlet in loop-B)

number of axial heat structures: 1		number of radial (r-) mesh points: 8	
geometry type: 3 (i.e., spherical)		left bound. coordinate: 1.6 m	
number of r-intervals	right bound. coordinate	r-composition no.	temperature
1	1.604 m	5 (i.e., stainless steel)	562.0 K
4	1.7 m	6 (i.e., carbon steel)	562.0 K
2	1.9 m	12 (i.e., calcium silicate)	562.0 K
left bound. no.	factor [left bound.]	right bound. no.	factor [right bound.]
228-01	0.1545	900-01	0.1545

***Note*:** In loop-B, the heat structure geometry no. 2281 for SG outlet is spherical, being composed of stainless steel, carbon steel, and calcium silicate. The factor is defined as the surface area of spherical zone divided by the surface area of hemisphere. Thus, for a single heat structure, the factor for the left boundary no. 228 for SG outlet is consistent with that for the right boundary no. 900 for environment (containment).

heat structure geometry no. (cccg): 4321 (COL in loop-A)

number of axial heat structures: 9		number of radial (r-) mesh points: 5	
geometry type: 2 (i.e., cylindrical)		left bound. coordinate: 0.3937 m	
number of r-intervals	right bound. coordinate	r-composition no.	temperature
2	0.4717 m	5 (i.e., stainless steel)	562.0 K
2	0.6417 m	12 (i.e., calcium silicate)	562.0 K
left bound. no.	length [left bound.]	right bound. no.	length [right bound.]
432-01	1.629 m	900-01	1.629 m
432-02	3.24 m	900-01	3.24 m
432-03	3.24 m	900-01	3.24 m
432-04	2.85 m	900-01	2.85 m

432-05	2.85 m	900-01	2.85 m
436-01	5.529 m	900-01	5.529 m
436-02	2.85 m	900-01	2.85 m
436-03	2.85 m	900-01	2.85 m
436-04	5.7564 m	900-01	5.7564 m

***Note*:** In loop-A, the heat structure geometry no. 4321 for COL is cylindrical, being composed of stainless steel and calcium silicate. Thus, for each of nine axial heat structures, the length of the left boundary no. 432 or 436 for COL is consistent with that of the right boundary no. 900 for environment (containment).

heat structure geometry no. (cccg): 2321 (COL in loop-B)

number of axial heat structures: 9 number of radial (r-) mesh points: 5
geometry type: 2 (i.e., cylindrical) left bound. coordinate: 0.3937 m

number of r-intervals	right bound. coordinate	r-composition no.	temperature
2	0.4717 m	5 (i.e., stainless steel)	562.0 K
2	0.6417 m	12 (i.e., calcium silicate)	562.0 K

left bound. no.	length [left bound.]	right bound. no.	length [right bound.]
232-01	0.543 m	900-01	0.543 m
232-02	1.08 m	900-01	1.08 m
232-03	1.08 m	900-01	1.08 m
232-04	0.95 m	900-01	0.95 m
232-05	0.95 m	900-01	0.95 m
236-01	1.843 m	900-01	1.843 m
236-02	0.95 m	900-01	0.95 m
236-03	0.95 m	900-01	0.95 m
236-04	1.9188 m	900-01	1.9188 m

***Note*:** In loop-B, the heat structure geometry no. 2321 for COL is cylindrical, being composed of stainless steel and calcium silicate. Thus, for each of nine axial heat structures, the length of the left boundary no. 232 or 236 for COL is consistent with that of the right boundary no. 900 for environment (containment).

heat structure geometry no. (cccg): 4401 (reactor coolant pump in loop-A)

number of axial heat structures: 1 number of radial (r-) mesh points: 5
geometry type: 2 (i.e., cylindrical) left bound. coordinate: 1.319 m

number of r-intervals	right bound. coordinate	r-composition no.	temperature
2	1.719 m	5 (i.e., stainless steel)	562.0 K
2	1.889 m	12 (i.e., calcium silicate)	562.0 K

left bound. no.	length [left bound.]	right bound. no.	length [right bound.]
440	3.72 m	900-01	3.72 m

***Note*:** In loop-A, the heat structure geometry no. 4401 for reactor coolant pump is cylindrical, being composed of stainless steel and calcium silicate. Thus, for a single heat structure, the length of the left boundary no. 440 for reactor coolant pump is consistent with that of the right boundary no. 900 for environment (containment).

heat structure geometry no. (cccg): 2401 (reactor coolant pump in loop-B)

number of axial heat structures: 1 number of radial (r-) mesh points: 5
geometry type: 2 (i.e., cylindrical) left bound. coordinate: 1.319 m

number of r-intervals	right bound. coordinate	r-composition no.	temperature
2	1.719 m	5 (i.e., stainless steel)	562.0 K
2	1.889 m	12 (i.e., calcium silicate)	562.0 K

left bound. no.	length [left bound.]	right bound. no.	length [right bound.]
240	1.24 m	900-01	1.24 m

***Note*:** In loop-B, the heat structure geometry no. 2401 for reactor coolant pump is cylindrical, being composed of stainless steel and calcium silicate. Thus, for a single heat structure, the length of the left boundary no. 240 for reactor coolant pump is consistent with that of the right boundary no. 900 for environment (containment).

heat structure geometry no. (cccg): 4481 (cold leg in loop-A)

number of axial heat structures: 4		number of radial (r-) mesh points: 5	
geometry type: 2 (i.e., cylindrical)		left bound. coordinate: 0.3493 m	
number of r-intervals	right bound. coordinate	r-composition no.	temperature
2	0.4183 m	5 (i.e., stainless steel)	562.0 K
2	0.5883 m	12 (i.e., calcium silicate)	562.0 K
left bound. no.	length [left bound.]	right bound. no.	length [right bound.]
444-01	6.294 m	900-01	6.294 m
448-01	6.294 m	900-01	6.294 m
452-01	6.294 m	900-01	6.294 m
452-02	2.859 m	900-01	2.859 m

***Note*:** In loop-A, the heat structure geometry no. 4481 for cold leg is cylindrical, being composed of stainless steel and calcium silicate. Thus, for each of four axial heat structures, the length of the left boundary no. 444, 448, or 452 for cold leg is consistent with that of the right boundary no. 900 for environment (containment).

heat structure geometry no. (cccg): 2481 (cold leg in loop-B)

number of axial heat structures: 4		number of radial (r-) mesh points: 5	
geometry type: 2 (i.e., cylindrical)		left bound. coordinate: 0.3493 m	
number of r-intervals	right bound. coordinate	r-composition no.	temperature
2	0.4183 m	5 (i.e., stainless steel)	562.0 K
2	0.5883 m	12 (i.e., calcium silicate)	562.0 K
left bound. no.	length [left bound.]	right bound. no.	length [right bound.]
244-01	2.098 m	900-01	2.098 m
248-01	2.098 m	900-01	2.098 m
252-01	2.098 m	900-01	2.098 m
252-02	0.953 m	900-01	0.953 m

***Note*:** In loop-B, the heat structure geometry no. 2481 for cold leg is cylindrical, being composed of stainless steel and calcium silicate. Thus, for each of four axial heat structures, the length of the left boundary no. 244, 248, or 252 for cold leg is consistent with that of the right boundary no. 900 for environment (containment).

heat structure geometry no. (cccg): 5001 (SG wall in loop-A)

number of axial heat structures: 1		number of radial (r-) mesh points: 8	
geometry type: 2 (i.e., cylindrical)		left bound. coordinate: 1.954 m	
number of r-intervals	right bound. coordinate	r-composition no.	temperature
1	1.958 m	5 (i.e., stainless steel)	528.9 K
4	2.036 m	6 (i.e., carbon steel)	528.9 K
2	2.236 m	12 (i.e., calcium silicate)	528.9 K
left bound. no.	length [left bound.]	right bound. no.	length [right bound.]
500-01	5.748 m	900-01	5.748 m

***Note*:** In loop-A, the heat structure geometry no. 5001 for SG wall is cylindrical, being composed of stainless steel, carbon steel, and calcium silicate. Thus, for a single heat structure, the length of the left boundary no. 500 for SG DC is consistent with that of the right boundary no. 900 for environment (containment).

heat structure geometry no. (cccg): 3001 (SG wall in loop-B)

number of axial heat structures: 1		number of radial (r-) mesh points: 8	
geometry type: 2 (i.e., cylindrical)		left bound. coordinate: 1.954 m	
number of r-intervals	right bound. coordinate	r-composition no.	temperature
1	1.958 m	5 (i.e., stainless steel)	528.9 K
4	2.036 m	6 (i.e., carbon steel)	528.9 K
2	2.236 m	12 (i.e., calcium silicate)	528.9 K
left bound. no.	length [left bound.]	right bound. no.	length [right bound.]
300-01	1.916 m	900-01	1.916 m

***Note*:** In loop-B, the heat structure geometry no. 3001 for SG wall is cylindrical, being composed of stainless steel, carbon steel, and calcium silicate. Thus, for a single heat structure, the length of the left boundary no. 300 for SG DC is consistent with that of the right boundary no. 900 for environment (containment).

heat structure geometry no. (cccg): 5002 (SG wall in loop-A)

number of axial heat structures: 4		number of radial (r-) mesh points: 8	
geometry type: 2 (i.e., cylindrical)		left bound. coordinate: 1.643 m	
number of r-intervals	right bound. coordinate	r-composition no.	temperature
1	1.647 m	5 (i.e., stainless steel)	528.9 K
4	1.7 m	6 (i.e., carbon steel)	528.9 K
2	1.9 m	12 (i.e., calcium silicate)	528.9 K
left bound. no.	length [left bound.]	right bound. no.	length [right bound.]
500-02	6.774 m	900-01	6.774 m
500-03	6.774 m	900-01	6.774 m
500-04	6.774 m	900-01	6.774 m
500-05	6.774 m	900-01	6.774 m

***Note*:** In loop-A, the heat structure geometry no. 5002 for SG wall is cylindrical, being composed of stainless steel, carbon steel, and calcium silicate. Thus, for each of four axial heat structures, the length of the left boundary no. 500 for SG DC is consistent with that of the right boundary no. 900 for environment (containment).

heat structure geometry no. (cccg): 3002 (SG wall in loop-B)

number of axial heat structures: 4		number of radial (r-) mesh points: 8	
geometry type: 2 (i.e., cylindrical)		left bound. coordinate: 1.643 m	
number of r-intervals	right bound. coordinate	r-composition no.	temperature
1	1.647 m	5 (i.e., stainless steel)	528.9 K
4	1.7 m	6 (i.e., carbon steel)	528.9 K
2	1.9 m	12 (i.e., calcium silicate)	528.9 K
left bound. no.	length [left bound.]	right bound. no.	length [right bound.]
300-02	2.258 m	900-01	2.258 m
300-03	2.258 m	900-01	2.258 m
300-04	2.258 m	900-01	2.258 m
300-05	2.258 m	900-01	2.258 m

***Note*:** In loop-B, the heat structure geometry no. 3002 for SG wall is cylindrical, being composed of stainless steel, carbon steel, and calcium silicate. Thus, for each of four axial heat structures, the length of the left boundary no. 300 for SG DC is consistent with that of the right boundary no. 900 for environment (containment).

heat structure geometry no. (cccg): 5041 (SG DC shroud in loop-A)

number of axial heat structures: 1		number of radial (r-) mesh points: 5	
geometry type: 2 (i.e., cylindrical)		left bound. coordinate: 1.637 m	
number of r-intervals	right bound. coordinate	r-composition no.	temperature
4	1.646 m	5 (i.e., stainless steel)	550.1 K
left bound. no.	length [left bound.]	right bound. no.	length [right bound.]
504-05	5.748 m	500-01	5.748 m

***Note*:** In loop-A, the heat structure geometry no. 5041 for SG DC shroud is cylindrical, being composed of stainless steel. Thus, for a single heat structure, the length of the left boundary no. 504 for SG riser is consistent with that of the right boundary no. 500 for SG DC.

heat structure geometry no. (cccg): 3041 (SG DC shroud in loop-B)

number of axial heat structures: 1		number of radial (r-) mesh points: 5	
geometry type: 2 (i.e., cylindrical)		left bound. coordinate: 1.637 m	
number of r-intervals	right bound. coordinate	r-composition no.	temperature
4	1.646 m	5 (i.e., stainless steel)	550.1 K
left bound. no.	length [left bound.]	right bound. no.	length [right bound.]
304-05	1.916 m	300-01	1.916 m

***Note*:** In loop-B, the heat structure geometry no. 3041 for SG DC shroud is cylindrical, being composed of stainless steel. Thus, for a single heat structure, the length of the left boundary no. 304 for SG riser is consistent with that of the right boundary no. 300 for SG DC.

heat structure geometry no. (cccg): 5042 (SG DC shroud in loop-A)

number of axial heat structures: 4		number of radial (r-) mesh points: 5	
geometry type: 2 (i.e., cylindrical)		left bound. coordinate: 1.5685 m	
number of r-intervals	right bound. coordinate	r-composition no.	temperature
4	1.5775 m	5 (i.e., stainless steel)	550.1 K
left bound. no.	length [left bound.]	right bound. no.	length [right bound.]
504-04	6.774 m	500-02	6.774 m
504-03	6.774 m	500-03	6.774 m
504-02	6.774 m	500-04	6.774 m
504-01	6.774 m	500-05	6.774 m

***Note*:** In loop-A, the heat structure geometry no. 5042 for SG DC shroud is cylindrical, being composed of stainless steel. Thus, for each of four axial heat structures, the length of the left boundary no. 504 for SG riser is consistent with that of the right boundary no. 500 for SG DC.

heat structure geometry no. (cccg): 3042 (SG DC shroud in loop-B)

number of axial heat structures: 4		number of radial (r-) mesh points: 5	
geometry type: 2 (i.e., cylindrical)		left bound. coordinate: 1.5685 m	
number of r-intervals	right bound. coordinate	r-composition no.	temperature
4	1.647 m	5 (i.e., stainless steel)	550.1 K
left bound. no.	length [left bound.]	right bound. no.	length [right bound.]
304-04	2.258 m	300-02	2.258 m
304-03	2.258 m	300-03	2.258 m
304-02	2.258 m	300-04	2.258 m
304-01	2.258 m	300-05	2.258 m

***Note*:** In loop-B, the heat structure geometry no. 3042 for SG DC shroud is cylindrical, being composed of stainless steel. Thus, for each of four axial heat structures, the length of the left boundary no. 304 for SG riser is consistent with that of the right boundary no. 300 for SG DC.

heat structure geometry no. (cccg): 5121 (SG wall in loop-A)

number of axial heat structures: 3		number of radial (r-) mesh points: 8	
geometry type: 2 (i.e., cylindrical)		left bound. coordinate: 2.14 m	
number of r-intervals	right bound. coordinate	r-composition no.	temperature
1	2.144 m	5 (i.e., stainless steel)	550.1 K
4	2.25 m	6 (i.e., carbon steel)	550.1 K
2	2.45 m	12 (i.e., calcium silicate)	550.1 K
left bound. no.	length [left bound.]	right bound. no.	length [right bound.]
512-01	3.153 m	900-01	3.153 m
512-02	3.153 m	900-01	3.153 m
512-03	3.153 m	900-01	3.153 m

***Note*:** In loop-A, the heat structure geometry no. 5121 for SG wall is cylindrical, being composed of stainless steel, carbon steel, and calcium silicate. Thus, for each of three axial heat structures, the length of the left boundary no. 512 for SG riser is consistent with that of the right boundary no. 900 for environment (containment).

heat structure geometry no. (cccg): 3121 (SG wall in loop-B)

number of axial heat structures: 3		number of radial (r-) mesh points: 8	
geometry type: 2 (i.e., cylindrical)		left bound. coordinate: 2.14 m	
number of r-intervals	right bound. coordinate	r-composition no.	temperature
1	2.144 m	5 (i.e., stainless steel)	550.1 K
4	2.25 m	6 (i.e., carbon steel)	550.1 K
2	2.45 m	12 (i.e., calcium silicate)	550.1 K
left bound. no.	length [left bound.]	right bound. no.	length [right bound.]
312-01	1.051 m	900-01	1.051 m
312-02	1.051 m	900-01	1.051 m
312-03	1.051 m	900-01	1.051 m

***Note*:** In loop-B, the heat structure geometry no. 3121 for SG wall is cylindrical, being composed of stainless steel, carbon steel, and calcium silicate. Thus, for each of three axial heat structures, the length of the left boundary no. 312 for SG riser is consistent with that of the right boundary no. 900 for environment (containment).

heat structure geometry no. (cccg): 5122 (SG riser wall in loop-A)

number of axial heat structures: 3		number of radial (r-) mesh points: 3	
geometry type: 2 (i.e., cylindrical)		left bound. coordinate: 0.706 m	
number of r-intervals	right bound. coordinate	r-composition no.	temperature
2	2.144 m	5 (i.e., stainless steel)	550.1 K
left bound. no.	surface area [left bound.]	right bound. no.	surface area [right bound.]
506-01	41.958 m^2	512-01	42.493 m^2
508-01	41.958 m^2	512-02	42.493 m^2
508-01	41.958 m^2	512-03	42.493 m^2

***Note*:** In loop-A, the heat structure geometry no. 5122 for SG riser wall is cylindrical, being composed of stainless steel. The left and right boundary coordinates are 0.706 m and 2.144 m, respectively, away from the center. Thus, for each of three axial heat structures, the surface area of the left boundary no. 506 for SG steam dome or no. 508 for SG steam separator is smaller than that of the right boundary no. 512 for SG riser.

heat structure geometry no. (cccg): 3122 (SG riser wall in loop-B)

number of axial heat structures: 3		number of radial (r-) mesh points: 3	
geometry type: 2 (i.e., cylindrical)		left bound. coordinate: 0.706 m	
number of r-intervals	right bound. coordinate	r-composition no.	temperature
2	2.144 m	5 (i.e., stainless steel)	550.1 K
left bound. no.	surface area [left bound.]	right bound. no.	surface area [right bound.]
306-01	13.986 m^2	312-01	14.164 m^2
308-01	13.986 m^2	312-02	14.164 m^2
308-01	13.986 m^2	312-03	14.164 m^2

***Note*:** In loop-B, the heat structure geometry no. 3122 for SG riser wall is cylindrical, being composed of stainless steel. The left and right boundary coordinates are 0.706 m and 2.144 m, respectively, away from the center. Thus, for each of three axial heat structures, the surface area of the left boundary no. 306 for SG steam dome or no. 308 for SG steam separator is smaller than that of the right boundary no. 312 for SG riser.

heat structure geometry no. (cccg): 5123 (SG internals in loop-A)

number of axial heat structures: 3		number of radial (r-) mesh points: 3	
geometry type: 2 (i.e., cylindrical)		left bound. coordinate: 0.7 m	
number of r-intervals	right bound. coordinate	r-composition no.	temperature
2	0.70335 m	5 (i.e., stainless steel)	550.1 K
left bound. no.	surface area [left bound.]	right bound. no.	surface area [right bound.]
512-01	111.861 m^2	0	112.395 m^2
512-02	111.861 m^2	0	112.395 m^2
512-03	111.861 m^2	0	112.395 m^2

***Note*:** In loop-A, the heat structure geometry no. 5123 for SG internals is cylindrical, being composed of stainless steel. The left and right boundary coordinates are 0.7 m and 0.70335 m, respectively, away from the center. Thus, for each of three axial heat structures, the surface area of the left boundary no. 512 for SG riser is smaller than that of the right boundary no. zero.

heat structure geometry no. (cccg): 3123 (SG internals in loop-B)

	number of axial heat structures: 3	number of radial (r-) mesh points: 3	
	geometry type: 2 (i.e., cylindrical)	left bound. coordinate: 0.7 m	
number of r-intervals	right bound. coordinate	r-composition no.	temperature
2	0.70335 m	5 (i.e., stainless steel)	550.1 K
left bound. no.	surface area [left bound.]	right bound. no.	surface area [right bound.]
312-01	37.287 m^2	0	37.465 m^2
312-02	37.287 m^2	0	37.465 m^2
312-03	37.287 m^2	0	37.465 m^2

***Note*:** In loop-B, the heat structure geometry no. 3123 for SG internals is cylindrical, being composed of stainless steel. The left and right boundary coordinates are 0.7 m and 0.70335 m, respectively, away from the center. Thus, for each of three axial heat structures, the surface area of the left boundary no. 312 for SG riser is smaller than that of the right boundary no. zero.

heat structure geometry no. (cccg): 5161 (SG wall in loop-A)

	number of axial heat structures: 1	number of radial (r-) mesh points: 8	
	geometry type: 2 (i.e., cylindrical)	left bound. coordinate: 2.14 m	
number of r-intervals	right bound. coordinate	r-composition no.	temperature
1	2.144 m	5 (i.e., stainless steel)	550.1 K
4	2.25 m	6 (i.e., carbon steel)	550.1 K
2	2.45 m	12 (i.e., calcium silicate)	550.1 K
left bound. no.	length [left bound.]	right bound. no.	length [right bound.]
516-01	12.657 m	900-01	12.657 m

***Note*:** In loop-A, the heat structure geometry no. 5161 for SG wall is cylindrical, being composed of stainless steel, carbon steel, and calcium silicate. Thus, for a single heat structure, the length of the left boundary no. 516 for SG steam dome is consistent with that of the right boundary no. 900 for environment (containment).

heat structure geometry no. (cccg): 3161 (SG wall in loop-B)

	number of axial heat structures: 1	number of radial (r-) mesh points: 8	
	geometry type: 2 (i.e., cylindrical)	left bound. coordinate: 2.14 m	
number of r-intervals	right bound. coordinate	r-composition no.	temperature
1	2.144 m	5 (i.e., stainless steel)	550.1 K
4	2.25 m	6 (i.e., carbon steel)	550.1 K
2	2.45 m	12 (i.e., calcium silicate)	550.1 K
left bound. no.	length [left bound.]	right bound. no.	length [right bound.]
316-01	4.219 m	900-01	4.219 m

***Note*:** In loop-B, the heat structure geometry no. 3161 for SG wall is cylindrical, being composed of stainless steel, carbon steel, and calcium silicate. Thus, for a single heat structure, the length of the left boundary no. 316 for SG steam dome is consistent with that of the right boundary no. 900 for environment (containment).

heat structure geometry no. (cccg): 5162 (SG internals in loop-A)

	number of axial heat structures: 1	number of radial (r-) mesh points: 3	
	geometry type: 1 (i.e., rectangular)	left bound. coordinate: 2.0 m	
number of r-intervals	right bound. coordinate	r-composition no.	temperature
2	2.003 m	5 (i.e., stainless steel)	550.1 K
left bound. no.	surface area [left bound.]	right bound. no.	surface area [right bound.]
516-01	1370.1 m^2	0	1370.1 m^2

***Note*:** In loop-A, the heat structure geometry no. 5162 for SG internals is rectangular, being composed of stainless steel. Thus, for a single heat structure, the surface area of the left boundary no. 516 for SG steam dome is consistent with that of the right boundary no. zero.

heat structure geometry no. (cccg): 3162 (SG internals in loop-B)

	number of axial heat structures: 1	number of radial (r-) mesh points: 3	
	geometry type: 1 (i.e., rectangular)	left bound. coordinate: 2.0 m	
number of r-intervals	right bound. coordinate	r-composition no.	temperature
2	2.003 m	5 (i.e., stainless steel)	550.1 K
left bound. no.	surface area [left bound.]	right bound. no.	surface area [right bound.]
316-01	456.7 m^2	0	456.7 m^2

***Note*:** In loop-B, the heat structure geometry no. 3162 for SG internals is rectangular, being composed of stainless steel. Thus, for a single heat structure, the surface area of the left boundary no. 316 for SG steam dome is consistent with that of the right boundary no. zero.

heat structure geometry no. (cccg): 6001 (PZR surge line)

	number of axial heat structures: 9	number of radial (r-) mesh points: 5	
	geometry type: 2 (i.e., cylindrical)	left bound. coordinate: 0.1421 m	
number of r-intervals	right bound. coordinate	r-composition no.	temperature
2	0.1778 m	5 (i.e., stainless steel)	607.9 K
2	0.3278 m	12 (i.e., calcium silicate)	607.9 K
left bound. no.	length [left bound.]	right bound. no.	length [right bound.]
600-01	0.76 m	900-01	0.76 m
600-02	1.3577 m	900-01	1.3577 m
600-03	1.74 m	900-01	1.74 m
600-04	4.6 m	900-01	4.6 m
600-05	5.1 m	900-01	5.1 m
600-06	3.585 m	900-01	3.585 m
600-07	1.3576 m	900-01	1.3576 m
600-08	1.24 m	900-01	1.24 m
600-09	0.5657 m	900-01	0.5657 m

***Note*:** The heat structure geometry no. 6001 for PZR surge line is cylindrical, being composed of stainless steel and calcium silicate. Thus, for each of nine axial heat structures, the length of the left boundary no. 600 for PZR surge line is consistent with that of the right boundary no. 900 for environment (containment).

heat structure geometry no. (cccg): 6101 (PZR shell)

	number of axial heat structures: 2	number of radial (r-) mesh points: 8	
	geometry type: 3 (i.e., spherical)	left bound. coordinate: 1.05 m	
number of r-intervals	right bound. coordinate	r-composition no.	temperature
1	1.054 m	5 (i.e., stainless steel)	617.7 K
4	1.13 m	6 (i.e., carbon steel)	617.7 K
2	1.31 m	12 (i.e., calcium silicate)	617.7 K
left bound. no.	factor [left bound.]	right bound. no.	factor [right bound.]
610-01	0.5	900-01	0.5
610-10	0.5	900-01	0.5

***Note*:** The heat structure geometry no. 6101 for PZR shell is spherical, being composed of stainless steel, carbon steel, and calcium silicate. The factor is defined as the surface area of spherical zone divided by the surface area of hemisphere. Thus, for each of two axial heat structures, the factor for the left boundary no. 610 for PZR is consistent with that for the right boundary no. 900 for environment (containment).

heat structure geometry no. (cccg): 6102 (PZR vessel)

number of axial heat structures: 9 — number of radial (r-) mesh points: 8
geometry type: 2 (i.e., cylindrical) — left bound. coordinate: 1.05 m

number of r-intervals	right bound. coordinate	r-composition no.	temperature
1	1.054 m	5 (i.e., stainless steel)	617.7 K
4	1.2 m	6 (i.e., carbon steel)	617.7 K
2	1.38 m	12 (i.e., calcium silicate)	617.7 K

left bound. no.	length [left bound.]	right bound. no.	length [right bound.]
610-02	1.61 m	900-01	1.61 m
610-03	1.61 m	900-01	1.61 m
610-04	1.61 m	900-01	1.61 m
610-05	1.61 m	900-01	1.61 m
610-06	1.61 m	900-01	1.61 m
610-07	1.61 m	900-01	1.61 m
610-08	1.61 m	900-01	1.61 m
610-09	1.61 m	900-01	1.61 m
610-10	0.52 m	900-01	0.52 m

***Note*:** The heat structure geometry no. 6102 for PZR vessel is cylindrical, being composed of stainless steel, carbon steel, and calcium silicate. Thus, for each of nine axial heat structures, the length of the left boundary no. 610 for PZR is consistent with that of the right boundary no. 900 for environment (containment).

heat structure geometry no. (cccg): 6103 (PZR heater)

number of axial heat structures: 1 — number of radial (r-) mesh points: 9
geometry type: 2 (i.e., cylindrical) — left bound. coordinate: 0.0 m

number of r-intervals	right bound. coordinate	r-composition no.	temperature
3	0.005 m	1 (i.e., magnesium oxide)	650.0 K
1	0.007 m	2 (i.e., nichrome)	650.0 K
2	0.01 m	1 (i.e., magnesium oxide)	650.0 K
2	0.015 m	5 (i.e., stainless steel)	650.0 K

left bound. no.	surface area [left bound.]	right bound. no.	surface area [right bound.]
0	0.0 m^2	610-10	13.147 m^2

***Note*:** The heat structure geometry no. 6103 for PZR heater is cylindrical, being composed of magnesium oxide, nichrome, and stainless steel. The left boundary coordinate corresponding to the cylindrical center is zero. Thus, for a single heat structure, the surface area of the left boundary no. zero is smaller than that of the right boundary no. 610 for PZR.

F. Heat structure thermal property data (cards 201mmmnn)

Tables that indicate temperature versus thermal conductivity, and volumetric heat capacity (namely, specific heat times density) are prepared in accordance with the requirements for the heat structure thermal property data for each composition.

<composition type and data format>

material type: tbl/fctn (Namely, user-supplied table is used.)
thermal conductivity format flag: 1
(Namely, table containing temperature and thermal conductivity is to be entered.)
volumetric heat capacity format flag: 1
(Namely, table containing temperature and volumetric heat capacity is to be entered.)

Among the compositions to be applied, thermal property data stored in the RELAP5 code program are used for carbon steel (denoted as the composition no. 6), uranium dioxide (denoted as the composition no. 15), and zirconium (denoted as the composition no. 17).

composition no. (mmm): 001 (magnesium oxide)

temp.	therm. conduct.	temp.	therm. conduct.	temp.	therm. conduct.
300.0 K	5.0385 W/m･K	473.15 K	3.95 W/m･K	573.15 K	3.37 W/m･K
temp.	therm. conduct.	temp.	therm. conduct.	temp.	therm. conduct.
673.15 K	2.96 W/m･K	773.15 K	2.61 W/m･K	873.15 K	2.32 W/m･K
temp.	therm. conduct.	temp.	therm. conduct.	temp.	therm. conduct.
973.15 K	2.09 W/m･K	1273.15 K	1.86 W/m･K	1473.15 K	1.72 W/m･K
temp.	vol. heat capacity	temp.	vol. heat capacity	temp.	vol. heat capacity
293.15 K	2.88d+6 J/m^3･K	373.15 K	3.04d+6 J/m^3･K	473.15 K	3.15d+6 J/m^3･K
temp.	vol. heat capacity	temp.	vol. heat capacity	temp.	vol. heat capacity
573.15 K	3.20d+6 J/m^3･K	673.15 K	3.25d+6 J/m^3･K	773.15 K	3.29d+6 J/m^3･K
temp.	vol. heat capacity	temp.	vol. heat capacity	temp.	vol. heat capacity
873.15 K	3.34d+6 J/m^3･K	973.15 K	3.44d+6 J/m^3･K	1073.15 K	3.53d+6 J/m^3･K
temp.	vol. heat capacity	temp.	vol. heat capacity		
1173.15 K	3.63d+6 J/m^3･K	1473.15 K	3.93d+6 J/m^3･K		

***Note*:** The thermal conductivity and volumetric heat capacity of magnesium oxide, denoted as the composition no. 1, are defined as a function of temperature.

composition no. (mmm): 002 (nichrome)

temp.	therm. conduct.	temp.	therm. conduct.	temp.	therm. conduct.
293.15 K	8.78 W/m･K	573.15 K	11.30 W/m･K	773.15 K	13.81 W/m･K
temp.	therm. conduct.	temp.	therm. conduct.	temp.	therm. conduct.
1073.15 K	18.8 W/m･K	1273.15 K	22.18 W/m･K	1473.15 K	25.52 W/m･K
temp.	vol. heat capacity	temp.	vol. heat capacity	temp.	vol. heat capacity
373.15 K	3.23d+6 J/m^3･K	573.15 K	3.62d+6 J/m^3･K	773.15 K	4.10d+6 J/m^3･K
temp.	vol. heat capacity	temp.	vol. heat capacity	temp.	vol. heat capacity
1073.15 K	4.61d+6 J/m^3･K	1273.15 K	4.73d+6 J/m^3･K	1473.15 K	4.95d+6 J/m^3･K

***Note*:** The thermal conductivity and volumetric heat capacity of nichrome, denoted as the composition no. 2, are defined as a function of temperature.

composition no. (mmm): 005 (stainless steel)

temp.	therm. conduct.	temp.	therm. conduct.		
273.15 K	12.98 W/m･K	1199.81 K	25.10 W/m･K		
temp.	vol. heat capacity	temp.	vol. heat capacity	temp.	vol. heat capacity
300.0 K	3.67d+6 J/m^3･K	366.48 K	3.83d+6 J/m^3･K	422.04 K	3.96d+6 J/m^3･K
temp.	vol. heat capacity	temp.	vol. heat capacity	temp.	vol. heat capacity
477.59 K	4.10d+6 J/m^3･K	533.15 K	4.23d+6 J/m^3･K	588.70 K	4.33d+6 J/m^3･K
temp.	vol. heat capacity	temp.	vol. heat capacity	temp.	vol. heat capacity
644.26 K	4.43d+6 J/m^3･K	699.81 K	4.50d+6 J/m^3･K	810.93 K	4.63d+6 J/m^3･K
temp.	vol. heat capacity				
1366.48 K	5.37d+6 J/m^3･K				

***Note*:** The thermal conductivity and volumetric heat capacity of stainless steel, denoted as the composition no. 5, are defined as a function of temperature.

composition no. (mmm): 012 (calcium silicate as insulator)

temp.	therm. conduct.	temp.	therm. conduct.	temp.	therm. conduct.
273.15 K	0.0465 W/m･K	373.15 K	0.0581 W/m･K	473.15 K	0.07 W/m･K
temp.	therm. conduct.	temp.	therm. conduct.	temp.	therm. conduct.
573.15 K	0.0879 W/m･K	673.15 K	0.1131 W/m･K	773.15 K	0.1458 W/m･K
temp.	therm. conduct.				
873.15 K	0.186 W/･mK				
temp.	vol. heat capacity	temp.	vol. heat capacity		
273.15 K	1.38d+5 J/m^3･K	873.15 K	1.38d+5 J/m^3･K		

***Note*:** The thermal conductivity and volumetric heat capacity of calcium silicate as insulator, denoted as the composition no. 12, are defined as a function of temperature.

composition no. (mmm): 016 (helium gas in gap)

temp.	therm. conduct.	temp.	therm. conduct.
273.15 K	0.51 W/m・K	3000.0 K	0.51 W/m・K
temp.	vol. heat capacity	temp.	vol. heat capacity
273.15 K	6.23d+3 J/m^3・K	3000.0 K	6.23d+3 J/m^3・K

***Note*:** The thermal conductivity and volumetric heat capacity of helium gas in gap, denoted as the composition no. 16, are given as constant values.

composition no. (mmm): 018 (Inconel 600)

temp.	therm. conduct.	temp.	therm. conduct.	temp.	therm. conduct.
273.15 K	11.8 W/m・K	373.15 K	13.0 W/m・K	473.15 K	14.2 W/m・K
temp.	therm. conduct.	temp.	therm. conduct.	temp.	therm. conduct.
573.15 K	15.5 W/m・K	673.15 K	16.9 W/m・K	873.15 K	19.8 W/m・K
Temp.	therm. conduct.				
1073.15 K	22.7 W/m・K				
temp.	vol. heat capacity	temp.	vol. heat capacity	temp.	vol. heat capacity
273.15 K	3.79d+6 J/m^3・K	373.15 K	4.05d+6 J/m^3・K	473.15 K	4.23d+6 J/m^3・K
temp.	vol. heat capacity	temp.	vol. heat capacity	temp.	vol. heat capacity
573.15 K	4.38d+6 J/m^3・K	673.15 K	4.50d+6 J/m^3・K	873.15 K	4.71d+6 J/m^3・K
temp.	vol. heat capacity				
1073.15 K	4.88d+6 J/m^3・K				

***Note*:** The thermal conductivity and volumetric heat capacity of Inconel 600, denoted as the composition no. 18, are defined as a function of temperature.

G. General table data (cards 202tttnn)

general table no. (ttt): 308 (SG secondary narrow-range liquid level)

table type: power (i.e., SG secondary narrow-range liquid level versus estimated value)

liquid level	estimated value	liquid level	estimated value
0.0 m	0.0 %	1.76 m	44.0 %
liquid level	estimated value		
4.0 m	100.0 %		

***Note*:** The general table no. 308 indicates that SG secondary narrow-range liquid levels of 4 m and 1.76 m correspond to the estimated values of 100% and 44%, respectively.

general table no. (ttt): 656 for PZR proportional heater power

table type: reac-t (i.e., control value versus heater power) trip card no.: 0

control value	heater power	control value	heater power
0.0 (-)	0.0 W	100.0 (-)	400.0 W
control value	heater power		
200.0 (-)	400.0 W		

***Note*:** The general table no. 656 indicates that the control value, computed based on the difference between PZR pressure and PZR reference pressure (15.5 MPa as PZR initial pressure), versus PZR proportional heater power. Setting a trip card no. to zero means no trip.

general table no. (ttt): 900 for environment

table type: htc-t (i.e., time versus heat transfer coefficient)

time	heat transfer coefficient	time	heat transfer coefficient
0.0 s	5.0 W/m^2・K	10000.0 s	5.0 W/m^2・K

***Note*:** The general table no. 900 indicates that heat transfer coefficient of environment (containment) is kept constant at 5 W/m^2・K as general heat transfer coefficient for natural convection.

general table no. (ttt): 002 (scram curve)

table type: reac-t (i.e., time versus scram reactivity) trip card no.: 673

time	reactivity	time	reactivity	time	reactivity
0.0 s	0.0 $	0.78 s	-0.0826 $	1.0 s	-0.1652 $
time	reactivity	time	reactivity	time	reactivity
1.22 s	-0.2974 $	1.44 s	-0.4956 $	1.62 s	-0.826 $
time	reactivity	time	reactivity	time	reactivity
1.83 s	-1.4703 $	1.96 s	-2.0485 $	2.02 s	-3.0397 $
time	reactivity	time	reactivity	time	reactivity
2.15 s	-4.7082 $	2.25 s	-7.2688 $	2.37 s	-7.9048 $
time	reactivity	time	reactivity		
2.6 s	-8.26 $	1000.0 s	-8.26 $		

***Note*:** The general table no. 2 indicates that scram reactivity is defined as a function of time following a reactor scram signal according to a trip card no. 673. This value is evaluated based on the reactivity curve described in the FSAR of the US Prairie Island Nuclear Generating Plant Units.

H. Reactor kinetics input (cards 30000000 through 39999999)

<reactor kinetics type>

kinetics type: point (i.e., point reactor kinetics option)

feedback type: separabl (Namely, reactor kinetics feedback due to moderator density reactivity and doppler reactivity is assumed to be separable.)

<reactor kinetics information>

fission product decay type: gamma-ac (i.e., fission product decay plus actinide decay calculation)

total reactor power: 3423.0d+6 W

initial reactivity: 0.0 $

delayed neutron fraction over prompt neutron generation time: 293.333 s^{-1}

***Note*:** The delayed neutron fraction over prompt neutron generation time is evaluated by dividing the delayed neutron fraction of 0.0044 into the prompt neutron generation time of 1.5×10^{-5} s.

fission product yield factor: 1.0 U-239 yield factor: 1.0

<fission product decay information>

As card 30000002 is not entered, both the default 1973 ANS Standard fission product data and the default energy release per fission value of 200 MeV/fission are employed.

<feedback information>

number of tables: 2 (i.e., tables for moderator density reactivity and Doppler reactivity)

(1) moderator density reactivity table (i.e., table for moderator density versus reactivity)

density	reactivity	density	reactivity	density	reactivity
427.174 kg/m^3	-5.700 $	462.771 kg/m^3	-4.482 $	498.369 kg/m^3	-3.454 $
density	reactivity	density	reactivity	density	reactivity
533.967 kg/m^3	-2.587 $	569.565 kg/m^3	-1.856 $	605.163 kg/m^3	-1.246 $
density	reactivity	density	reactivity	density	reactivity
640.761 kg/m^3	-0.743 $	676.359 kg/m^3	-0.331 $	711.956 kg/m^3	0.0 $

***Note*:** The moderator density reactivity is defined as a function of moderator density. This value is evaluated based on the WCAP-8330 reactivity curve.

(2) Doppler reactivity table (i.e., table for temperature versus Doppler reactivity)

temperature	reactivity	temperature	reactivity	temperature	reactivity
571.9 K	1.701 $	675.3 K	1.075 $	778.6 K	0.488 $
Temperature	reactivity	temperature	reactivity	temperature	reactivity
869.0 K	0.0 $	972.4 K	-0.535 $	1075.8 K	-1.048 $
Temperature	reactivity				
1500.0 K	-2.996 $				

***Note*:** The Doppler reactivity is defined as a function of temperature. This value is evaluated based on the reactivity curve described in the FSAR of the US Surry Power Plant Units.

(3) volume weighting factor for density feedback

volume no.	weight. factor	volume no.	weight. factor	volume no.	weight. factor
124010000	0.11111	124020000	0.11111	124030000	0.11111
124040000	0.11111	124050000	0.11111	124060000	0.11111
124070000	0.11111	124080000	0.11111	124090000	0.11111

***Note*:** The volume weighting factor for density feedback for each of nine vertically divided volumes of core is adjusted to 0.11111.

(4) heat structure weighting factor for Doppler feedback

The number of fuel rods in the PWR is 50952. On the other hand, the number of electric heater rods in the LSTF is 360, 180, and 468 for high-power, mean-power, and low-power heater rods, respectively. The radial power peaking factors in the LSTF are 1.51, 1.00, and 0.66 for high-power, mean-power, and low-power heater rods, respectively.

The following base factor for the heat structure geometry no. for each fuel rod in the PWR is set referring to the number of electric heater rods and the radial power peaking factor in the LSTF.

A. The base factor for the heat structure geometry no. 1241 for high-power fuel rods is 0.5265. This value is calculated as (1.51*360)/(1.51*360+1.00*180+0.66*468).
B. The base factor for the heat structure geometry no. 1242 for mean-power fuel rods is 0.1743. This value is calculated as (1.00*180)/(1.51*360+1.00*180+0.66*468).
C. The base factor for the heat structure geometry no. 1243 for low-power fuel rods is 0.2992. This value is calculated as (0.66*468)/(1.51*360+1.00*180+0.66*468).

The following reference coefficient for axial heat structure end no. for each fuel rod in the PWR is set considering the axial power peaking factor in the LSTF.

a. The reference coefficient for each of axial structure end no. 1 and 9 is 0.04032. This value is calculated as 0.3633/(0.3633*2+0.8135*2+1.1736*2+1.4071*2+1.4945).
b. The reference coefficient for each of axial structure end no. 2 and 8 is 0.090294. This value is calculated as 0.8135/(0.3633*2+0.8135*2+1.1736*2+1.4071*2+1.4945).
c. The reference coefficient for each of axial structure end no. 3 and 7 is 0.130262. This value is calculated as 1.1736/(0.3633*2+0.8135*2+1.1736*2+1.4071*2+1.4945).
d. The reference coefficient for each of axial structure end no. 4 and 6 is 0.15618. This value is calculated as 1.4071/(0.3633*2+0.8135*2+1.1736*2+1.4071*2+1.4945).
e. The reference coefficient for axial structure end no. 5 is 0.16588. This value is calculated as 1.4945/(0.3633*2+0.8135*2+1.1736*2+1.4071*2+1.4945).

The heat structure weighting factor for Doppler feedback for each heat structure no. for high-power, mean-power, and low-power fuel rods in the PWR shown below is obtained by multiplying the above base factor by the above reference coefficient.

structure no.	weight. factor	structure no.	weight. factor	structure no.	weight. factor
1241001	0.021230	1242001	0.007028	1243001	0.012065
structure no.	weight. factor	structure no.	weight. factor	structure no.	weight. factor
1241002	0.047540	1242002	0.015738	1243002	0.027016
structure no.	weight. factor	structure no.	weight. factor	structure no.	weight. factor
1241003	0.068583	1242003	0.022705	1243003	0.038974

structure no.	weight. factor	structure no.	weight. factor	structure no.	weight. factor
1241004	0.082229	1242004	0.027222	1243004	0.046729
1241005	0.087336	1242005	0.028913	1243005	0.049631
1241006	0.082229	1242006	0.027222	1243006	0.046729
1241007	0.068583	1242007	0.022705	1243007	0.038974
1241008	0.047540	1242008	0.015738	1243008	0.027016
1241009	0.021230	1242009	0.007028	1243009	0.012065

I. Control system input data (cards 205cccnn)

The variable ‘cntrlvar’ corresponds to control variable command used in RELAP5 code.

Control components employed with self-initialization option are composed of various component types; sum, integrating, unit trip, multiplier, lag, and functional.

As for alphanumeric name of the variable code denoted in the sum component, ‘voidf’ and ‘p’ are volume liquid fraction and pressure, respectively.

Control system input data related to the PZR heater power are as follows.

control component no. (ccc): 612 (PZR liquid volume)
control component type: sum (i.e., sum) scaling factor s: 1.952903773 initial value: 0.0
initial value flag: 1 (i.e., initial condition computation) constant a_0: 0.0
constant a_1: 1.0 alphanumeric name for v_1: cntrlvar integer name for v_1: 611
Control variable y defined by the sum component is expressed as: $y = s(a_0+a_1*v_1)$
***Note*:** The ‘cntrlvar 612’ is defined by the sum component using the ‘cntrlvar 611’.

control component no. (ccc): 611 (PZR liquid volume)
control component type: sum (i.e., sum) scaling factor s: 1.0 initial value: 0.0
initial value flag: 1 (i.e., initial condition computation) constant a_0: 0.0
constant a_1: 2.4382 alphanumeric name for v_1: voidf integer name for v_1: 61001
constant a_2: 5.5764 alphanumeric name for v_2: voidf integer name for v_2: 61002
constant a_3: 5.5764 alphanumeric name for v_3: voidf integer name for v_3: 61003
constant a_4: 5.5764 alphanumeric name for v_4: voidf integer name for v_4: 61004
constant a_5: 5.5764 alphanumeric name for v_5: voidf integer name for v_5: 61005
constant a_6: 5.5764 alphanumeric name for v_6: voidf integer name for v_6: 61006
constant a_7: 5.5764 alphanumeric name for v_7: voidf integer name for v_7: 61007
constant a_8: 5.5764 alphanumeric name for v_8: voidf integer name for v_8: 61008
constant a_9: 5.5764 alphanumeric name for v_9: voidf integer name for v_9: 61009
constant a_{10}: 5.5764 alphanumeric name for v_{10}: voidf integer name for v_{10}: 61010
Control variable y defined by the sum component is expressed as:
$y = s(a_0+a_1*v_1+a_2*v_2+a_3*v_3+a_4*v_4+a_5*v_5+a_6*v_6+a_7*v_7+a_8*v_8+a_9*v_9+a_{10}*v_{10})$
***Note*:** The ‘cntrlvar 611’ is defined by the sum component using liquid fraction of each of ten vertically divided volumes of PZR.

control component no. (ccc): 651 (difference between PZR pressure and PZR reference pressure)
control component type: sum (i.e., sum) scaling factor s: 1.0 initial value: 0.0
initial value flag: 1 (i.e., initial condition computation) constant a_0: -2248.10295
constant a_1: 1.450389e-4 alphanumeric name for v_1: p integer name for v_1: 61001
Control variable y defined by the sum component is expressed as: $y = s(a_0+a_1*v_1)$
***Note*:** The 'cntrlvar 651' is defined by the sum component using pressure of the pipe component no. 610 for PZR.

control component no. (ccc): 652 (difference between PZR pressure and PZR reference pressure)
control component type: integral (i.e., integrating) scaling factor s: 0.00167 initial value: 0.0
initial value flag: 1 (i.e., initial condition computation)
alphanumeric name for v_1: cntrlvar integer name for v_1: 651
Control variable y defined by the integrating component is expressed as: $y = s\int v_1 dt$
***Note*:** The 'cntrlvar 652' is defined by the integrating component using the 'cntrlvar 651'.

control component no. (ccc): 653 (difference between PZR pressure and PZR reference pressure)
control component type: sum (i.e., sum) scaling factor s: 0.5 initial value: 0.0
initial value flag: 1 (i.e., initial condition computation) constant a_0: 0.0
constant a_1: 1.0 alphanumeric name for v_1: cntrlvar integer name for v_1: 651
constant a_2: 1.0 alphanumeric name for v_2: cntrlvar integer name for v_2: 652
Control variable y defined by the sum component is expressed as: $y = s(a_0+a_1*v_1+a_2*v_2)$
***Note*:** The 'cntrlvar 653' is defined by the sum component using the 'cntrlvar 651' and 'cntrlvar 652'.

control component no. (ccc): 654 (difference between PZR pressure and PZR reference pressure)
control component type: sum (i.e., sum) scaling factor s: 1.0 initial value: 0.0
initial value flag: 1 (i.e., initial condition computation) constant a_0: 42.5
constant a_1: 1.0 alphanumeric name for v_1: cntrlvar integer name for v_1: 653
Control variable y defined by the sum component is expressed as: $y = s(a_0+a_1*v_1)$
***Note*:** The 'cntrlvar 654' is defined by the sum component using the 'cntrlvar 653'.

control component no. (ccc): 655 (PZR proportional heater power)
control component type: sum (i.e., sum) scaling factor s: -6.666667 initial value: 0.0
initial value flag: 1 (i.e., initial condition computation) constant a_0: -50.0
constant a_1: 1.0 alphanumeric name for v_1: cntrlvar integer name for v_1: 654
Control variable y defined by the sum component is expressed as: $y = s(a_0+a_1*v_1)$
***Note*:** The 'cntrlvar 655' is defined by the sum component using the 'cntrlvar 654' which invokes the 'cntrvar 651'.

control component no. (ccc): 656 (PZR proportional heater power)
control component type: function (i.e., functional) scaling factor s: 1.0d+3 initial value: 0.0
initial value flag: 1 (i.e., initial condition computation)
limiter control: 3 (Namely, both the minimum and maximum limits are to be imposed.)
minimum value: 0.0 maximum value: 4.0e+5
alphanumeric name for v_1: cntrlvar integer name for v_1: 655 general table no.: 656
Control variable y defined by the functional component is expressed as: $y = s*[\text{function } (v_1)]$
***Note*:** The 'cntrlvar 656' is defined by the functional component using the 'cntrlvar 655' which concerns the general table no. 656.

control component no. (ccc): 657 (on/off signal for PZR heater)
control component type: tripunit (i.e., unit trip) scaling factor s: 1.0 initial value: 0.0
initial value flag: 0 (Namely, initial value of zero is used as initial condition.)
trip card no.: 581 (Namely, u is 0.0 or 1.0 when trip is 'on' or 'off', respectively.)
Control variable y defined by the unit trip component is expressed as: $y = s*u$
***Note*:** The 'cntrlvar 657' is defined by the unit trip component which concerns a trip card no. 581.

control component no. (ccc): 658 (PZR proportional heater power)
control component type: sum (i.e., sum) scaling factor s: -1.0 initial value: 1.0
initial value flag: 1 (i.e., initial condition computation)
limiter control: 3 (Namely, both the minimum and maximum limits are to be imposed.)
minimum value: 0.0 maximum value: 1.0 constant a_0: -1.0
constant a_1: 1.0 alphanumeric name for v_1: cntrlvar integer name for v_1: 657
Control variable y defined by the sum component is expressed as: $y = s(a_0+a_1*v_1)$
***Note*:** The 'cntrlvar 658' is defined by the sum component using the 'cntrlvar 657'.

control component no. (ccc): 659 (PZR proportional heater power)
control component type: mult (i.e., multiplier) scaling factor s: 1.0 initial value: 0.0
initial value flag: 1 (i.e., initial condition computation)
limiter control: 3 (Namely, both the minimum and maximum limits are to be imposed.)
minimum value: 0.0 maximum value: 4.0e+5
alphanumeric name for v_1: cntrlvar integer name for v_1: 656
alphanumeric name for v_2: cntrlvar integer name for v_2: 658
Control variable y defined by the multiplier component is expressed as: $y = s*v_1*v_2$
***Note*:** The 'cntrlvar 659' is defined by the multiplier component using the 'cntrlvar 656' and 'cntrvar 658'.

control component no. (ccc): 660 (PZR backup heater power)
control component type: sum (i.e., sum) scaling factor s: 1.0 initial value: 0.0
initial value flag: 1 (i.e., initial condition computation) constant a_0: -30.0
constant a_1: 1.0 alphanumeric name for v_1: cntrlvar integer name for v_1: 654
Control variable y defined by the sum component is expressed as: $y = s(a_0+a_1*v_1)$
***Note*:** The 'cntrlvar 660' is defined by the sum component using the 'cntrlvar 654' which invokes the 'cntrvar 651'.

control component no. (ccc): 661 (on/off signal for PZR heater)
control component type: tripunit (i.e., unit trip) scaling factor s: 1.0 initial value: 0.0
initial value flag: 0 (Namely, initial value of zero is used as initial condition.)
trip card no.: 582 (Namely, u is 0.0 or 1.0 when trip is 'on' or 'off', respectively.)
Control variable y defined by the unit trip component is expressed as: $y = s*u$
***Note*:** The 'cntrlvar 661' is defined by the unit trip component which concerns a trip card no. 582.

control component no. (ccc): 662 (PZR backup heater power)
control component type: mult (i.e., multiplier) scaling factor s: 1.4e+6 initial value: 0.0
initial value flag: 1 (i.e., initial condition computation)
limiter control: 3 (Namely, both the minimum and maximum limits are to be imposed.)
minimum value: 0.0 maximum value: 1.4e+6
alphanumeric name for v_1: cntrlvar integer name for v_1: 661
alphanumeric name for v_2: cntrlvar integer name for v_2: 658
Control variable y defined by the multiplier component is expressed as: $y = s*v_1*v_2$
***Note*:** The 'cntrlvar 662' is defined by the multiplier component using the 'cntrlvar 661' and 'cntrvar 658'.

control component no. (ccc): 663 (PZR backup heater power)
control component type: lag (i.e., lag) scaling factor s: 1.0 initial value: 0.0
initial value flag: 1 (i.e., initial condition computation)
limiter control: 3 (Namely, both the minimum and maximum limits are posed.)
minimum value: 0.0 maximum value: 1.4e+6
lag time a_1: 10.0 alphanumeric name for v_1: cntrlvar integer name for v_1: 662
Control variable y defined by the lag component is expressed as: $y = s*v_1/(1+a_1)$
***Note*:** The 'cntrlvar 663' is defined by the lag component using the 'cntrlvar 662'.

control component no. (ccc): 664 (PZR heater power)
control component type: sum (i.e., sum) scaling factor s: 1.0 initial value: 0.0
initial value flag: 1 (i.e., initial condition computation)
limiter control: 3 (Namely, both the minimum and maximum limits are to be imposed.)
minimum value: 0.0 maximum value: 1.8e+6 constant a_0: 0.0
constant a_1: 1.0 alphanumeric name for v_1: cntrlvar integer name for v_1: 659
constant a_2: 1.0 alphanumeric name for v_2: cntrlvar integer name for v_2: 663
Control variable y defined by the sum component is expressed as: $y = s(a_0+a_1*v_1+a_2*v_2)$
***Note*:** The 'cntrlvar 664' is defined by the sum component using the 'cntrlvar 659' which invokes the 'cntrvar 655', and the 'cntrlvar 663' which invokes the 'cntrvar 660'.

control component no. (ccc): 665 (PZR heater power)
control component type: sum (i.e., sum) scaling factor s: 1.0 initial value: 0.0
initial value flag: 1 (i.e., initial condition computation)
limiter control: 3 (Namely, both the minimum and maximum limits are to be imposed.)
minimum value: 0.0 maximum value: 1.6e+6 constant a_0: -200000.01
constant a_1: 1.0 alphanumeric name for v_1: cntrlvar integer name for v_1: 664
Control variable y defined by the sum component is expressed as: $y = s(a_0+a_1*v_1)$
***Note*:** The 'cntrlvar 665' is defined by the sum component using the 'cntrlvar 664'.

control component no. (ccc): 505 (reactor scram signal)
control component type: tripunit (i.e., unit trip) scaling factor s: 1.0 initial value: 0.0
initial value flag: 1 (i.e., initial condition computation)
trip card no.: 501 (Namely, u is 0.0 or 1.0 when trip is 'on' or 'off', respectively.)
Control variable y defined by the unit trip component is expressed as: y = s*u
***Note*:** The 'cntrlvar 505' is defined by the unit trip component which concerns a trip card no. 501.

control component no. (ccc): 666 (reactor scram signal)
control component type: sum (i.e., sum) scaling factor s: 1.0 initial value: 1.0
initial value flag: 1 (i.e., initial condition computation) constant a_0: 1.0
constant a_1: -1.0 alphanumeric name for v_1: cntrlvar integer name for v_1: 505
Control variable y defined by the sum component is expressed as: $y = s(a_0+a_1*v_1)$
***Note*:** The 'cntrlvar 666' is defined by the sum component using the 'cntrlvar 505'.

control component no. (ccc): 600 (PZR heater power)
control component type: mult (i.e., multiplier) scaling factor s: 1.0 initial value: 0.0
initial value flag: 1 (i.e., initial condition computation)
limiter control: 3 (Namely, both the minimum and maximum limits are to be imposed.)
minimum value: 0.0 maximum value: 1.6e+6
alphanumeric name for v_1: cntrlvar integer name for v_1: 665
alphanumeric name for v_2: cntrlvar integer name for v_2: 666
Control variable y defined by the multiplier component is expressed as: $y = s*v_1*v_2$
***Note*:** The 'cntrlvar 600' is defined by the multiplier component using the 'cntrlvar 665' and 'cntrvar 666'.

Control system input data relevant to the SG secondary narrow-range liquid level are as follows.

control component no. (ccc): 521 (SG secondary narrow-range liquid level in loop-A)
control component type: lag (i.e., lag) scaling factor s: 1.0 initial value: 44.0
initial value flag: 1 (i.e., initial condition computation)
limiter control: 3 (Namely, both the minimum and maximum limits are posed.)
minimum value: 0.0 maximum value: 100.0
lag time a_1: 5.0 alphanumeric name for v_1: cntrlvar integer name for v_1: 508
Control variable y defined by the lag component is expressed as: $y = s*v_1/(1+a_1)$
***Note*:** The 'cntrlvar 521' is defined by the lag component using the 'cntrlvar 508'.

control component no. (ccc): 321 (SG secondary narrow-range liquid level in loop-B)
control component type: lag (i.e., lag) scaling factor s: 1.0 initial value: 44.0
initial value flag: 1 (i.e., initial condition computation)
limiter control: 3 (Namely, both the minimum and maximum limits are posed.)
minimum value: 0.0 maximum value: 100.0
lag time a_1: 5.0 alphanumeric name for v_1: cntrlvar integer name for v_1: 308
Control variable y defined by lag component is expressed as: $y = s*v_1/(1+a_1)$
***Note*:** The 'cntrlvar 321' is defined by the lag component using the 'cntrlvar 308'.

control component no. (ccc): 508 (SG secondary narrow-range liquid level in loop-A)
control component type: function (i.e., functional) scaling factor s: 1.0 initial value: 0.0
initial value flag: 1 (i.e., initial condition computation)
alphanumeric name for v_1: cntrlvar integer name for v_1: 518 general table no.: 308
Control variable y defined by the functional component is expressed as: $y = s*[\text{function } (v_1)]$
***Note*:** The 'cntrlvar 508' is defined by the functional component using the 'cntrlvar 518' which concerns the general table no. 308.

control component no. (ccc): 518 (SG secondary narrow-range liquid level in loop-A)
control component type: sum (i.e., sum) scaling factor s: 1.0 initial value: 1.76
initial value flag: 1 (i.e., initial condition computation) constant a_0: 0.0
constant a_1: 1.051 alphanumeric name for v_1: voidf integer name for v_1: 51201
constant a_2: 1.051 alphanumeric name for v_2: voidf integer name for v_2: 51202
constant a_3: 1.898 alphanumeric name for v_3: voidf integer name for v_3: 51203
Control variable y defined by the sum component is expressed as: $y = s(a_0+a_1*v_1+a_2*v_2+a_3*v_3)$
***Note*:** The 'cntrlvar 518' is defined by the sum component using liquid fraction of each of three vertically divided volumes of SG riser in loop-A.

control component no. (ccc): 308 (SG secondary narrow-range liquid level in loop-B)
control component type: function (i.e., functional) scaling factor s: 1.0 initial value: 0.0
initial value flag: 1 (i.e., initial condition computation)
alphanumeric name for v_1: cntrlvar integer name for v_1: 318 general table no.: 308
Control variable y defined by the functional component is expressed as: $y = s*[\text{function } (v_1)]$
***Note*:** The 'cntrlvar 308' is defined by the functional component using the 'cntrlvar 318' which concerns the general table no. 308.

control component no. (ccc): 318 (SG secondary narrow-range liquid level in loop-B)
control component type: sum (i.e., sum) scaling factor s: 1.0 initial value: 1.76
initial value flag: 1 (i.e., initial condition computation) constant a_0: 0.0
constant a_1: 1.051 alphanumeric name for v_1: voidf integer name for v_1: 31201
constant a_2: 1.051 alphanumeric name for v_2: voidf integer name for v_2: 31202
constant a_3: 1.898 alphanumeric name for v_3: voidf integer name for v_3: 31203
Control variable y defined by the sum component is expressed as: $y = s(a_0+a_1*v_1+a_2*v_2+a_3*v_3)$
***Note*:** The 'cntrlvar 318' is defined by the sum component using liquid fraction of each of three vertically divided volumes of SG riser in loop-B.

Control system input data related to the opening degree of SG main feedwater valve are as follows.

control component no. (ccc): 530 (opening degree of SG main feedwater valve in loop-A)
control component type: integral (i.e., integrating) scaling factor s: 1.0 initial value: 0.0
initial value flag: 1 (i.e., initial condition computation)
limiter control: 3 (Namely, both the minimum and maximum limits are posed.)
minimum value: -1.0 maximum value: 1.0
alphanumeric name for v_1: cntrlvar integer name for v_1: 529
Control variable y defined by the integrating component is expressed as: $y = s\int v_1 dt$

***Note*:** The 'cntrlvar 530' is defined by the integrating component using the 'cntrlvar 529' which calculates the difference between SG reference secondary liquid level and SG secondary narrow-range liquid level in loop-A.

control component no. (ccc): 531 (opening degree of SG main feedwater valve in loop-A)
control component type: sum (i.e., sum) scaling factor s: 1.0 initial value: 0.0
initial value flag: 1 (i.e., initial condition computation)
limiter control: 3 (Namely, both the minimum and maximum limits are to be imposed.)
minimum value: -1.0 maximum value: 1.0 constant a_0: 0.0
constant a_1: 1.0 alphanumeric name for v_1: cntrlvar integer name for v_1: 530
constant a_2: -10.0 alphanumeric name for v_2: cntrlvar integer name for v_2: 505
Control variable y defined by the sum component is expressed as: $y = s(a_0+a_1*v_1+a_2*v_2)$
***Note*:** The 'cntrlvar 531' is defined by the sum component using the 'cntrlvar 530', and the 'cntrlvar 505' which concerns a trip card no. 501.

control component no. (ccc): 330 (opening degree of SG main feedwater valve in loop-B)
control component type: integral (i.e., integrating) scaling factor s: 1.0 initial value: 0.0
initial value flag: 1 (i.e., initial condition computation)
limiter control: 3 (Namely, both the minimum and maximum limits are posed.)
minimum value: -1.0 maximum value: 1.0
alphanumeric name for v_1: cntrlvar integer name for v_1: 329
Control variable y defined by the integrating component is expressed as: $y = s\int v_1 dt$
***Note*:** The 'cntrlvar 330' is defined by the integrating component using the 'cntrlvar 329' which calculates the difference between SG reference secondary liquid level and SG secondary narrow-range liquid level in loop-B.

control component no. (ccc): 331 (opening degree of SG main feedwater valve in loop-B)
control component type: sum (i.e., sum) scaling factor s: 1.0 initial value: 0.0
initial value flag: 1 (i.e., initial condition computation)
limiter control: 3 (Namely, both the minimum and maximum limits are to be imposed.)
minimum value: -1.0 maximum value: 1.0 constant a_0: 0.0
constant a_1: 1.0 alphanumeric name for v_1: cntrlvar integer name for v_1: 330
constant a_2: -10.0 alphanumeric name for v_2: cntrlvar integer name for v_2: 505
Control variable y defined by the sum component is expressed as: $y = s(a_0+a_1*v_1+a_2*v_2)$
***Note*:** The 'cntrlvar 331' is defined by the sum component using the 'cntrlvar 330', and the 'cntrlvar 505' which concerns a trip card no. 501.

Additionally, control system input data relevant to various liquid levels in reactor vessel are as follows.

control component no. (ccc): 124 (core liquid level)
control component type: sum (i.e., sum) scaling factor s: 1.0 initial value: 0.0
initial value flag: 1 (i.e., initial condition computation) constant a_0: 0.0
constant a_1: 0.406666 alphanumeric name for v_1: voidf integer name for v_1: 12401
constant a_2: 0.406666 alphanumeric name for v_2: voidf integer name for v_2: 12402
constant a_3: 0.406666 alphanumeric name for v_3: voidf integer name for v_3: 12403
constant a_4: 0.406666 alphanumeric name for v_4: voidf integer name for v_4: 12404
constant a_5: 0.406666 alphanumeric name for v_5: voidf integer name for v_5: 12405
constant a_6: 0.406666 alphanumeric name for v_6: voidf integer name for v_6: 12406
constant a_7: 0.406666 alphanumeric name for v_7: voidf integer name for v_7: 12407
constant a_8: 0.406666 alphanumeric name for v_8: voidf integer name for v_8: 12408
constant a_9: 0.406666 alphanumeric name for v_9: voidf integer name for v_9: 12409
Control variable y defined by the sum component is expressed as:
$y = s(a_0+a_1*v_1+a_2*v_2+a_3*v_3+a_4*v_4+a_5*v_5+a_6*v_6+a_7*v_7+a_8*v_8+a_9*v_9)$
***Note*:** The 'cntrlvar 124' is defined by the sum component using liquid fraction of each of nine vertically divided volumes of core.

control component no. (ccc): 125 (liquid level from core top to reactor vessel bottom)
control component type: sum (i.e., sum) scaling factor s: 1.0 initial value: 0.0
initial value flag: 1 (i.e., initial condition computation) constant a_0: 3.0988
constant a_1: 1.0 alphanumeric name for v_1: cntrlvar integer name for v_1: 124
Control variable y defined by the sum component is expressed as: $y = s(a_0+a_1*v_1)$

***Note*:** The 'cntrlvar 125' is defined by the sum component using the 'cntrlvar 124' and length of 3.0988 m from core bottom to reactor vessel bottom. This length is equal to the combined length of the component no. 120 for core inlet and the components no. 116 and 112 for lower plenum.

control component no. (ccc): 109 (liquid level from vessel DC top to reactor vessel bottom)
control component type: sum (i.e., sum) scaling factor s: 1.0 initial value: 0.0
initial value flag: 1 (i.e., initial condition computation) constant a_0: 1.84
constant a_1: 0.8245 alphanumeric name for v_1: voidf integer name for v_1: 10401
constant a_2: 0.51075 alphanumeric name for v_2: voidf integer name for v_2: 10801
constant a_3: 0.655 alphanumeric name for v_3: voidf integer name for v_3: 10802
constant a_4: 0.406666 alphanumeric name for v_4: voidf integer name for v_4: 10803
constant a_5: 0.406666 alphanumeric name for v_5: voidf integer name for v_5: 10804
constant a_6: 0.406666 alphanumeric name for v_6: voidf integer name for v_6: 10805
constant a_7: 0.406666 alphanumeric name for v_7: voidf integer name for v_7: 10806
constant a_8: 0.406666 alphanumeric name for v_8: voidf integer name for v_8: 10807
constant a_9: 0.406666 alphanumeric name for v_9: voidf integer name for v_9: 10808
constant a_{10}: 0.406666 alphanumeric name for v_{10}: voidf integer name for v_{10}: 10809
constant a_{11}: 0.406666 alphanumeric name for v_{11}: voidf integer name for v_{11}: 10810
constant a_{12}: 0.406666 alphanumeric name for v_{12}: voidf integer name for v_{12}: 10811
constant a_{13}: 1.2588 alphanumeric name for v_{13}: voidf integer name for v_{13}: 10812
Control variable y defined by the sum component is expressed as: $y = s(a_0+a_1*v_1+a_2*v_2+a_3*v_3+a_4*v_4+a_5*v_5+a_6*v_6+a_7*v_7+a_8*v_8+a_9*v_9+a_{10}*v_{10}+a_{11}*v_{11}+a_{12}*v_{12}+a_{13}*v_{13})$

***Note*:** The 'cntrlvar 109' is defined by the sum component using liquid fraction of each of twelve vertically divided volumes of vessel DC and length of 1.84 m from vessel DC bottom to reactor vessel bottom. This length is equal to the combined length of the components no. 116 and 112 for lower plenum.

control component no. (ccc): 512 (SG secondary wide-range liquid level in loop-A)
control component type: sum (i.e., sum) scaling factor s: 1.0 initial value: 0.0
initial value flag: 1 (i.e., initial condition computation) constant a_0: 0.0
constant a_1: 2.258 alphanumeric name for v_1: voidf integer name for v_1: 50401
constant a_2: 2.258 alphanumeric name for v_2: voidf integer name for v_2: 50402
constant a_3: 2.258 alphanumeric name for v_3: voidf integer name for v_3: 50403
constant a_4: 2.258 alphanumeric name for v_4: voidf integer name for v_4: 50404
constant a_5: 1.916 alphanumeric name for v_5: voidf integer name for v_5: 50405
constant a_6: 1.051 alphanumeric name for v_6: voidf integer name for v_6: 50601
constant a_7: 2.949 alphanumeric name for v_7: voidf integer name for v_7: 50801
constant a_8: 3.372 alphanumeric name for v_8: voidf integer name for v_8: 51601
Control variable y defined by the sum component is expressed as:
$y = s(a_0+a_1*v_1+a_2*v_2+a_3*v_3+a_4*v_4+a_5*v_5+a_6*v_6+a_7*v_7+a_8*v_8)$

***Note*:** The 'cntrlvar 512' is defined by the sum component using liquid fraction of each of five vertically divided volumes of SG riser and that of each volume of SG steam dome and SG separator in loop-A.

control component no. (ccc): 312 (SG secondary wide-range liquid level in loop-B)

control component type: sum (i.e., sum) scaling factor s: 1.0 initial value: 0.0

initial value flag: 1 (i.e., initial condition computation) constant a_0: 0.0

constant a_1: 2.258	alphanumeric name for v_1: voidf	integer name for v_1: 30401
constant a_2: 2.258	alphanumeric name for v_2: voidf	integer name for v_2: 30402
constant a_3: 2.258	alphanumeric name for v_3: voidf	integer name for v_3: 30403
constant a_4: 2.258	alphanumeric name for v_4: voidf	integer name for v_4: 30404
constant a_5: 1.916	alphanumeric name for v_5: voidf	integer name for v_5: 30405
constant a_6: 1.051	alphanumeric name for v_6: voidf	integer name for v_6: 30601
constant a_7: 2.949	alphanumeric name for v_7: voidf	integer name for v_7: 30801
constant a_8: 3.372	alphanumeric name for v_8: voidf	integer name for v_8: 31601

Control variable y defined by the sum component is expressed as:

$y = s(a_0+a_1*v_1+a_2*v_2+a_3*v_3+a_4*v_4+a_5*v_5+a_6*v_6+a_7*v_7+a_8*v_8)$

***Note*:** The ‘cntrlvar 312’ is defined by the sum component using liquid fraction of each of five vertically divided volumes of SG riser and that of each volume of SG steam dome and SG separator in loop-B.